Università degli Studi di Cagliari
Dipartimento di Scienze della Vita e dell'Ambiente
Sezione di Scienze del Farmaco

DOTTORATO DI RICERCA

Scienze e Tecnologie Farmaceutiche

Ciclo XXVI

Secondary Metabolites from *Otanthus maritimus*, *Stachys glutinosa* and *Withania somnifera*: Isolation, Structure Elucidation and Interactions with Cannabinoid and Opioid Systems

Settore scientifico disciplinare di afferenza

CHIM/08

Presentata da: Nicola Anzani
Coordinatore Dottorato Prof. Elias Maccioni
Tutor Dott. Filippo Cottiglia

anno accademico 2012 – 2013

UNIONE EUROPEA
Fondo sociale europeo

FSE 2007-2013
POR SARDEGNA
obiettivo competitività regionale e occupazione

ACKNOWLEDGEMENTS

I am most grateful to my supervisor, Dr. Filippo Cottiglia, for general help and many fruitful discussion about my work. To him goes all my gratitude for being always an example at work and for his continuous support and encouragement.

Special thanks to Dr. Stefania Ruiu and Dr. Alessandro Orrù (Institute of Translational Pharmacology, UOS of Cagliari, National Research Council, Parco Scientifico e Tecnologico, Pula, Italy) for binding assays and analgesia experiments.

Thanks are also due to Dr. Simona Distinto (Department of Life and Environmental Sciences, Cagliari) for molecular modeling studies.

I wish to thank Dr. Marco Leonti (Department of Life and Environmental Sciences, Cagliari) for the identification of the plant material.

I am grateful to Dr. Amit Agarwal (Natural Remedies Pvt. Ltd., Bangalore, India) for providing the methanol extract of *Withania somnifera* roots.

I would like to express my gratitude to my colleagues at the Laboratory of Medicinal Chemistry of the Department of Life and Enviromental Sciences for creating a friendly and stimulating working atmosphere.

Last but not least, I would like to give special thanks to my family that always believed in me and to my girlfriend Michela for her infinite patience and love that allowed me to overcome all obstacles. You're my lighthouse in the storm.



Nicola Anzani gratefully acknowledges Sardinia Regional Government for the financial support of her PhD scholarship (P.O.R. Sardegna F.S.E. Operational Programme of the Autonomous Region of Sardinia, European Social Fund 2007-2013 - Axis IV Human Resources, Objective l.3, Line of Activity l.3.1.)".

TABLE OF CONTENTS

ABBREVIATIONS

ACN	acetonitrile
APT	attached proton test
CB	cannabinoid
$CDCl_3$	deuterated chloroform
CD_4O	deuterated methanol
CPP	conditioned place preference
d	doublet
DCM	dichloromethane
DEPT	distortionless enhancement by polarization tranfer
DQF-COSY	double-quantum filtered correlation spectroscopy
DOR	δ opioid receptor
ESI MS	electrospray mass spectrometry
EtOAc	ethyl acetate
FDA	food and drugs administration
GABA	gamma-aminobutyric acid
[^{3}H]-DAMGO	[(D-Ala^2, N-Me-Phe^4, Gly^5-ol-) enkephalin]
[^{3}H]-DPDPE	[(D-Pen 2,5)-enkephalin]
HMBC	heteronuclear multiple bond correlation
HPLC	high performance liquid chromatography

HR ESI MS	high resolution electrospray mass spectrometry
HSQC	heteronuclear single quantum coherence
IC_{50}	inhibition concentration (50% inhibition)
µg	microgram
µl	microliter
K_i	inhibition constant
KOR	k opioid rceptor
MeOH	methanol
MOR	µ opioid receptor
NMDA	N-methyl-d-aspartate
NMR	nuclear magnetic resonance
NP	normal phase
OME	*Otanthus maritimus* extract
PAg	Periaqueductal grey
PMF_s	polymethoxyflavones
RP	reversed phase
s	singlet
spp	species
TOF	time of flight
THC	tetrahydrocannabinol
t	triplet
TFAA	trifluoroacetic acid

TLC	thin layer chromatography
SGE	*Stachys glutinosa* extract
UV	ultraviolet
VLC	vacuum liquid chromatography
WSAE	*Withania somnifera* alkaloid extract
WSE	*Withania somnifera* methanol extract

1. INTRODUCTION

Plants have been used for thousands of years to treat diseases and today too, they are the almost exclusive source of drugs for the majority of the world's population.

In the 19th century, with the isolation of morphine from opium, it was begun to employ the pure active ingredients rather than whole extracts.[1] After the discovery of morphine a lot of plant-originated drugs have been discovered and various secondary metabolites are currently in use such as, for example, quinine from *Cinchona* species, cardiac glicosides from *Digitalis purpurea*, vinblasine and vincristine from *Catharanthus roseus*, taxol from *Taxus brevifolia* and the antimalarian compound, artemisinin, from *Artemisia annua*.

Higher plants are also an important source of drugs that act as agonist to opioid receptors and among all, morphine, isolated from the opium poppy, *Papaver somniferum*. Morphine is a μ opioid receptor agonist and is the most potent analgesic currently used in clinic for the treatment of moderate or severe pain. Salvinorin is another receptor opioid ligand (k agonist) isolated from plants (*Salvia divinorum*) but it does not show any analgesic activity and has been classified as a hallucinogenic agent.[2]

A consistent number of medicinal and dietary plants have been reported to contain secondary metabolites that interact with the endocannabinoid system. These compounds, also called phytocannabinoids, are capable of either directly interacting with cannabinoid receptors (CB_1 and CB_2) or sharing chemical similarity with cannabinoids or both.[3] Δ^9-tetrahydrocannabinol (Δ^9-THC) from *Cannabis sativa* is a non-selective agonist to cannabinoid receptors and is used for the treatment of neuropathic pain or for refractory forms of treatment with morphine derivatives.[4]

Recently, N-alkylamides from *Echinacea* spp. have been identified as CB_2 receptor selective agonists and are responsible of the immunomodulatory effect of this plant.[5]

Powerful new technologies such as high-throughput screening and combinatorial chemistry dramatically increase the possibility of drug discovery. Nevertheless, natural products still offer unmatched structural variety when compared to synthetic compounds. For example, natural products are more likely to be rich in stereochemistry and concatenated rings than the structures obtained by the combinatorial libraries.

To date, natural products still represent a very important source in the discovery and development of new medicines and a significant part of the therapeutic armamentarium of doctors is represented by

natural medicines or natural-derived products.[6] If we consider the new drugs approved in 2010 by Food and Drugs Administration (FDA), half of the 20 fully approved small molecules were natural products or directly derived therefrom, confirming the importance of natural products as source of new drugs.[6]

2. OPIOID RECEPTORS

The term opioid applies to any substance that produces effects similar to those of morphine and that are blocked from specific antagonists (naloxone). Among these there are natural alkaloids, synthesis or semisynthesis compounds, endogenous opioid peptides. These substances act on specific receptors of the peripheral and central nervous system (that take the generic name of opioid receptors) acting mainly as modulators of the painful sensations but also through specific transcription factors nuclear receptors. The term opioid is frequently used improperly to indicate, more restrictively, the alkaloids that can be found in opium, a mixture of substances derived from the latex of *Papaver somniferum*, and their semi-synthetic derivatives; the correct term to describe these substances is, instead, opiates. The evidence of the use of opium as a medicine as well as a substance for luxury, dates back to many centuries before Christ, given in Latin texts and Homer, and to Roman imperial and Republican.[7] Opioids act on a family of receptors in the central and peripheral nervous system, which includes four subtypes: μ opioid receptor (MOR), δ opioid receptor (DOR) and κ opioid receptor (KOR). All these receptors belong to the superfamily of G protein-coupled

receptors. The activation of these receptors leads to: inhibition of adenylate cyclase and thereby reduced synthesis of cAMP, the inhibition of Ca^{2+} channels that results in a reduction in the release of neurotransmitter, the opening of K^{+} channels that results in hyperpolarization of the membrane and reduction of nerve activity.[7]

G proteins involved in signal transduction are Gi (inhibitor). These cellular effects are reflected in a wide variety of physical symptoms such as analgesia and sedation, sleep induction, respiratory depression (caused by opioid action at the level of the bulbar respiratory centre sensitive to arterial pCO2), central nervous depression, gastrointestinal motility inhibition and inhibition of the cough reflex.[7] All opioid receptors modulate the analgesic action although they operate at different levels. MOR: generating analgesia (sovraspinal level), miosis, and respiratory depression, decrease in gastrointestinal activity, euphoria; KOR: produces analgesia (spinal level), miosis, and respiratory depression, dysphoria (unlike μ receptors); DOR: no analgesia, but decreases the intestinal transit and depresses the immune system.[7] Opioids tend to inhibit neuronal transmission at both pre and post synaptic level. In fact, the activation of presinaptic μ receptors causes inhibition of N-type calcium channels and thus a reduction in the production of neurotransmitters, while the activation of μ postsynaptic receptors produces

hyperpolarization by activating potassium channels and inhibiting calcium L-type.

MOR is the most widespread receptor and mediate most of the pharmacological effects of opioid analgesics.

Physiologically active molecules on these receptors are the endogenous opioids peptides, β- endorphins, dynorphines A and B, and enkephalins, endogenous substances better defined as opioid peptides which are synthesized respectively starting from large precursor peptide, proopiomelanocortin, proenkephaline and prodinorphine, splitting by specific endopeptidase.[7]

The endogenous opioids, β-endorphins, dynorphines A and B, and enkephalins exert their analgesic action at spinal and sovraspinal level. They also cause analgesia with a peripheral action mechanism associated with the inflammatory process. In the central nervous system, opioids exert an inhibitory action on neurotransmitters. At sovraspinal level, activation of opioid receptors inhibit neuronal activity and therefore the release of noradrenaline from the *locus coeruleus* and *nucleus reticularis paragigantocellularis* (NRPG), and the release of serotonin from *nucleus Raphe Magnus* (NRM), with inhibition of pain transmission. MOR agonists prevent the release of the inhibitory transmitter GABA activating the *Periaqueductal grey* (PAG) systems that regulate the activity of the bulb.[8] In particular, the

GABA transmission can have opposite effects on pain processing in relation to its location within the central nervous system; its activation causes analgesia at spinal level, while it is pronociceptive at sopraspinal level.[9,10] The systemic administration of $GABA_A$ and $GABA_B$ agonists such as benzodiazepines increases the opioid-induced analgesia[11,12] and attenuates the development of tolerance.[13]

Opioids also exert a neuromodulator action of pain signal on afferent neurons located in the dorsal horn of the spinal cord and neuronal interconnection paths for pain signal transmission in the brain.

At spinal level, the activation of k and μ receptors blocks the release of substance P, peptide released following a skin lesion from the fibers relating to the rear horns of the spinal cord. Substance P is a neurotransmitter of the anguished transmission, so blocking its release also locks the transmission of pain information.[14]

Glutamate is the primary excitatory neurotransmitter involved in the transmission of nociceptive stimuli at spinal level.[10] In addition, N-Methyl-D-Aspartate (NMDA) receptor sensitization on spinal neurons play a key role in the development of tolerance induced by opioids.[8] Consistently, the co-administration of NMDA receptor antagonists enhances the opioid-induced analgesia.[15]

2.1 Natural Opioids Ligands

As mentioned before, the investigation of natural products has proven to be an excellent source of clinical agents for a number of therapeutic areas including pain.[6]

Morphine (Figure 1) is the most abundant opiate found in opium (8-14% of dry weight), the dried latex is obtained by shallowly slicing the unripe seedpods of the *Papaver somniferum* poppy. Morphine was the first active principle purified from a plant source and is one of at least 50 alkaloids of several different types present in opium.

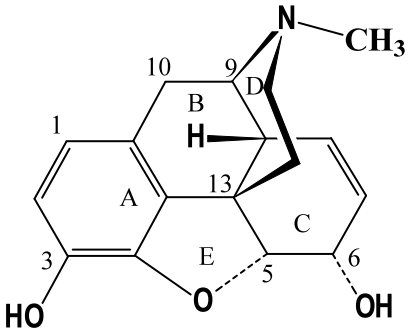

Figure 1. Structure of morphine

Morphine is primarily used to treat both acute and chronic severe pain for example in myocardial infarction, in cancer pain and for labour pains.[7]

In fact like other opioids, it acts directly on μ receptor of the central nervous system (CNS) to relieve pain. Morphine has a high potential for addiction; tolerance and psychological dependence develop rapidly. Tolerance to respiratory depression and euphoria develops more rapidly than tolerance to analgesia, and many chronic pain patients are being maintained on a stable dose, for many years.[7]

In addition morphine acts on the myenteric plexus in the intestinal tract, reducing gut motility, causing constipation. The gastrointestinal effects of morphine are mediated primarily by μ receptors in the bowel.[7]

New natural therapies are currently being explored as analgesic potential alternatives to morphine and derivatives.[17]

Kratom (*Mitragyna speciosa* Korth., Rubiaceae) is an indigenous herb of Southeast Asia that is traditionally used to treat fever, diarrhea, fatigue, pain, and as a substitute for morphine in treating opioid addicts. The main component of kratom is the indole alkaloid mitragynine (Figure 2), which has been reported to have affinities for all three opioid receptors, though it appears to be relatively selective

for MOP receptors. Additionally, other constituents of kratom and derivatives of mitragynine, as pseudoindoxyl and 7-hydroxymitragynine, have also been found to have affinity for opioid receptors (Figure 2).[17]

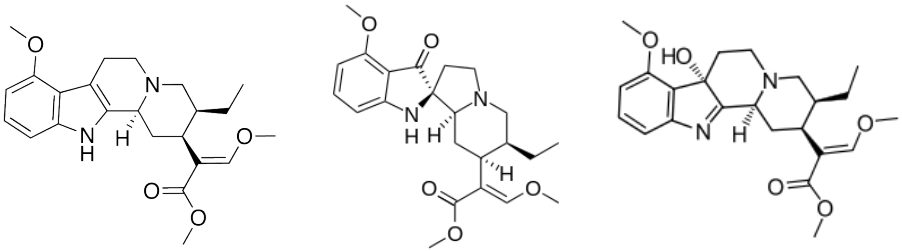

mitragynine pseudoindoxyl-mitragynine 7-hydroxymitragynine

Figure 2. Structures of *Mitragyna speciosa* alkaloids

Research interest in mitragynine stems from its increasing use as a remedy for opioid withdrawal by individuals who self-treat chronic pain. In addition this compound is known to produce antinociception in mice in the hot-plate and in the tail-flick tests.[17] However, the exact mechanisms underlying the effect of mitragynine are currently unknown. It has been hypothesized that the MOP agonism of mitragynine might avert withdrawal symptoms, while KOP agonism

might attenuate reinforcement and blunt cravings. The collective findings of the effects of mitragynine indicate that the molecule and its derivatives may be useful for the development of new analgesics and possibly for the treatment of opioid abuse.[17]

Selective KOP agonists are also capable of producing clinically useful analgesia, but lack the respiratory depression, constipation, and addictive properties associated with MOP agonists. However, a side effect associated with activation of KOP receptors is dysphoria. Still, KOP agonists are targets for achieving pain relief without the negative side effects associated with MOP agonists. Although KOP agonists are known to produce dysphoric effects, there is still some hope that a clinically useful analgesic may be found.[17]

Salvinorin A, a *neo*-clerodane diterpene (Figure 3), is the active hallucinogenic component in the Mexican mint plant *Salvia divinorum* (Lamiaceae). This plant has been used by the Mazatec Indians in Oaxaca, Mexico, as a hallucinogenic agent, and to relieve diarrhea, headache, and rheumatism.

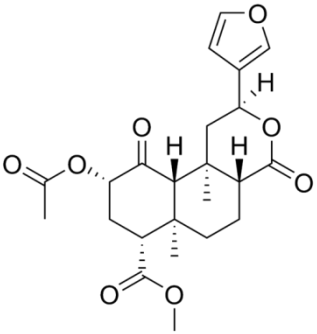

Figure 3. Structure of salvinorin A

However, until recently, the target of the hallucinogenic effects was not clear, as Salvinorin A lacks activity at the targets of other known hallucinogens, specifically serotonin receptors, cholinergic receptors, and cannabinoid receptors.

In 2002, Salvinorin A was identified as a potent and selective KOP agonist. This result is surprising considering that Salvinorin A lacks the basic nitrogen that has long been thought to be required for opioid activity. However, given the known hallucinogenic effects of other KOP agonists, this finding is not unprecedented. Salvinorin A produces a discriminative effect in both rats and non-human primates that is similar to other KOP agonists. It has also been shown to produce analgesia in mice that can be blocked by a KOP receptor antagonist.[17]

Another natural opioid is ibogaine (Figure 4), an indole alkaloid isolated from the root, root-bark, stems, and leaves of the African shrub *Tabernanthe iboga*. This plant has been used by indigenous people in low doses to combat fatigue and hunger and in higher doses as a sacrament in religious rituals. The psychopharmacology of ibogaine is complex due to its affinity for several receptors, transporters, and ion channels. In addition, its primary metabolite, 12-hydroxyibogamine, is also biologically active. The most-studied therapeutic effect of ibogaine is the reduction or elimination of addiction to opioids. The mechanism by which ibogaine exerts its anti-addictive effects is presently unknown although several receptor systems have been implicated in its activity. However, it has been speculated that its k agonist actions contribute to its effects on stimulant self-administration and analogs of ibogaine are currently being explored as potentially safer medications**.**[18]

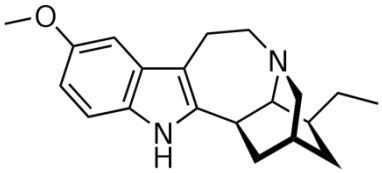

Figure 4. Structure of ibogaine

3. CANNABINOID RECEPTORS

The cannabinoid receptors are a class of cell membrane receptors under the G protein-coupled receptor superfamily[19-21] which contain seven transmembrane spanning domains.[22]

There are currently two known subtypes, termed CB1 and CB2[23,24]. (Figure 5). The CB1 receptor is expressed mainly in the brain, but also in the lungs, liver and kidneys. The CB2 receptor is expressed mainly in the immune system and in hematopoietic cells.[25]

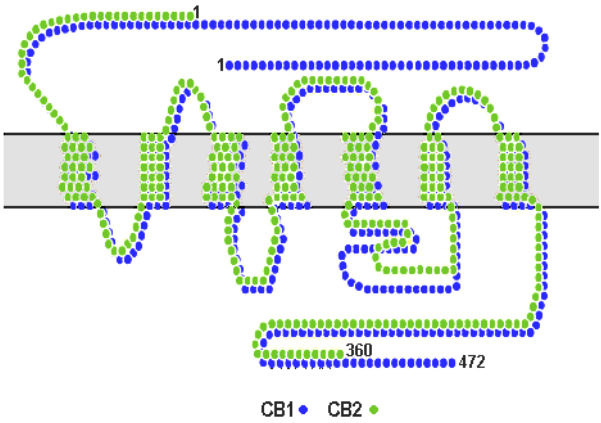

Figure 5. CB1 and CB2 receptors

Cannabinoid receptors are activated by three major groups of ligands, endocannabinoids (such as anandamide and 2-arachidonoylglycerol (2-AG) (Figure 6), phytocannabinoids (such as Δ^9-THC and alkylamides, found in *Cannabis* and *Echinacea* species, respectively) (Figure 7) and synthetic cannabinoids (such as HU-210). All of the endocannabinoids and phytocannabinoids are lipophilic, i.e. fat soluble, compounds. Cannabinoids bind reversibly and stereo-selectively to the cannabinoid receptors.

(1)

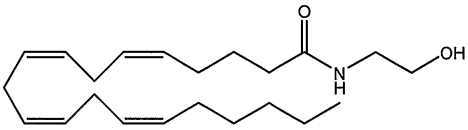

(2)

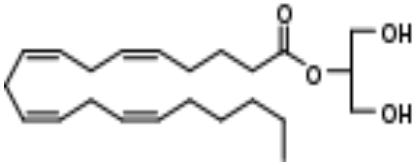

Figure 6. Structures of anandamide (1) and 2-arachidonoylglycerol (2)

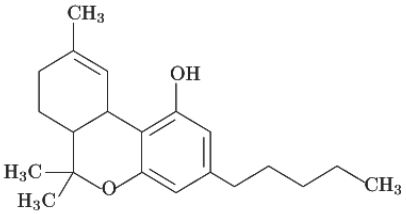

Figure. 7 Structure of Δ^9-THC

After the receptor is engaged, multiple intracellular signal transduction pathways are activated. At first, it was thought that cannabinoid receptors mainly inhibited the enzyme adenylate cyclase (and thereby the production of the second messenger molecule cyclic AMP), and positively influenced inwardly rectifying potassium channels (=Kir or IRK). However, a much more complex picture has appeared in different cell types, implicating other potassium ion channels, Ca2+ channels, protein kinase A and C, Raf-1, ERK, p38, c-fos, c-jun and many more.[26]

Separation between the therapeutically undesirable psychotropic effects, and the clinically desirable ones has not been reported with agonists that bind to cannabinoid receptors. Δ^9-THC, as well as the two major endogenous compounds identified so far, anandamide and 2-arachidonylglycerol, that bind to the cannabinoid receptor, produce

most of their effects by binding to both the CB1 and CB2 receptors. While the effects mediated by CB1, mostly in the central nervous system, have been thoroughly investigated, those mediated by CB2 are not equally well defined.[27]

3.1 CB1 Receptor

CB1 receptors are expressed most densely in the central nervous system and are largely responsible for mediating the effects of cannabinoid binding in the brain.

The analgesic effects of cannabinoids are based on the interaction of these compounds with CB1 receptors on spinal cord interneurons in the superficial levels of the dorsal horn. Signals on this track are also transmitted to the periaqueductal gray (PAG) of the midbrain. Endogenous cannabinoids are believed to exhibit an analgesic effect on these receptors by limiting both GABA and glutamate of PAG cells that relate to nociceptive input.[28]

They are also found in other parts of the body. For instance, in the liver, activation of the CB1 receptor is known to increase de novo lipogenesis.[29] Activation of presynaptic CB1 receptors is also known to inhibit sympathetic innervation of blood vessels and contributes to

the suppression of the neurogenic vasopressor response in septic shock.[30]

Inhibition of gastrointestinal activity has been observed after administration of Δ^9-THC or anandamide. This effect is assumed to be CB1-mediated, since this receptor is expressed by the peptide hormone cholecystokinin, and application of the CB1-specific antagonist SR 141716A Rimonabant blocks the effect.[31]

Cannabinoids are well known for their cardiovascular activity. Activation of peripheral CB1 receptors contributes to hemorrhagic and endotoxin-induced hypotension. Anandamide and 2-AG, produced by macrophages and platelets, respectively, may mediate this effect.[32]

Many studies suggest that the effects of endocannabinoids on memory are dependent on what type of neurons are being targeted (excitatory vs. inhibitory) and the location of these networks in the brain.[33]

Evidence for the role of the endocannabinoid system in food-seeking behavior comes from a variety of cannabinoid studies. Emerging data suggest that Δ^9-THC acts via CB1 receptors in the hypothalamic nuclei to directly increase appetite.[34]

3.2 CB2 Receptor

CB2 receptors are found throughout tissues of the spleen, tonsils, and thymus gland mainly expressed on T cells of the immune system, on macrophages and B cells, and in hematopoietic cells. When activated, they too can affect the release of chemical messengers, in this case the secretion of cytokines by immune cells, and can in addition modulate immune cell trafficking.[35] They are also expressed on peripheral nerve terminals, playing a role in antinociception, or the relief of pain. In the brain, they are mainly expressed by microglial cells, where their role remains unclear.

To be specific, this receptor has been implicated in a variety of modulatory functions, including immune suppression, induction of apoptosis and of cell migration.[36]

Therefore, they are also expressed in the brain, though not as densely as the CB1 receptor and are located on different cells.[37] Unlike the CB1 receptor, in the brain, CB2 receptors are found primarily on microglia, but not on neurons.

CB2 receptors are also found throughout the gastrointestinal system, where they modulate intestinal inflammatory response. Thus, CB2

receptor agonists are a potential therapeutic target for inflammatory bowel diseases, such as Crohn's disease and ulcerative colitis.[38,39]

The endocannabinoid system, through CB2 signaling, plays a key role in the maintenance of bone mass: CB2 are expressed in osteoblast, osteocytes and osteoclast. CB2 agonists enhance endocortical osteoblast number and activity while restraining trabecular osteoclastogenesis. Another important effect is that CB2 agonists attenuate ovariectomy-induced bone loss while increasing cortical thickness. These findings suggest CB2 offers a potential molecular target for the diagnosis and treatment of osteoporosis.[40]

3.3 Natural Cannabinoids Ligands

Cannabis sativa have been used for centuries and are known to produce an analgesic effect in addition to hallucinogenic effects such as feelings of dissociation from reality. Cannabinoids are divided into two categories: classical cannabinoids and non-classical cannabinoids.[41]

Classical cannabinoids are tricyclic dibenzopyran derivatives that are both natural and obtained by semisynthesis starting from the first one. This group of molecules is exemplified by Δ^9-THC; the main

psychotropic principle of cannabis. Non-classical cannabinoids emerged from Pfizer SAR studies of the classical cannabinoids.[41]

These compounds are devoided of the dihydropyran ring present in Δ9-THC, as for example CP47497 (Figure 8).[42]

Δ9-THC acts as an agonist with efficacy similar to that of anandamide. It has been suggested that the hallucinogenic effects of Δ^9-THC arise from the compound's ability to mimic the action of anandamide at cannabinoid receptors, while simultaneously antagonizing 2-AG at these same receptors. This hypothesis is supported by the observation that a single high dose of a CB1 receptor antagonist has only a limited ability to block the subjective effects of cannabis ingestion.[43]

Dronabinol[44,48] is the pure isomer of Δ^9-THC, which is the main isomer found in cannabis. It is sold as Marinol (Figure 8) and considered to be non-narcotic with low risk of physical or mental dependence. Marinol has been approved by the U.S. Food and Drugs Administration (FDA) for the treatment of anorexia in AIDS patients, as well as for refractory nausea and vomiting of patients undergoing chemiotherapy.

An analog of Dronabinol, Nabilon[44,48] (Figure 8), is available commercially in Canada under the trade name Cesamet,

manufactured by Valeant Pharmaceuticals. Cesamet has also received FDA approval and began being marketed in the U.S. in 2006.

Female cannabis plants contain more than 60 cannabinoids including cannabindiol, thought to be the major anticonvulsivant that helps multiplesclerosis patients[45], and cannabichromene (Figure 8), an anti-inflammatory which may contribute to the pain-killing effect of cannabis.[46] It takes over one hour for Marinol to reach full systemic effect[47]compared to seconds or minutes for smoked or vaporized cannabis.[48]

Recent advances in the understanding of the endocannabinoid system have broadened the therapeutic possibilities resulting from its manipulation. CB1 receptor antagonists have received the most of the attention of the potential drugs affecting the endocannabinoid system. Their primary indication is for obesity. The rationale behind this indication lies in the generally accepted notion that ingestion of cannabis enhances the appetite, resulting in increased consumption of rich foods. Therefore, CB1 receptor antagonists should function to reduce the appetite, thereby reducing caloric intake and body weight.[49,50] The first reported CB1 receptor antagonist was rimonabant (SR141716, Accomplia)[51] (Figure 8) wich show nanomolar affinity for CB1 receptors, and little affinity for CB2 receptors.

Another indication for CB1 receptor antagonists is in the treatment of drug abuse. Several studies in animals have observed that CB1 receptor antagonists such as rimonabant reduce the rewarding properties of opioid receptor agonists.[52-55] In fact, these rewarding properties are absent in CB1 receptor knock-out mice.[57] However, opioid receptors do not seem to be involved in the hallucinogenic effects of CB1 receptor agonists, as opioid receptor antagonists do not block these effects.[58] Also, the CB1 receptor seems to be involved in responses to both nicotine and alcohol; CB1 receptor antagonists are able to block nicotine-induced conditioned place preference (CPP) and to decrease alcohol consumption.[58] In October 2008, the European Medicines Agency's Committee for Medicinal Products for Human Use (CHMP) had determined that the risks of Accomplia outweighed its benefits, and subsequently recommended the product be suspended from the UK market and doctors not prescribe the drug due to the risk of serious psychiatric problems and even suicide.

Extracts of *Cannabis* are known to produce analgesic effect. In April 2005, Canadian authorities approved the marketing of Sativex, a mouth spray for multiple sclerosis patients, who can use it to alleviate neuropathic pain and spasticity. Sativex contains tetrahydrocannabinol together with cannabindiol and is a preparation of whole cannabis rather than individual cannabinoids.[45] It is

marketed in Canada by GW Pharmaceuticals and is the first cannabis-based prescription drug in the world (in modern times). In addition, Sativex received European regulatory approval in 2010.

A particularly attractive feature of selective CB2 receptor agonists as therapeutics is that they are devoid of any known hallucinogenic effects such as those associated with CB1 receptor agonists.[50]

Since CB2 receptors are believed to play an important role in distinct pathophysiological processes, including metabolic dysregulation, inflammation, pain, and bone loss, they have, therefore, become of interest as new targets in drug discovery. Recently, some phytocannabinoids have been identified as selective CB2 agonist and, among all, a few fatty acid amides isolated from *Echinacea purpurea* that justify the use of *Echinacea* as herbal immunomodulators worldwide plant.[59]

Another phytocannabinoid that act as potent and selective CB2 agonist is the sesquiterpene β-caryophyllene.[5] This compound have been identified in many food plants and also in *Cannabis sativa* L. essential oil. β-caryophyllene showed high oral bioavailabilty and strong anti-inflammatory and analgesic effects and may be considered a good candidate for clinical trials targeting the CB2 receptor.[60]

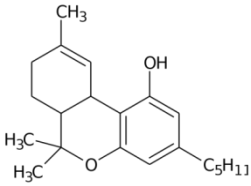

Dronabinol

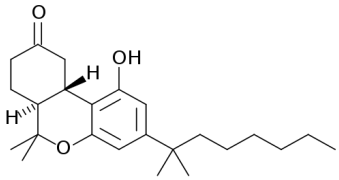

Nabilon

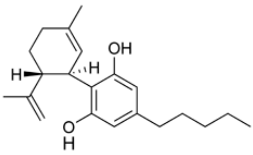

Cannabindiol

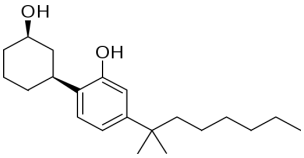

CP47497

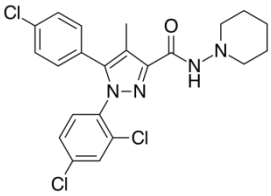

Rimonabant

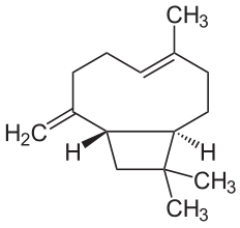

β-caryophyllene

Figure 8. Natural and synthetic cannabinoids structures

4. AIM OF THE WORK

In our continuous search for plant secondary metabolites that bind to CB and/or opioid receptors, we selected four extracts that showed interesting affinity *versus* the above mentioned receptors (Table 1). In particular: the DCM extract obtained from the aerial parts of *Stachys glutinosa* (SGE) was able to bind with a good affinity both MOR and DOR with a K_i of 10.3 and 9 μg/mL, respectively while the DCM extract from the leaves of *Otanthus maritimus* (OME) showed good binding affinity to CB1 (K_i = 2.2 μg/mL) and CB2 (K_i = 1.3 μg/mL) and moderate affinity to MOR and DOR. The third was an alkaloid fraction obtained from the MeOH extract of the roots of *Withania somnifera* (WSAE) that displayed appreciable affinity versus DOR (K_i = 25.5 μg/mL), CB1 (K_i = 23.5 μg/mL), CB2 (K_i = 20.3 μg/mL) and $GABA_A$ (K_i = 14 μg/mL). The *in toto* MeOH extract (WSE) bound with very low affinity to CB and opioid receptors but displayed interesting affinity to $GABA_A$ receptors (K_i = 14 μg/mL) (Table 1).

Based on this results this study, carried out in collaboration with the group of Dr. Stefania Ruiu of CNR-Institute of Translational Pharmacology of Cagliari, aimed to:

1. Isolate the secondary metabolites that were responsible of the observed binding affinity
2. Identify the compounds by spectrometric and spectroscopic methods
3. Evaluate the binding affinity of the isolated metabolites to opioid and cannabinoid receptors.
4. Evaluate the most potent and abundant compounds in antinociceptive experiments in mice.

Table 1. K_i values of OME, SGE, WSE, and WSAE extracts for opioid, cannabinoid, $GABA_A$ receptors

	Receptor affinity (μg/ml)					
Extract	**μ**	**δ**	**k**	**CB_1**	**CB_2**	**$GABA_A$**
OME	10 ± 0.7	8.5 ± 1.3	-	2.2 ± 0.9	1.3 ± 0.3	-
SGE	10.3± 0.2	9.0 ± 1	-	-	-	-
WSE	385 ± 14	166 ± 11	775 ± 56	837 ± 74	>1000	13 ± 2
WSAE	60 ± 7	25.5 ± 6	700 ± 120	23.5 ± 1	20.3 ± 2	14 ± 0.5

Results are mean ± SEM of four independent experiments assayed in triplicate.

5. METHODOLOGY OF ISOLATION PROCEDURE

The isolation of a natural product can be divided into three main stages: extraction, fractionation, and purification.

5.1 Extraction

The first stage of the isolation procedure is the release of compounds from the cell mass and the removal of bulk of the biomass. Most of the bulk of biomass exists as fairly inert, insoluble, and often polymeric material, such as the cellulose of plants. The first step of the extraction is to release and solubilize the smaller secondary metabolites by a thorough extraction with an organic solvent or water. This can be done by a series of of stepwise extractions, using solvents of varying polarity, which acts as the first fractionation step, or by using a single solvent such as methanol, which should dissolve most natural products.

5.2 Fractionation

The second stage, the fractionation, consists to remove the most part of the unwanted material and to obtain a crude separation of the compounds mixture. Such step may involve vacuum liquid chromatography and liquid-liquid extractions.

5.3 Vacuum Liquid Chromatography (VLC)

VLC is a very convenient and simple chromatograpy method that is able to produce good resolution in short time. This technique involves the use of reduced pressure to increase the flow rate of the mobile phase through a short bed of stationary phase: most of the stationary phase could be used (silica gel, reversed phase material or aluminium oxide) and the technique is applicable to large scale separations. The advantage of this procedure includes its simplicity of equipment, low cost of operation and low solvent consumption, as well as the speed of separation. The disadvantage is that the resolution is only moderate.

5.4 Purification

The purification is the last step and consists in a high-resolution separation giving a single pure compound. This procedure involves

chromatographic techniques such as open column chromatography and High Performance Liquid Chromatography.

5.5 Open Column Chromatography

The gravity-driven open column chromatography method is still widely used in natural product chemistry, as it reprsents a rapid and efficent techiques to obtain pure compouds. The separation is based on differential partitioning between the mobile and stationary phases. Subtle differences in a compound's partition coefficient result in differential retention on the stationary phase and thus changing the separation. The main advantage of column chromatography is the relatively low cost and disposability of the stationary phase used in the process. The most used stationary phase is silica gel. The chemical nature of the surface of silica gel consists of exposed silanol groups. These hydroxyl groups are the active centers and potentially can form strong hydrogen bonds with compounds being chromatographed. Thus, in general, the stronger the hydrogen-bonding potential of a compound, the stronger it will be retained by silica gel, so that polar compounds are strongly adsorbed, while non-polar molecules are poorly or non-retained on silica gel. Other stationary phases are aluminium oxide, reversed phase (RP) and Sephadex.

5.6 High Performance Liquid Chromatography

Preparative High Performance Liquid Chromatography (HPLC) is a versatile and widely used technique for the final purification of natural compound. The main difference between HPLC and other models of column chromatography is that the diameter of the stationary phase particles is comparatively low (3-10 μm) and these particles are tightly packed to give a very uniform column bed structure. The low particle diameter means that a high pressure is needed to drive the eluent through the bed. However, because of the very high total surface area available for interations with solutes, the resolving power of HPLC is very high.

6. METHODOLOGY OF STRUCTURE ELUCIDATION

6.1 Nuclear Magnetic Resonance Spectroscopy

The process of structural determination involves the accumulation of data from numerous sources, each giving some structural informations. All the available structural informations have to be assimilated into a chemical structure that rigorously fits all the parameters.

Of all modern methods for structure elucidation, Nuclear Magnetic Resonance (NMR) Spectroscopy, provides the most complete information, with or without prior structural knowledge. When a single radiofrequency pulse of a few microsecond duration is applied to atoms that in nature possess a non zero spin quantum number as ^{1}H or ^{13}C, their nuclei has been excite and results in the emission of a signal knows as free induction decays (FID). Fourier transformation of this decay yelds the NMR spectrum.

In the **^{1}H NMR** spectrum we observe different resonance lines that rapresent the chemical shift interaction for the protons in different position in a molecule. Thus it is a convenient method for the determination of the chemical shift of each resonance calculated

from their integrated intensities. Where the multiplicity and the coupling pattern of a signal is interpretable, the number and the stereochemical orientation of adjacent protons can be proposed as well.

The **^{13}C NMR** spectrum provides important structural information, since it arises directly from the nuclei that form the framework of the organic molecules. The normal ^{13}C spectrum is acquired with full proton decoupling: in the absence of coupling to ^{1}H nuclei, all of the ^{13}C signals in the spectrum appear as single lines, allowing the number of carbons in the molecule to be readly determined. The ^{13}C spectrum also confirms the presence of quaternary carbons but multiplicity cannot be estabilished.

The number of hydrogens bonded to each carbon can be detected by **DEPT** experiment: **DEPT 135** shows all protonated carbon signals, with CH_3 and CH resonance being positive, while CH_2 signals are negative. To distinguish CH_3 from CH, DEPT 90 is used: in this experiment only CH gives a signal, while carbons with all other substituition patterns are not detected.

The Attached Proton Test (**APT**) experiment is another way to assign C-H multiplicities in ^{13}C NMR spectra. It provides the information on all sorts of carbons within one experiment. Depending on the number of hydrogens bound to a carbon atom, n, CHn spin vectors evolve

differently after the initial pulse: CH and CH_3 vectors have opposite phases compared to quaternary caarbons and CH_2.

Two dimensional NMR spectra are obtained by recording a series of 1D spectra differing only by a time increment. They could be divided into two groups: homonuclear and heteronuclear methods.

Within the homonuclear experiments, **DQF-COSY** (Double Quantum Filtered COrrelation Spectroscopy) shows vicinal and geminal protons correlated via scalar coupling.

The Nuclear Overhauser Effect (NOE) allows the identification of those nuclei within a molecule that are close in space. A 2D NOE experiment (**NOESY** or **ROESY**) therefore provides information on the three dimensionl molecular structure, hence the relative sterochemistry of the molecule.

Heteronuclear experiments are used in the form of **HSQC** (Heteronuclear Single Quantum Coherence) to assign the protons to their attached carbons. **HMBC** (Heteronuclear Multiple Bond Correlations) provides a wealth of structural information by the ability to identify ^{1}H-^{13}C correlations across carbon-carbon or carbon-heteroatom linkages.

6.2 Mass Spectrometry

Mass spectrometry (MS) is an analytical technique that produces spectra of the masses of the atoms or molecules comprising a sample of material. Mass spectrometry works by ionizing chemical compounds to generate charged molecules or molecule fragments and measuring their mass-to-charge ratios.

The ions are detected by a mechanism capable of detecting charged particles. Signal processing results are displayed as spectra of the relative abundance of ions as a function of the mass-to-charge ratio. The atoms or molecules can be identified by correlating known masses to the identified masses or through a characteristic fragmentation pattern.

A standard method is Electrospray Ionization Mass Spectrometry (**ESI MS**) that is typically used to determine the molecular weights of a wide range of molecules. Soft ionization is a useful technique when considering biological molecules of large molecular mass, such as the aformetioned, because this process does not fragment the macromolecules into smaller charged particles, rather it turns the macromolecule being ionized into small droplets. These droplets will then be further desolvated into even smaller droplets,

which creates molecules with attached protons. These protonated and desolvated molecular ions will then be passed through the mass analyzer to the detector, and the mass of the sample can be determined.

The High Resolution Electrospray Ionization Mass Spectrometry (**HR ESI MS**) allowed the determination of the exact molecular mass.

7. BIOLOGICAL EXPERIMENTS

7.1 Binding Assay

The main parameters that characterize a drug interaction with its specific interaction sites are generally determined through binding studies. Execution of binding studies involves incubation of a preparation containing the receptor, whether or not purified, with a ligand of this receptor, marked with a radioactive isotope. During the incubation period, a portion of the labeled ligand give, with a certain amount of receptor, the complex ligand-receptor. At the end of incubation, the portion of free ligand is separated from the complex. The most widely used method is to filter the sample at the end of incubation over glass fiber filters; cells (or membranes) and therefore the receptor therein contained, are retained by the filter, while the free ligand passes through it. The radioactivity of bound labeled ligand collected on the filters is counted; for β ray emitting isotopes e.g., ^{3}H-labeled ligands, the filters are dried, liquid scintillation fluid is added and radioactivity is counted in a liquid scintillation counter.

7.2 Tail Flick Test

The tail flick test is a test of the pain response in animals. It is used in basic pain research and to measure the effectiveness of analgesics, by observing the reaction to heat. A light beam is focused on the animal's tail and a timer starts. When the animal flicks its tail, the timer stops and the recorded time (latency) is a measure of the pain threshold.

7.3 Hot Plate Test

The hot plate test is another test of the pain response in animals, similar to the tail flick test. It is a behavioral model of nociception where behaviors such as jumping and hind paw-licking are elicited following a noxious thermal stimulus. Licking is a rapid response to painful thermal stimuli that is a direct indicator of nociceptive threshold. Jumping represents a more elaborated response, with a latency, and encompasses an emotional component of escaping. A transparent glass cylinder is used to keep the animal on the heated surface of the plate.

The temperature of the hot plate is set using a thermoregulated water-circulated pump.

The time of latency is defined as the time period between the zero point, when the animal is placed on the hot plate surface, and the time when the animal licks its paw or jumps off to avoid thermal pain.

8. *OTHANTUS MARITIMUS*

8.1 Botanical decription

Otanthus maritimus (L) Hoffmanns. & Link (Figure 9) is an evergreen chamaephyte plant belongs to the family of the Asteraceae and is the only species of the monotypic genus *Otanthus.*[62] It looks like a bushy plant 10-50 cm tall, with dense, silvery-white fluff with numerous woody stems at the base and hardened at the top. The plant possesses an effective adaptation to resist aridity and the direct sunlight.[63]

Figure 9. *O.maritimus*

The leaves are oblong or spatulate, sessile, obtuse, finely toothed. View spherical flower heads, 8-10 mm diameter, with short pedicles gathered to form corymbs at the top of the branches. Scarious bracts are present on the edge. The flowers (Figure 10) are yellow tubular shaped with two wings at the base. The fruit is an achene 4 mm curved. Flowering occurs between June and September.

Figure 10. Flowers of *O. maritimus*

8.2 Geographical Distribution and Habitat

O. maritimus is distributed along the European coasts of Atlantic and Mediterranean sea (Figure 11). It is a species related to the sandy beaches characterising with its silvery-white small bushes, growing especially at the shoreline and dunes at first colonizing with a long, deep root and with branches partly covered by sand.[63]

Figure 11. Areal of *O. maritimus*

O. maritimus may be considered very important in the consolidation of the dunes thanks to its impressive development of underground apparatus. The gradual degradation of coasts is drastically reducing the spread of this species.

8.3 Use in Folk Medicine

In traditional medicine *O. maritimus* is used to treat asthmatic bronchitis, dysentery and inflammation of the urinary bladder.[64]

8.4 Chemical Composition

The roots of *O. maritimus* contain fatty acid amides (Figure 12)[65], acetylene derivatives[65] (Figure 13), monoterpenes (Figure 14) and sesquiterpenes[66] (Figure 15), while from the aerial parts amides[67] (Figure 16) sesquiterpene lactons[68] (Figure 17), monoterpenes (Figure 18)[68,69], and lignanes[67] (Figure 19), have been isolated.

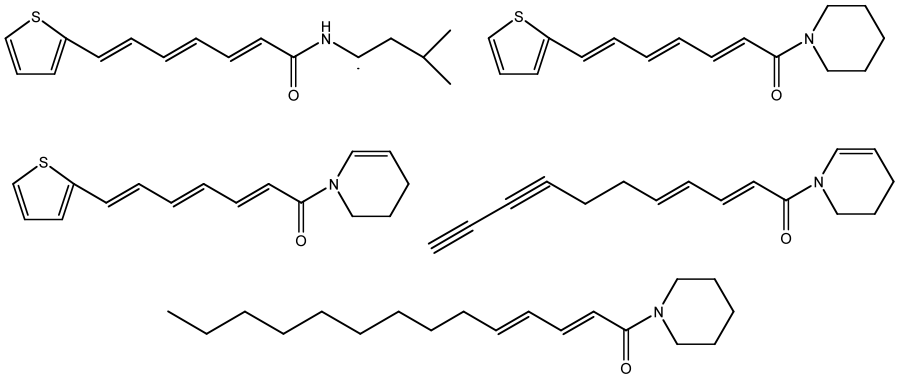

Figure 12. Fatty acid amides isolated from the roots of *O. maritimus*

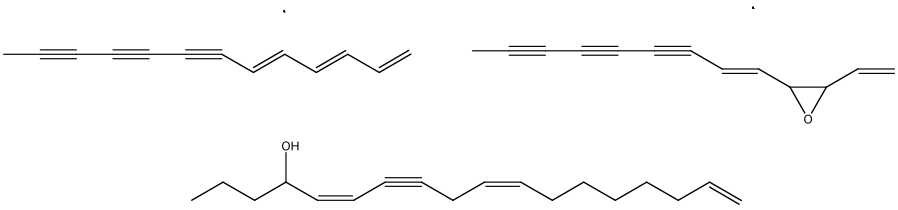

Figure 13. Acetylenes isolated from the roots of *O. maritimus*

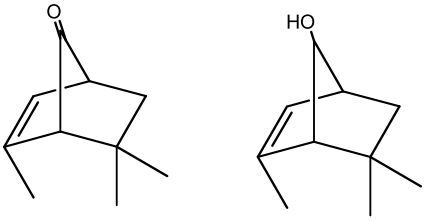

Chrysanthenone Chrysanthenol

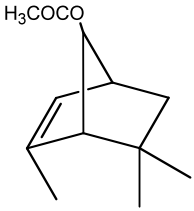

Chrysanthenol acetate

Figure 14 . Monoterpens isolated from the roots of *O. maritimus*

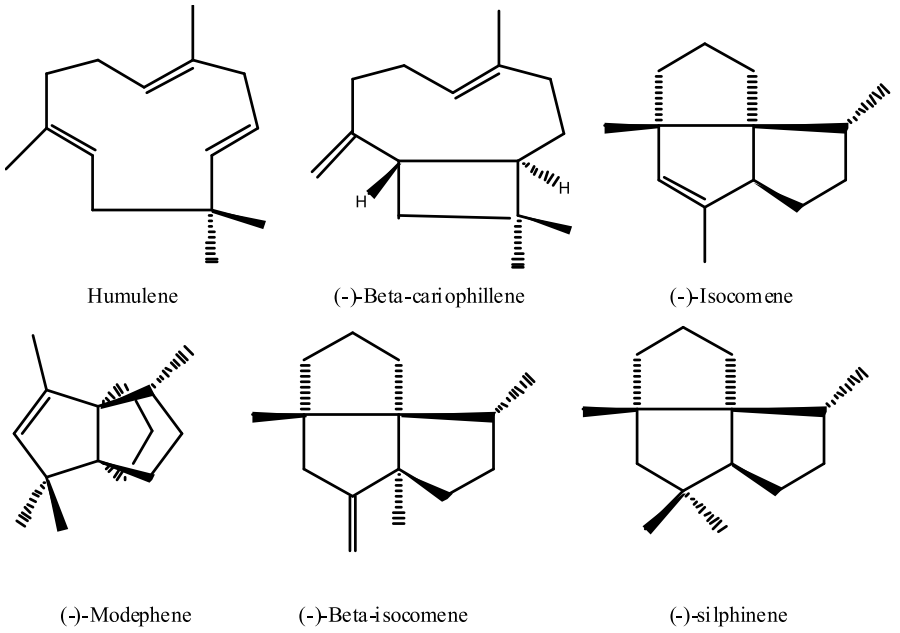

Figure 15. Sesquiterpens isolated from the roots of *O. maritimus*

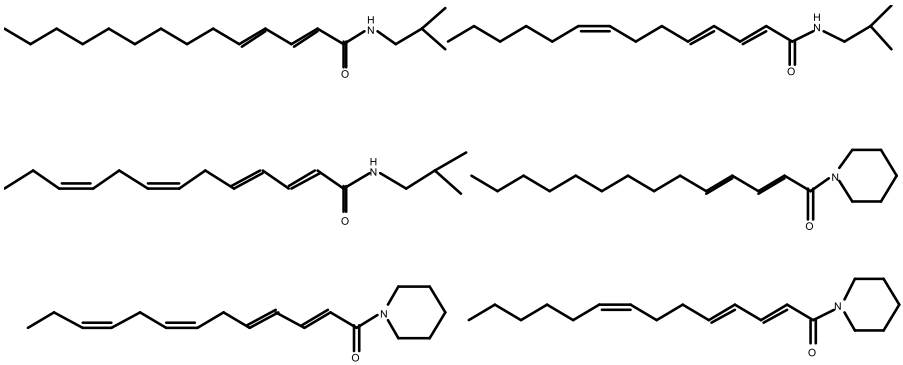

Figure 16. Amides isolated from the leaves of *O. maritimus*

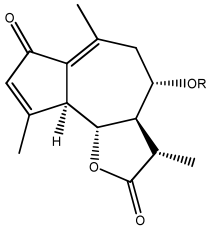

A a-d

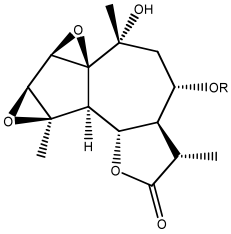

B a-d

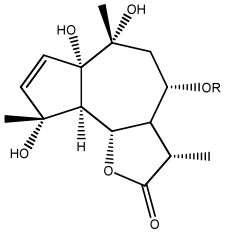

D a-d

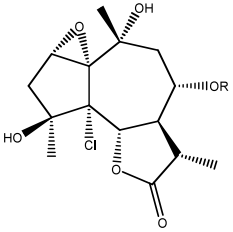

E a-d

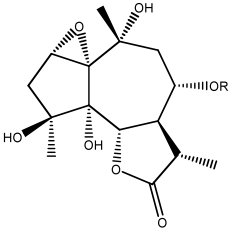

F a-d

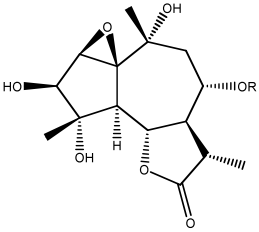

G a-f

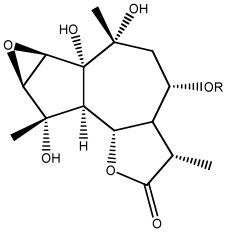

H a-d

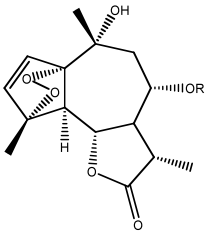

I a-d

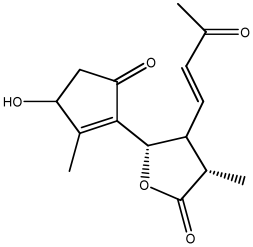

J

A a-I a R=Ang. A b-I b R=i-but. A c-I c R=i-val. A d-I d R=met-but G e R=prop
G f R=8-desacyloxy-11,13-dehydro G g R=ang; 3-OAc G h R=Ang; 10-OAc G i R=Ang; 3,10-OAc

Figure 17. Sesquiterpens lactones isolated from the leaves of *O. maritimus*

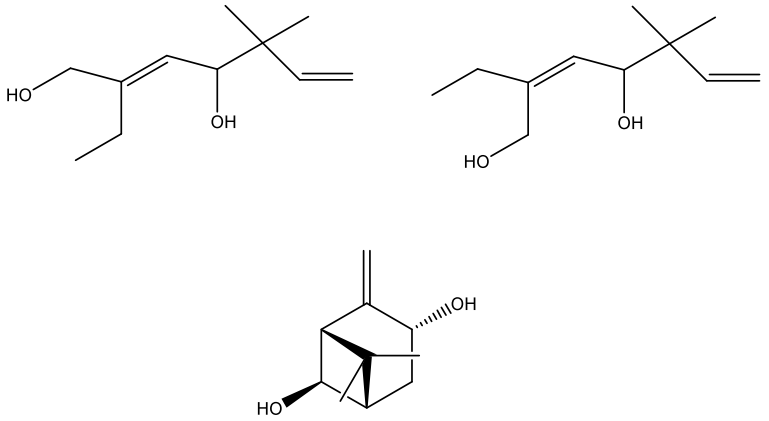

Figure 18. Monoterpens isolated from the leaves of *O. maritimus*

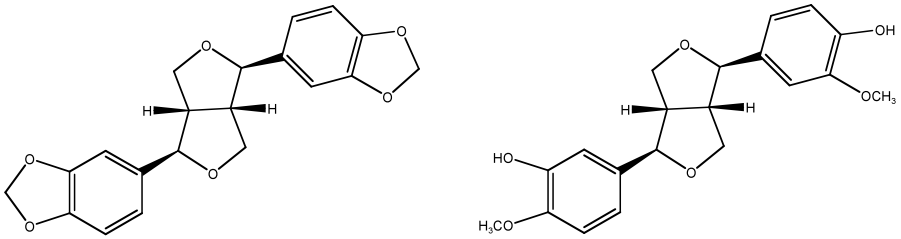

Saesamin Pinoresinol

Figure 19. Lignanes isolated from the leaves of *O. maritimus*

8.5 Biological Actvity of N-alkylamides

Certain alkylamides such as dodeca-2*E*,4*E*-dienoic acid isobutylamide and dodeca-2*E*,4*E*,8*Z*,10*Z*-tetraenoic acid isobutylamide (Figure 20) have been identified as the main active principles of *Echinacea purpurea* and *Echinacea angustifolia* preparations[5,71] that are remedies widely used for the prevention and treatment of common cold, bronchitis and coughts.[72]

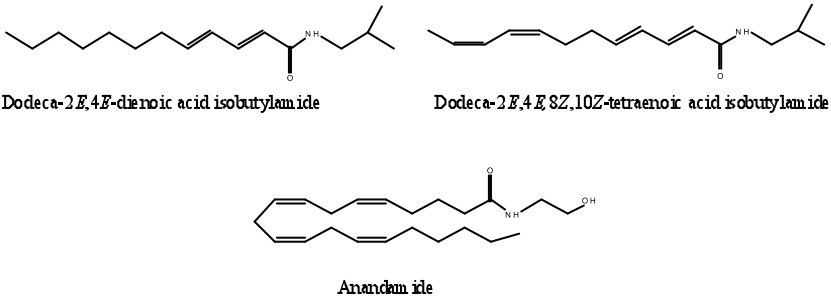

Figure 20. Chemical structures of *Echinacea* alkylamides and anandamide

Raduner and co-workers[5] demonstrated that the above mentioned alkylamides were able to act as full agonist at CB2 receptor in a nanomolar range showing a higher selectivity *versus* CB2 compared with CB1 receptors.

It has been postulated that the affinity of the alkylamides to CB receptor is due to their structural similarity with the endogenous cannabinoid anandamide (Figure 20). Alkylamides also showed to inhibit the fatty acid amidohydrolase (FAAH) and thereby able to enhance the activity of CB1 and CB2 ligands.[71] Again dodeca-2*E*,4*E*-dienoic acid isobutylamide and dodeca-2*E*,4*E*,8*Z*,10*Z*-tetraenoic acid isobutylamide elevated total intracellular Ca^{2+} in CB_2-positive but not in CB2-negative promyelocitic HL 60 cells[5].

This effect of dodeca-2*E*,4*E*-dienoic acid isobutylamide and dodeca-2*E*,4*E*,8*Z*,10*Z*-tetraenoic acid isobutylamide was blocked by treatment of the cells with SR144528, indicating that the effect of these compounds is mediated through the CB2 receptor[5]. Furthermore, it has been demonstrated that alkylamides are the only *Echinacea* compounds that after oral administration showed high bioavailability.[73-75] All this data highlight that the immunomodulatory effect of *Echinacea* could be connected to the interactions of alkylamides with the CB2 receptors.

Most of the isolated alkylamides of *O. maritimus* roots belongs to the class of the very unusual thienylheptatrienamides. In particular, no biological activity for these compounds have been reported in the literature, apart a study regarding an insecticidal effect.[67]

STACHYS GLUTINOSA

9.1 Botanical Decription

The plant, belonging to the family of Lamiaceae, looks like a densely branched frutex woody at the base, forming a hemispherical high bush until 50 cm; the look is thistly due to previous years branches that may persist for years buckets (Figure 21). Characteristic are the tetragon branches of the year and persistent unpleasant odor emanated from the same hence the adjective *"fetid"* associated with the common name.

Figure 21. *Stachys glutinosa* L.

The leaves are opposite and sessile with linear lanceolate or scrape leaf, around 4 cm length and few millimetres width, ruffled margin. The top page is glabrous and bottom covered with glandular trichomes in part.

Figure 22. Leaves and flowers of *S.glutinosa* L.

The flowers (Figure 22) are grouped, supported by long pedicels and calyx preceded by linear bracteoles. The tube-shaped and regular calyx ends with 5 teeth sharp; the corolla, typical of the Lamiacae, is symmetric and gamopetalous with lower lip longer than above, pubescent and very clear colour: white, pink, violet. The stamens are four with filaments inserted in corolla; the ovary is bicarpellary with stylus sandwiched between carpels. The long flowering and climbing, lasts from spring until autumn.[76]

9.2 Geographical Distribution and Habitat

S. glutinosa is a xerophilous plant that adapts to dry and sunny soils, typically beaten from strong winds with acidic or calcareous matrix. It does not tolerate shading, so its presence is sporadic in high scrub or forest; is found easily in reduced and rocky slopes. Characteristic of the plant is fire resistance as it is able to push through radical to fast-

growing suckers. *S. glutinosa* is an endemic shrub of Sardinia, Corsica and Capraia islands that grows on different substrata[77].

9.3 Use in Folk Medicine

The decoction produced from the leaves of *S. glutinosa* was used as an antispasmodic and antiseptic[78-80] while the whole plant was used as an insect repellent to ward off mallophaga (lice chickens).[81]

9.4 Chemical Composition

To date there are few works in the literature regarding chemical and biological studies *S. glutinosa*. Three articles reported the chemical composition of the essential oil and its antibacterial and antiviral activity.[82-84]

In only one work is reported the isolation of non-volatile components belonging to the class of iridoids from the aerial parts of *S. glutinosa* (Figure 23).[85]

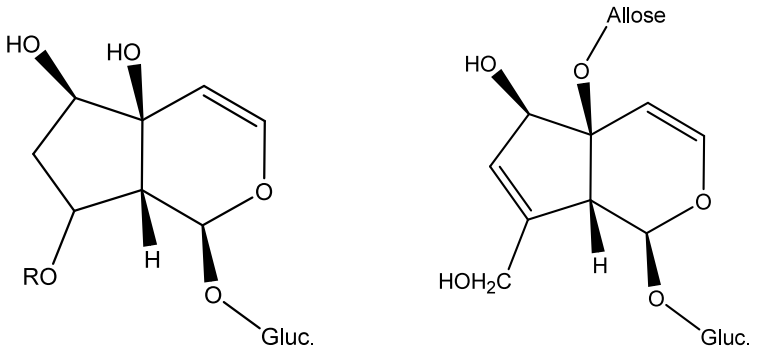

R=H : Arpagide

R=AcO : Acetil-arpagide

5-Allosil-aucubin

Figure 23. Iridoids from *S.glutinosa*

9.5 The Phytochemical Investigation on Genus *Stachys*

9.5.1 Diterpenes

Phytochemical studies of members of the genera *Stachys* have led to the isolation of a number of neo-clerodane and labdane diterpenoids (Figure 24).

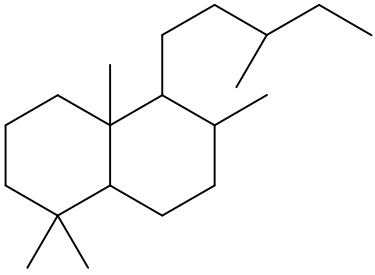

Labdanes

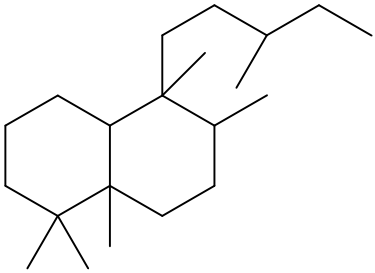

Clerodanes

Figure 24. Labdane and clerodane carbon skeleton

Both classes have been receiving increasing interest for their biological activities and especially as antifeedant, antimicrobial and cytotoxic agents.[86-88]

The first report of a diterpenoid from genus *Stachys* was from a Moldavia species, *S. annua.* Moldavian researchers[89,90] reported the occurrence of stachysolone (Figure 25) and its three acetylderivatives isolated from the aerial parts. The same compounds were also isolated from the aerial parts of *Stachys recta*[91] and *Stachys aegyptiaca.*[92]

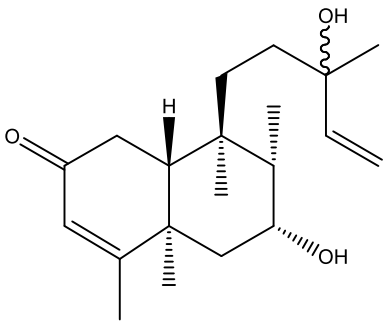

Figure 25. Structure of stachysolone

Continuing the investigation of *S. annua*, three further diterpenoids were isolated, annuanone, stachylone and stachone[93-95] (Figure 26) and they were later detected in several other species of *Stachys* of the flora of Ukraine[96].

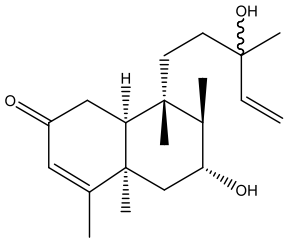

Annuanone

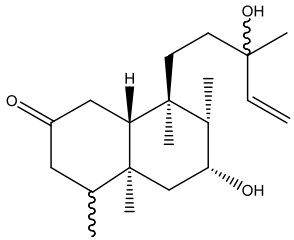

Stachylone

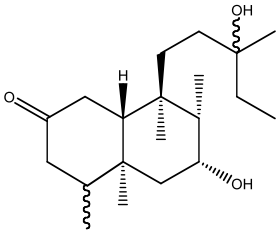

Stachone

Figure 26. Structures of annuanone, stachylone and stachone

A species collected in Cyrenaica, *Stachys rosea*, yielded two new neoclerodane diterpenoids, roseostachenone and roseostachone[97] A reinvestigation of the plant[98] led to the isolation of two new neoclerodanes, roseostachenol and roseotetrol (Figure 27).

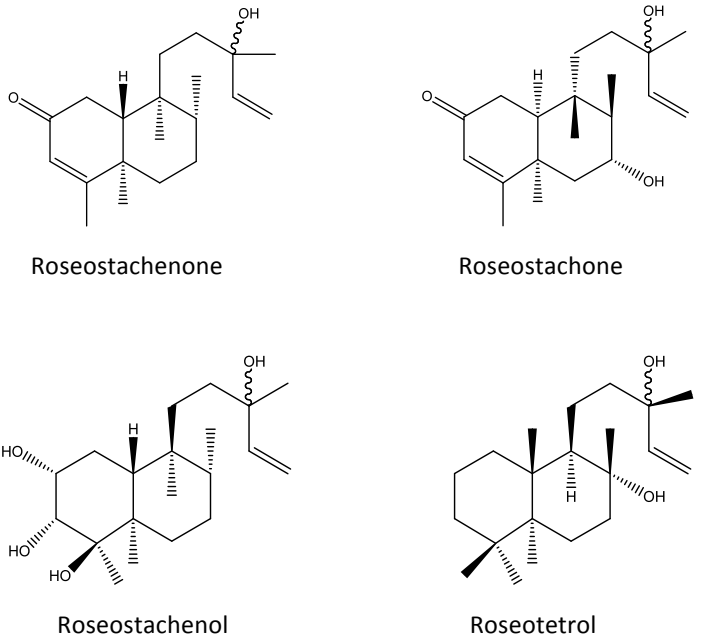

Roseostachenone Roseostachone

Roseostachenol Roseotetrol

Figure 27. Structure of roseostachenone, roseostachone, roseostachenol and roseotetrol

The pytochemical study of *Stachys mucronata*, collected in the island of Karpathos (Greece), gave two labdane diterpenoids, ribenone and ribenol (Figure 28).[99] Both products had been isolated from other plants. In literature many works reported these compounds as possible anti-tumor promoters[100-102] but also as antibacterial.[103]

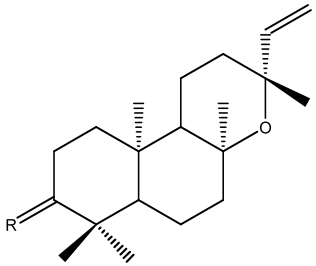

R=O Ribenone
R= α-OH Ribenol

Figure 28. Structure of ribenone and ribenol

The species *S. plumosa*, native of the Balkan peninsula, yielded three new labdane diterpenoids: (+)-6-deoxyandalusol, (+)-13-epijabugodiol, (+)-plumosol (Figure 29).[104]

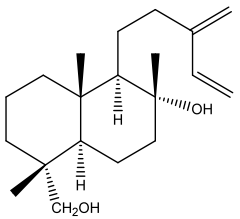

(+)-6-Deoxyandalusol

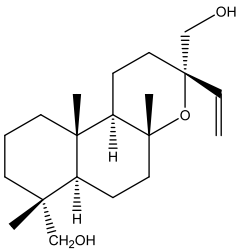

(+)-13-Epijabugodiol

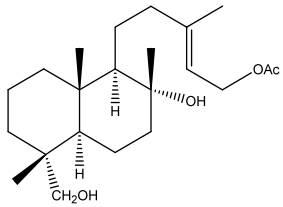

Plumosol

Figure 29. structures of (+)-6-deoxyandalusol, (+)-13-epijabugodiol, (+)-plumosol

Other compounds isolated from *S. rosea* were 13-epi-sclareol (Figure 30), which showed activity against Leishmania spp., as well as ribenone and ribenol.[105-107]

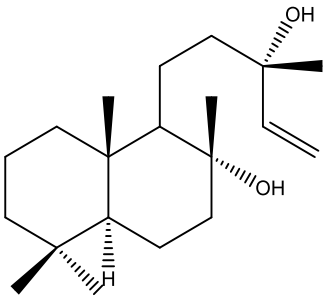

Figure 30. Structure of 13-epi-sclareol

10. *WITHANIA SOMNIFERA*

10.1 Botanical Description

W. somnifera (L.) Dunal also known as, Ashwaganda or indian ginseng, is a green shrub belonging to the family of Solanaceae. This species is 35 to 75 centimeters tall and possesses tomentose branches extend radially from a central stem. The flowers are small and green. The ripe fruit is orange-red. Roots are 20-30 cm long and 6-12 mm in diameter, with a few (2 to 3) lateral roots of slightly smaller size (Figure 31). Outer surface is buff to gray-yellow with longitudinal wrinkles and in the center soft, solid mass with scattered pores. The taste is bitter and acrid. The ripe fruit is orange-red.[108]

10.2 Geographical Distribution and Habitat

W. somnifera is found in many of the dry regions of India, such as Mandsaur district of Madhya Pradesh, Punjab, Sindh, Gujarat and Rajasthan. It is also found in Pakistan, Nepal, Afganistan, Sri Lanka, Congo, South Africa, Egypt and Morocco.[109]

Figure 31. *W. somnifera* leaves, fruits , flowers

10.3 Use in Folk Medicine

Ashwaganda holds a place in Ayurveda similar to that of Ginseng in Chinese medicine. It is reputed to be capable of imparting long life, youthful vigour and intellectual prowess and is an ingredient of many traditional preparations. The name Ashwaganda comes from the smell of horses, which the root (Figure 32) emits, and the botanical suffix somnifera from the use of the plant as a sedative The plant is used to to treat various neurological disorders, geriatric debilities, arthritis, stress and behavior-related problems.[110,111] In the traditional system of medicine Ayurveda, this plant is claimed to have potent aphrodisiac, rejuvenative and life prolonging propreties. It improves learning ability and memory capacity.[112,113]

Figure 32. *W. somnifera* roots

10.4 Pharmacological Studies of W. *somnifera* Extracts

Pharmacological studies have shown that *W. Somnifera* extracts have anticancer, antianxiety, antiinflammatory, immunomodulatory, adaptogenic, cardiovascular, free radical scavenging and central nervous system activities.[114] Among the central nervous system activities of *W. somnifera*, the action on neurodegenerative disorders have been well documented. In particular, *W. somnifera* preparations have shown beneficial effects against Huntington's[115], Alzheimer's[116], and Parkinson's diseases.[117]

W. somnifera root extract is widely used to reduce symptoms of anxiety and stress and these effects have been demonstrated in a study that showed a trend for the anxiolytic superiority of *W. somnifera* over placebo at week 2, and statistically significant superiority at week 6 in patients with anxiety disorders.[118]

10.5 CHEMICAL COMPOSITION

10.5.1 Withanolides

The major constituents of the *W. somnifera* roots and leaves are a group of steroidal lactones called withanolides that have been considered exclusive of Solanaceae plants. Withanolides are a group of at least 300 naturally occurring chemical compounds and structurally, they consists of a C-28-steroidal skelelton in which C-22 and C-26 are appropriately oxidized to form a six-membered lactone ring .

In the roots 17-hydroxy-27-deoxy withaferin A, withanolide A and withanone have been identified as the major withanolides (Figure 33) while 27-hydroxy withanone, withaferin A, 17-hydroxy withaferin A, 27-hydroxy withanolide B and 27-deoxy withaferin A were detected as minor constituents (Figure 34).

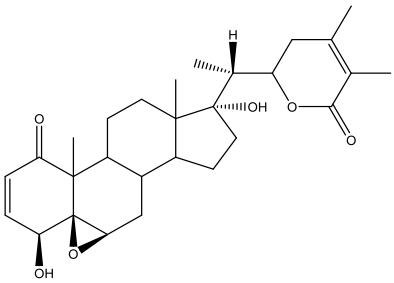

17-hydroxy-27-deoxy withaferin A

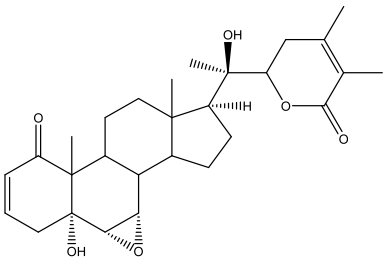

withanolide A

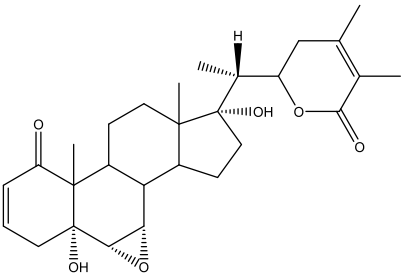

withanone

Figure 33. Main withanolides isolated from the roots of *Withania somnifera*

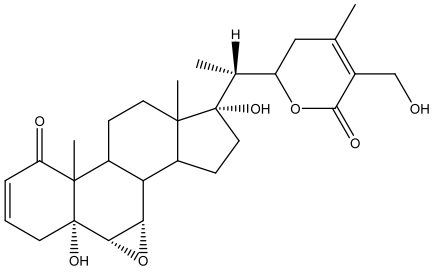

27-hydroxy withanone

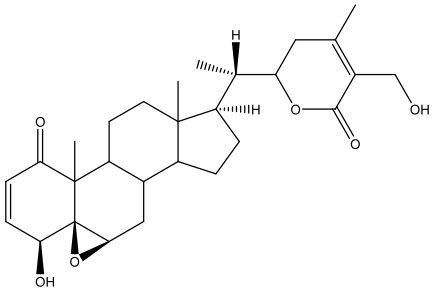

withaferin A

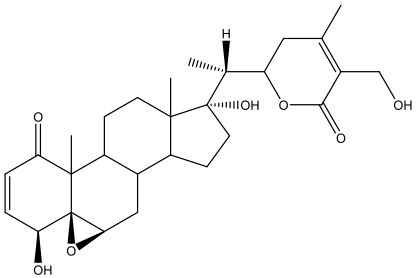

17-hydroxy withaferin A

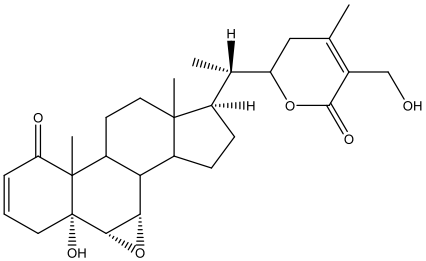

27-hydroxy withanolide B

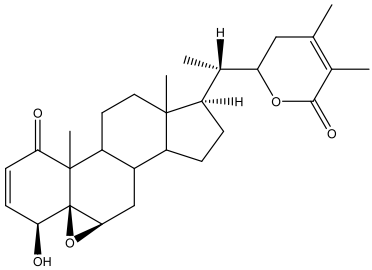

27-deoxy withaferin A

Figure 34. Minor withanolides from the roots of *Withania somnifera*

The withanolides composition of leaves differed only from a quantitative point of view with the exception of withanolide D (Figure 35) found only in the leaves. The minor withanolides of the leaves were 27-deoxy withaferin A and 27-hydroxy withanolide B (Figure 34) while all other seroidal lactones occurred substantially.[119]

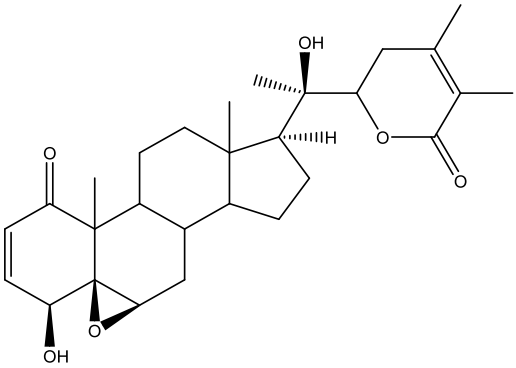

withanolide D

Figure 35. Structure of withanolide D isolated from the leaves of *Withania somnifera*

10.5.2 Alkaloids

In addition to withanolides, both leaves and roots contain relatively high amounts of alkaloids possessing a pyperidin, pyrrolidin or pyrazol ring. Up to now ten alkaloids have been isolated: D-L-isopelletierine, anaferine, hygrine, cuscohygrine, anahygrine, tropine, pseudotropine, 3alfa-tigloyloxytropane, withasomnine and coline[120,121] (Figure 36-37) Among the *W. somnifera* alkaloids, anaferine, has been found only in this plant (roots) and therefore can be considered a chemical marker for this species.

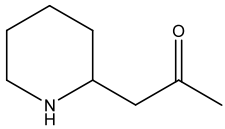

D,L-isopelletierine

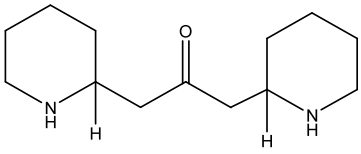

Anaferine

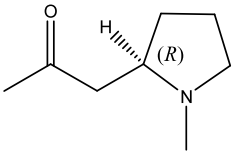

Hygrine

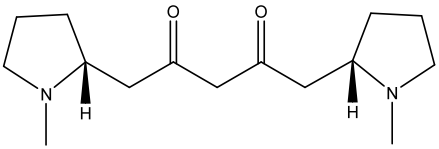

Cuscohygrine

Figure 36. Alkaloids isolated from *Withania somnifera*

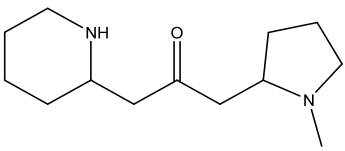

Anahygrine

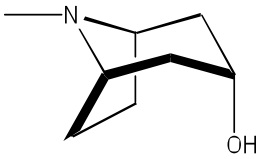

Tropina

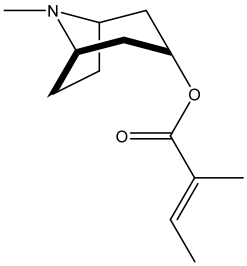

3 -α-tigloyloxytropane

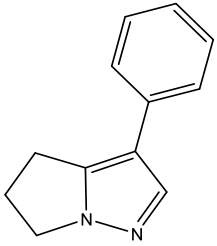

withasomnine

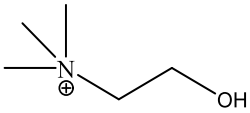

coline

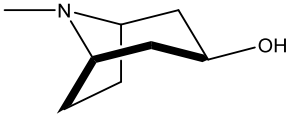

Pseudo tropine

Figure 37. Alkaloids isolated from *Withania somnifera*

10.5.3 Biological Activities of *Withania somnifera* Withanolides

The first compound of this group to be isolated was withaferin A, a highly oxygenated withanolide. Several studies indicated that withaferin A (figure 34) is one of the main biologically active withanolides, exerting a wide variety of activities, including anti-inflammatory, tumor preventive, cell death inducing, anti-tumor, radiosensitizing, as well as anti- angiogenic effects.[122] From a biological point of view, the others withanolids isolated from *W. somnifera* were much less studied respect to withaferin A and were mainly investigated as cytotoxic agents against cancer cells.[123]

In orden to justify the multiple targets of withaferin A (Figure 34), it has been postulated an acylation or alkylation of critical macromolecules or enzymatic active sites by covalent attachment.[124] These effects could be justified by at least three reactive position in the steroidal skeleton which might be involved in the alkylation reactions with nucleophilic sites like sulfhydryl groups of cysteine residues in target proteins. These include the double bond at C3 in A-ring, the epoxide moiety at position 5 and C-24 in its E-ring. These sites are potentially highly susceptible for nucleophilic attack, and by

Michael addition alkylation reaction, lead to a covalent binding of withaferin A with the target protein.[125]

The antiinflammatory, proapoptotic, antiangiogenic and anti-proliferative activities of withaferin A have been attributed to the inhibition of the transcription factor NF-kB,[126] of the members of the signal transducer and activator of transcription family (STAT1 and STAT3),[127] and to the activation the liver X receptor α (LXRα).[128]

Interestingly, withaferin A was also able to inhibit acetylcholesterinases and butyrylcholinesterases[129] justifing, at least in part, the positive effect of *W. Somnifera* exracts in the treatment of the neurodegenerative diseases such as Alzheimer's disease and related dementias.[130]

RESULTS

11. *OTHANTUS MARITIMUS*

11.1 Extraction of *O.maritimus* Roots

The powered dried roots of *O. maritimus* (780 g) were succesively extracted with DCM and MeOH yielding 23.9 g and 51 g , respectively. The extraction was carried out by percolation during the day and at night the roots were left to maceration.

11.2 Isolation of Metabolites from *O.maritimus*

The DCM extract showed significant binding affinity to CB1 and CB2 receptors and moderate affinity to μ and δ opioid receptors (Table 1) and was therefore subjected to fractionation by silica gel vacuum-liquid chromatography (VLC), column chromatography (silica gel and Sephadex LH 20) and semi-preparative NP (normal-phase) or RP (reversed-phase) HPLC to give two new thienylheptatrienamides namely (2*E*,4*E*,6*E*)-*N*-isopentyl-7-(2-thienyl)-2,4,6-heptatrienamide (**1**) and (2*Z*)-5-{[(2*E*,4*E*,6*E*)-7-(2-thienyl)-2,4,6-heptatrienoyl]amino}-2-pentenyl-3-methylbutanoate (**5**) (Figure 38), and one new neo-lignan 9-isovaleroxy balanophonin (**12**) (Figure 39), along with eight known

amides (**2**-**4**, **6**-**10**) (Figure 38), pontica epoxide (**11**), sesamin (**13**), puberulin (**14**), espeletone (**15**), and (2*Z*,6*E*,10*E*)-geranylgeraniol (**16**) (Figure 39).

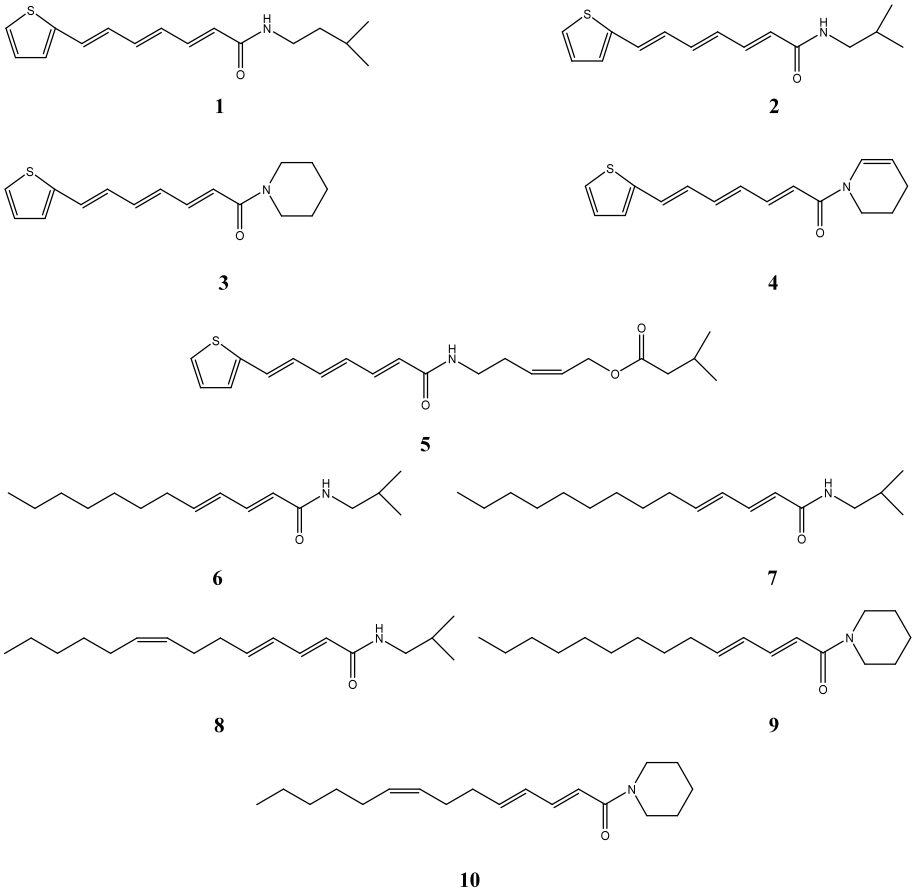

Figure 38. Isolated amides from *O. maritimus*

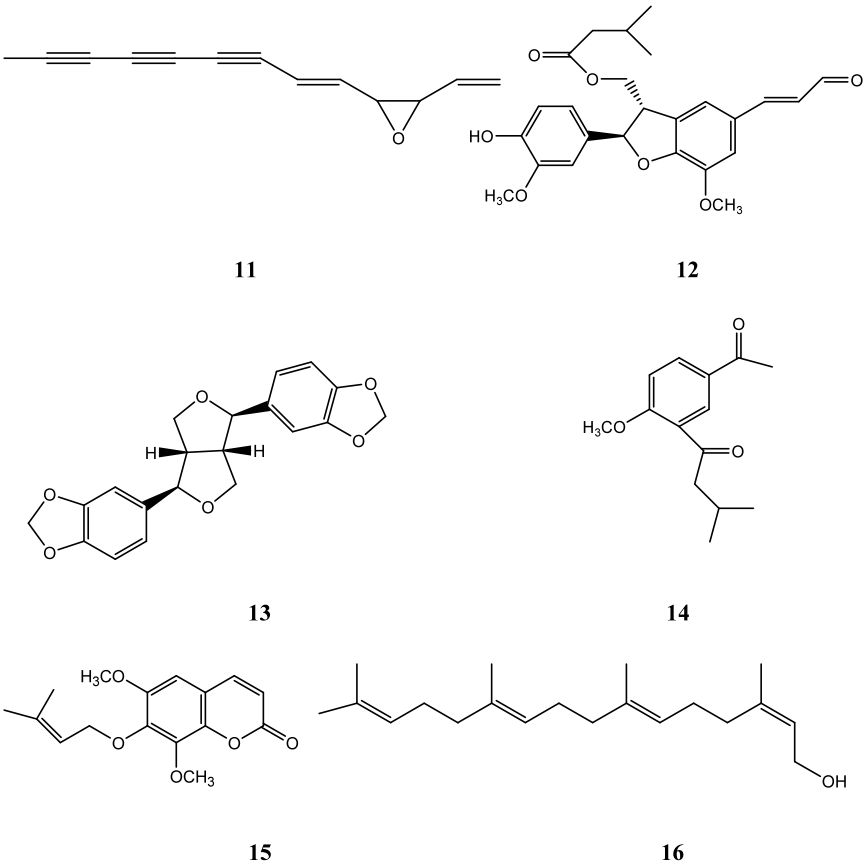

Figure 39. Other compounds isolated from *O. maritimus*

11.3 STRUCTURE ELUCIDATION OF METABOLITES FROM *O. MARITIMUS*

11.3.1 Structure Elucidation of Compound 1

The ESIMS and the HR-TOF-ESIMS of compound (**1**) showed the molecular ion peak at *m/z* 276 $[M + H]^+$ and 276.1408 (calc. 276.1417), respectively, accounting for the elemental composition of $C_{16}H_{21}NOS$, possessing seven degrees of unsaturation (Figure 40).

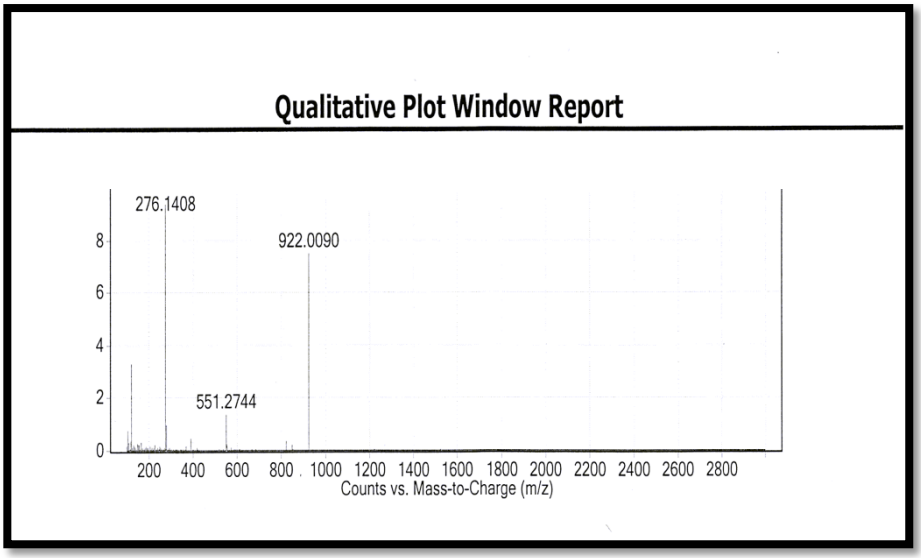

Figure 40. HR-TOF-ESIMS spectrum of **1**

The ^{1}H NMR spectrum of **1** suggested the presence of a conjugated trienamide by the presence of two doublet at δ_H 5.85 (*J* = 15 Hz, H-2) and 6.83 (*J* = 15 Hz, H-7) and four double doublet at 7.29 (*J* = 15, 10 Hz, H-3), 6.37 (*J* = 15, 10 Hz, H-4), 6.61 (*J* = 15, 10 Hz, H-5) and 6.65 (*J* = 15, 10 Hz, H-6) (Figure 41, table 2).

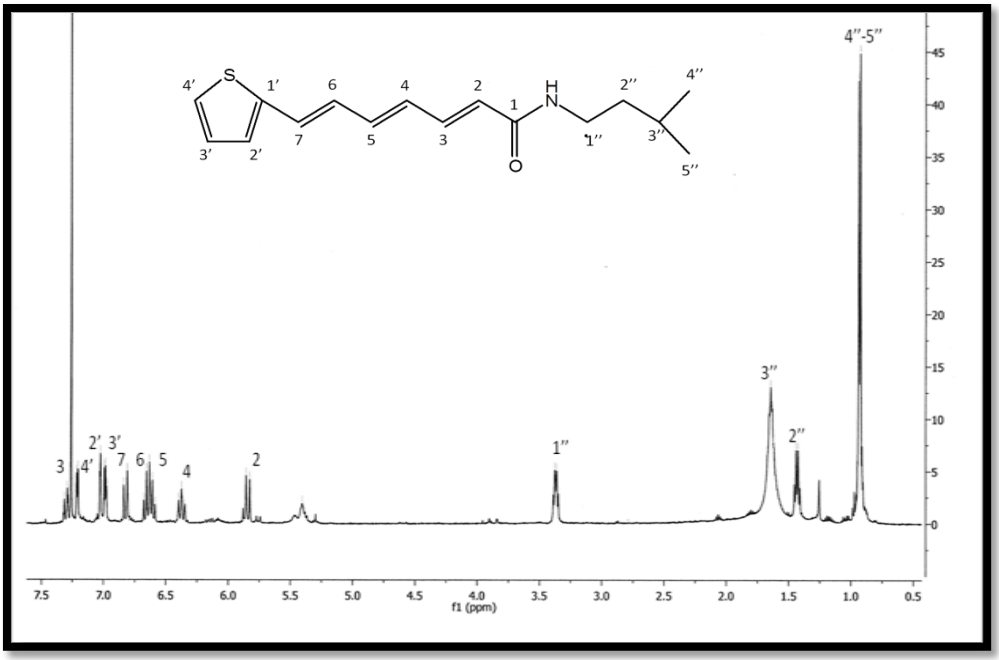

Figure 41. ^{1}H NMR spectrum (500 MHz) of compound **1** measured in $CDCl_3$

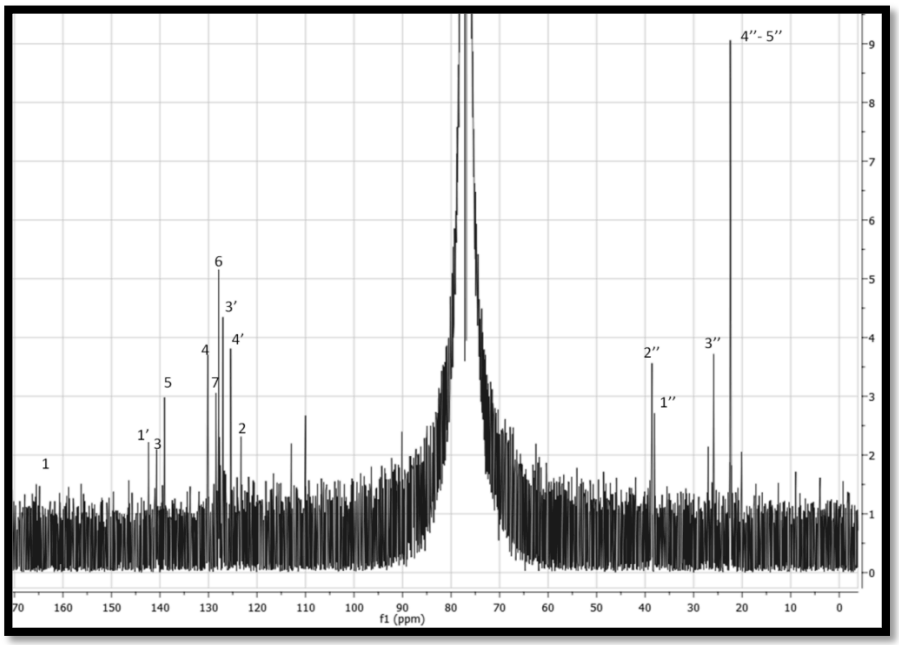

Figure 42. ^{13}C NMR spectrum (100 Mhz)of compound **1** measured in $CDCl_3$

The HSQC spectrum revealed the proton connectivities with the corresponding carbon (Figure 43).

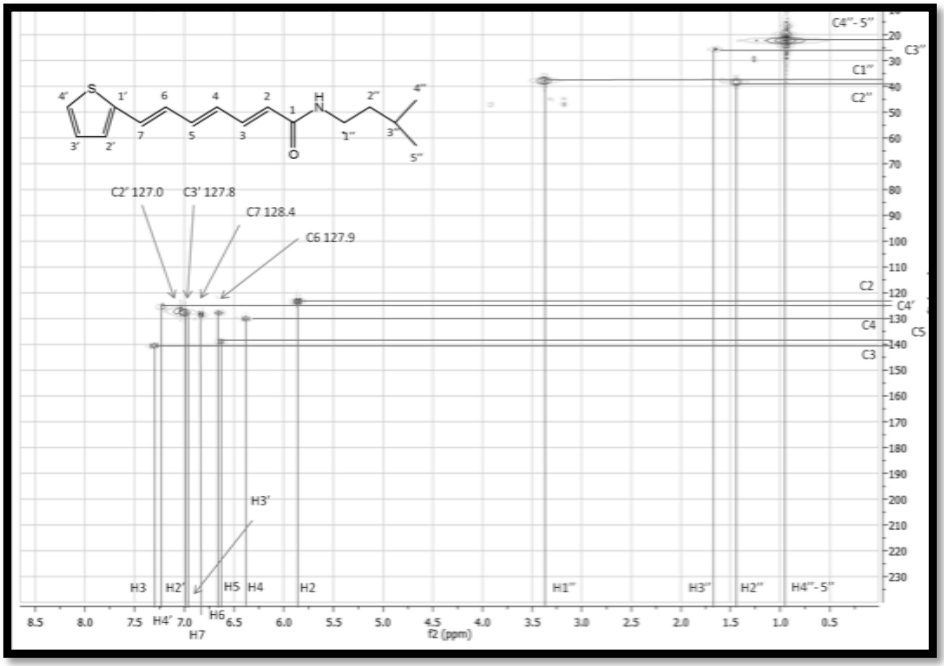

Figure 43. HSQC spectrum (500 MHz) of compound **1** measured in $CDCl_3$

The large coupling constants of the above mentioned protons, besides the HMBC correlations of the protons at 5.85 and 7.29 ppm with the carbonyl group at δ_H 166.0 ppm (Figure 44), clearly indicated the presence of *trans*-α, β, γ, δ, ε, ζ,- double bonds conjugated with a carbonyl group.

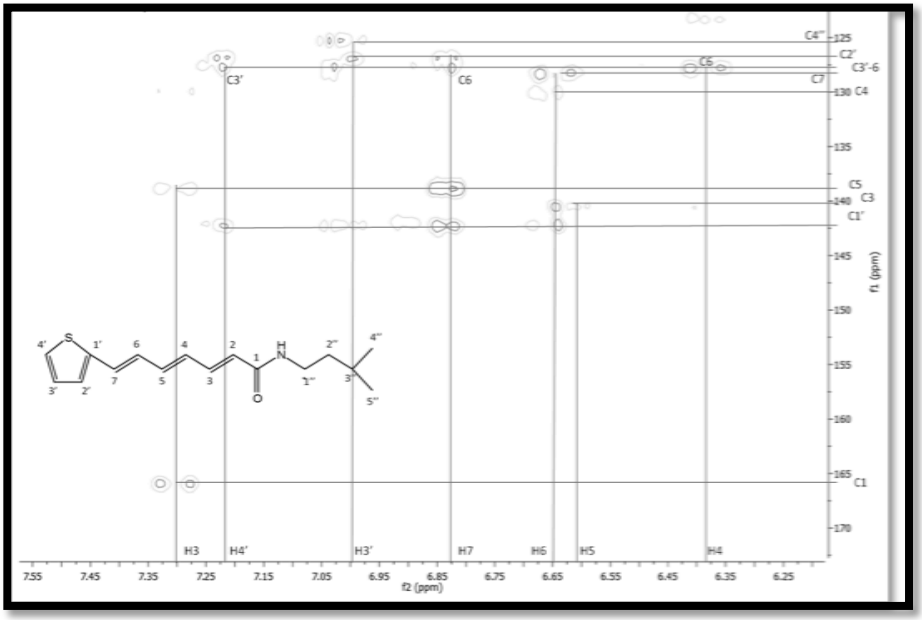

Figure 44. HMBC spectrum (500 MHz) of compound **1** measured in $CDCl_3$

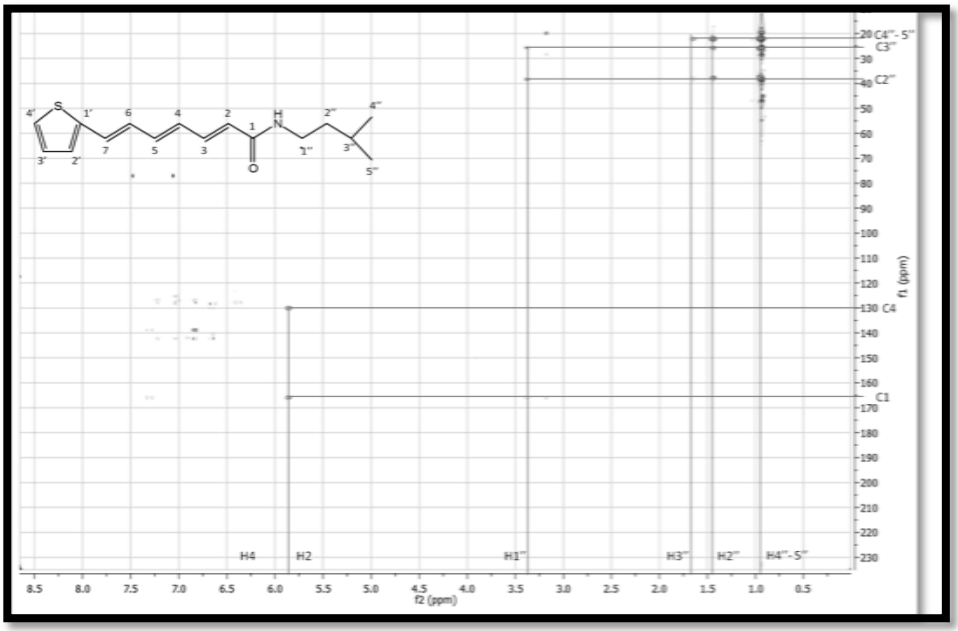

Figure 45. HMBC spectrum (500 MHz) of compound **1** measured in $CDCl_3$

The ^{1}H NMR spectrum revealed three further protons at δ_H 7.20 (1H, d, *J* = 5 Hz), 7.02 (1H, d, *J* = 5 Hz), and 6.98 (1H, dd, *J* = 5, 3.5 Hz) characteristic of a 2-thienyl moiety[131]. The connectivity of the sulphur heterocycle with the trienamide chain was confirmed by HMBC correlations between H-7 (δ_H = 6.83) and C-1′ (δ_C = 142.3) and C-2′ (δ_C = 127.0), and between H-6 and C-1′ (Figure 45). A quartet in the ^{1}H NMR spectrum at δ_H 3.37 (*J* = 5 Hz, H-1″), two multiplet at δ_H 1.43 (H-2″) and 1.64 (H-3″), and a six-proton doublet at 0.93 (*J* = 6.5 Hz, H-4″, H-5″), suggested the presence of an isopentyl group.

The ^{1}H-^{1}H COSY experiment showed correlations of H-1″/H-2″, H-2″/H-3″, and between H-3″ and H-4″ and H-5″ (Figure 46-47). This confirmed the presence of an isopentyl moiety, and the cross peak in the HMBC spectrum between the protons at δ_H 3.37 and C-1 (δ_C 166.0), demonstrated that this group was attached to the NH group. Thus, the structure of **1** was established as (2*E*,4*E*,6*E*)-*N*-isopentyl-7-(2-thienyl)-2,4,6-heptatrienamide.

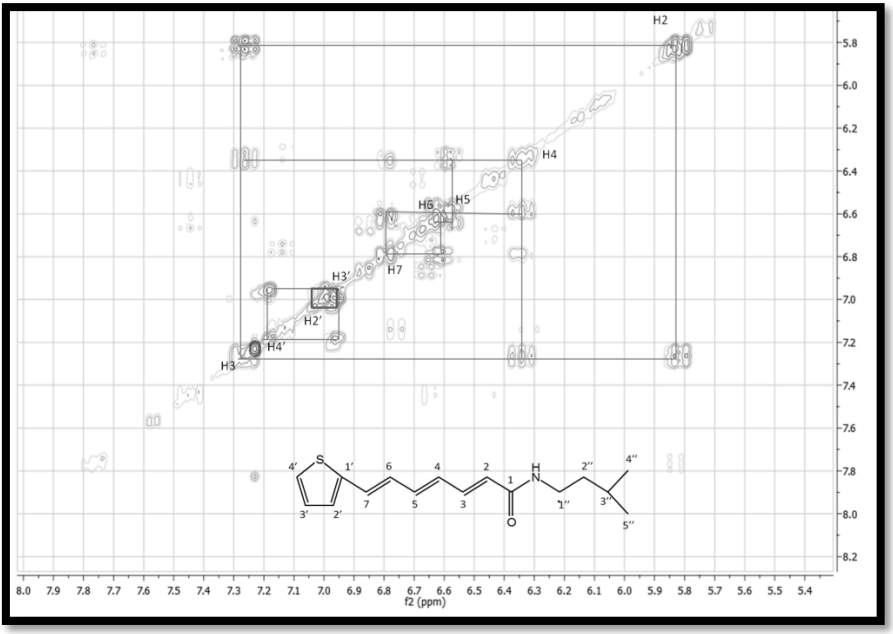

Figure 46. DQF-COSY (500 MHz) of compound **1**

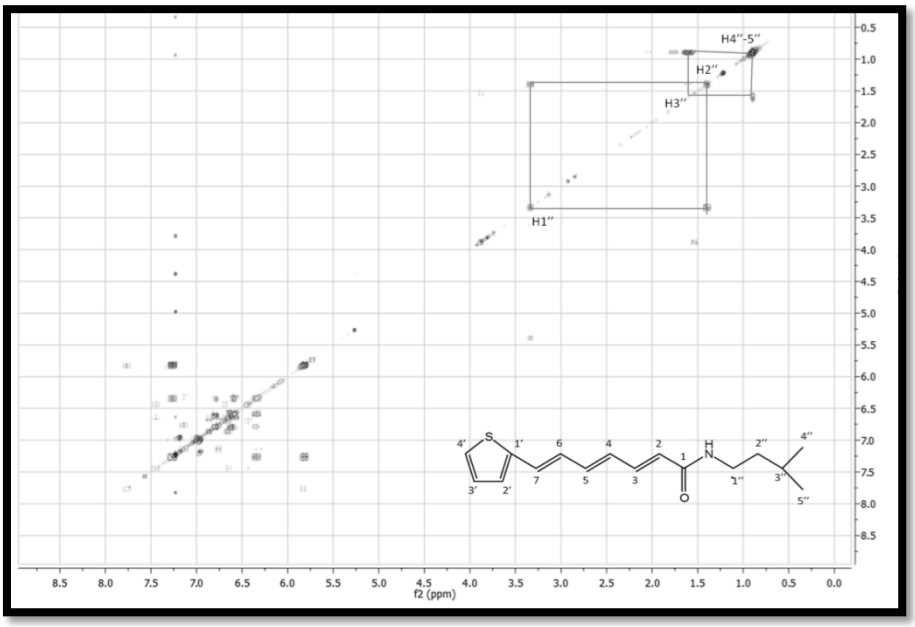

Figure 47. DQF-COSY (500 MHz) of compound **1**

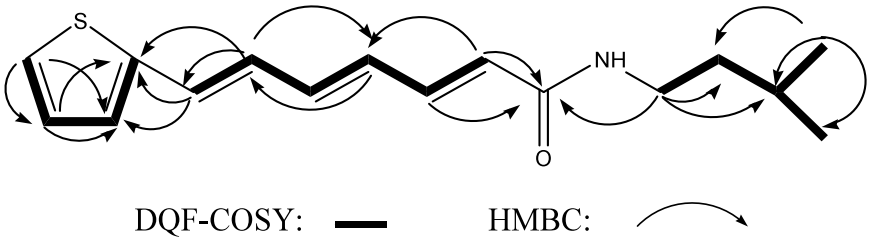

Figure 48. Main COSY and HMBC correlations of compound **1**

Table 2. ^{1}H (500 MHz) and ^{13}C (100 MHz) NMR spectral data of compound **1** ($CDCl_3$, δ in ppm)

	δ_C, multiplicity[a]	δ_H, multiplicity[b]
1	166.0, s	
2	123.3, d	5.85, d (15.0)
3	140.7, d	7.29, dd (15.0, 10.0)
4	130.2, d	6.37, dd (15.0, 10.0)
5	139.0, d	6.61, dd (15.0, 10.0)
6	127.9, d	6.65, dd (15.0, 10.0)
7	128.4, d	6.83, d (15.0)
1′	142.3, s	
2′	127.0, d	7.02, d (3.5)
3′	127.8, d	6.98, dd (5.0, 3.5)
4′	125.4, d	7.20, d (5.0)
1″	38.0, t	3.37, q, (5.0)
2″	38.6, t	1.43, m
3″	25.9, q	1.64, m
4″	22.5, q	0.93, d (6.5)
5″	22.5, q	0.93, d (6.5)
NH	5.40, br, s	

[a]Multiplicity was determined by analysis of the APT spectrum. [b]J values (Hz) in parentheses.

11.3.2 Structure Elucidation of Compound 5

Compound **5** showed a pseudomolecular ion peak at *m/z* 374 $[M + H]^+$, in low resolution ESIMS and a pseudomolecular ion at *m/z* 374.1785 $[M + H]^+$ (calc. 374.1784) in HR-TOF-ESI mass spectrum (Figure 49), accounting for the elemental composition of $C_{21}H_{27}NO_3S$, possessing nine degrees of unsaturation.

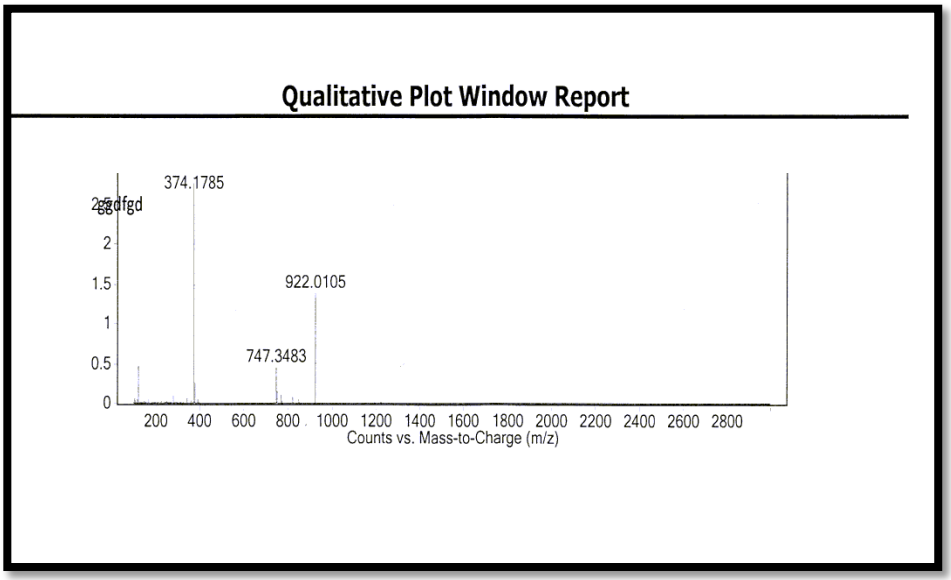

Figure 49. HR-TOF-ESIMS spectrum of **5**

Analysis of the ^{1}H (Figure 50) and APT (Figure 51) NMR data (Table 3) and the HSQC spectrum (Figure 53) of **5** revealed the presence of one sp^3 methine, four sp^3 methylene, two methyl, eleven sp^2 methine, and three sp^2 quaternary carbons. The downfield region ($5.7 < \delta_H < 7.5$) of the ^{1}H NMR spectrum of **5** was almost superimposable to those of **2**, suggesting the presence of a (2-thienyl)-2,4,6-heptatrienamidic moiety (Table 2), and the only significant difference between this spectrum portion of **2** with that of **5** was the downfield shift of the secondary amide proton signal to δ_H 6.16.

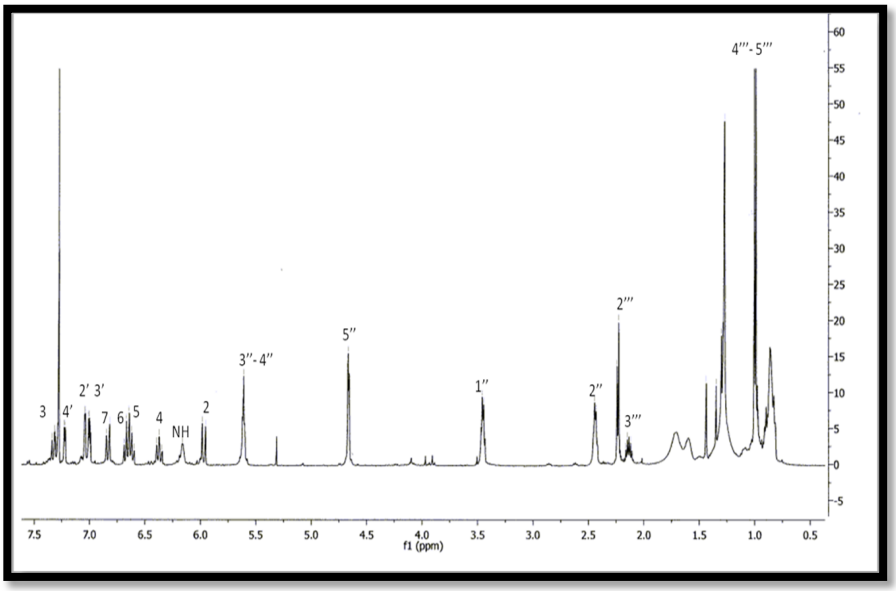

Figure 50. ^{1}H NMR spectrum (500 MHz) of **5** measured in $CDCl_3$

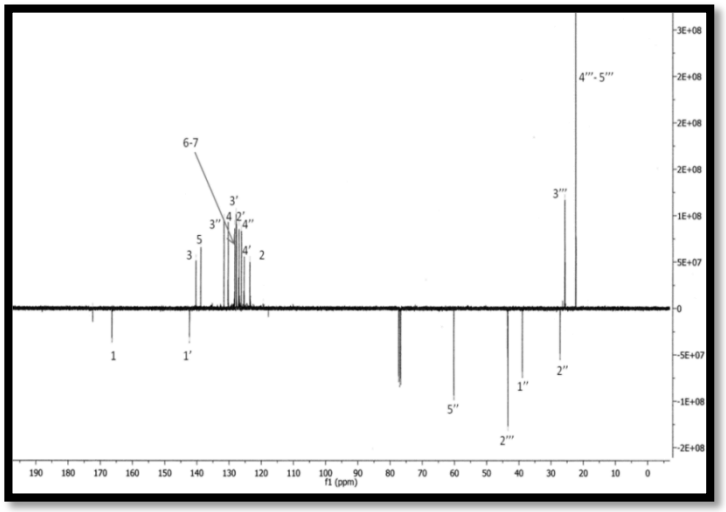

Figure 51. APT spectrum (100 MHz) of **5** measured in $CDCl_3$

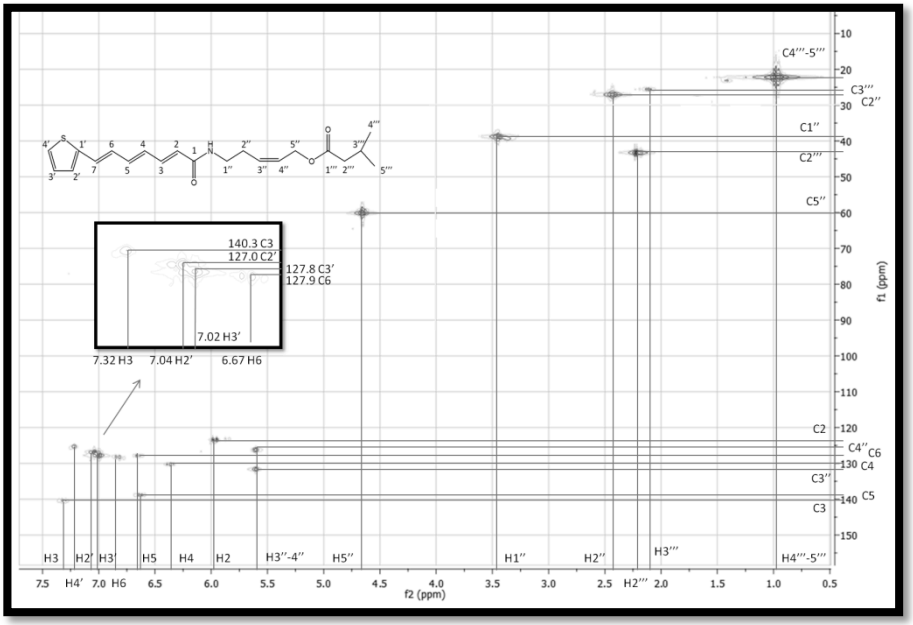

Figure 52. HSQC spectrum (500 MHz) of **5** measured in $CDCl_3$

In the same spectrum a doublet at δ_H 2.23 (J = 7 Hz, H-2‴), a multiplet at 2.13 (H-3‴) and a six-proton doublet at 1.0 (J = 6.5 Hz, H-4‴, H-5‴) suggested the presence of an isobutyl group which was substantiated by HMBC (Figure 53) and DQF-COSY (Figure 54,55) correlations.

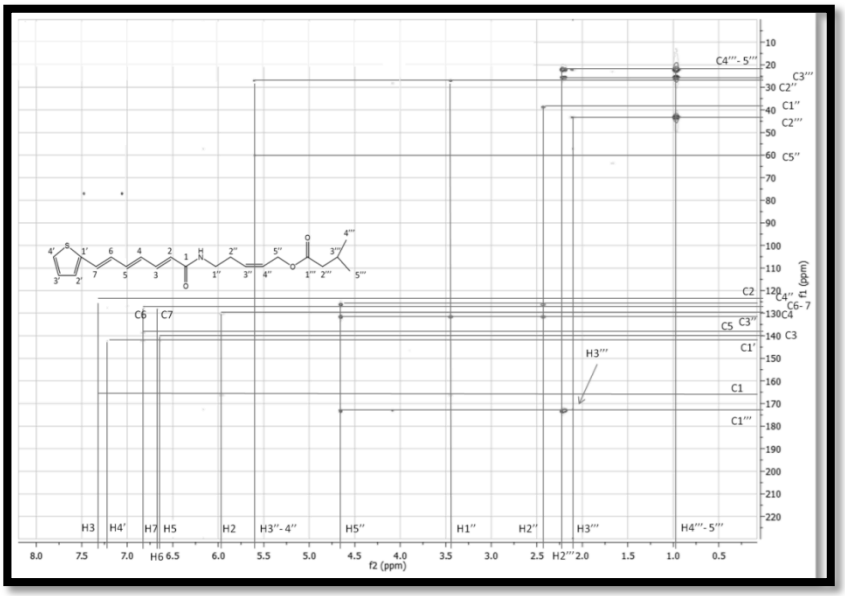

Figure 53. HMBC spectrum (500 MHz) of **5** measured in $CDCl_3$

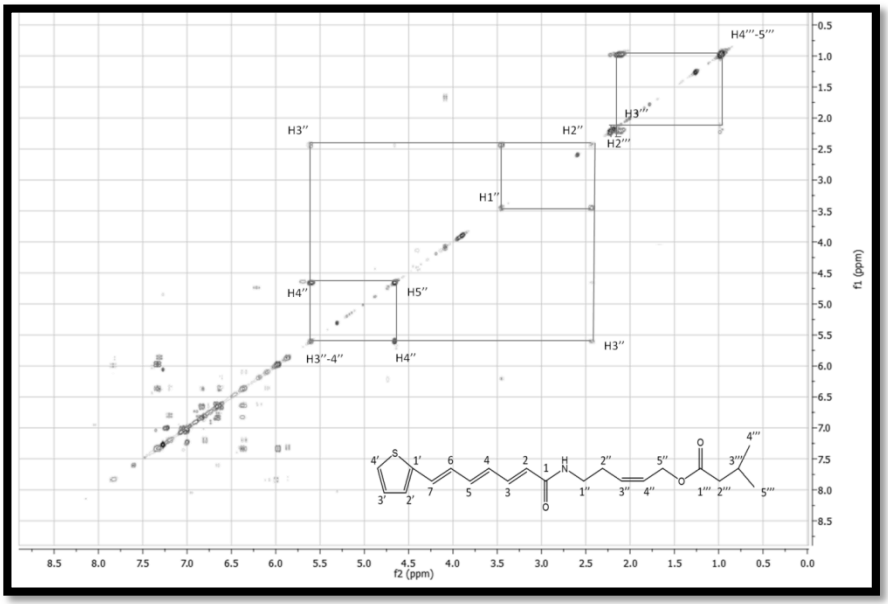

Figure 54. DQF-COSY (500 MHz) of compound **5**

This moiety was linked to an ester carbonyl group, judged by HMBC connectivities of the methylene and oxymethylene protons, respectively at 2.23 (*J* = 7.0 Hz, H-2‴) and 4.66 (*J* = 5.5 Hz, H-5″) ppm, with the quaternary carbon at δ_C 173.5 (Figure 53). HMBC cross-peaks of the protons at 4.66 and 2.43 (2H, m, H-2″) ppm with olefinic carbons at δ_C 131.6 and 126.2 (C-3″, C-4″), and of the methylene protons at δ_H 3.45 (H-1″, q, *J* = 6 Hz) with C-3″ (δ_C 131.6) revealed a 2-butenyl chain directly linked to C-5″ (δ_C = 60.2) (Figure 53). The

geometry of the C-3′′ and C-4′′ double ond was determined to be the *Z*-form by the same chemical shift of H-3′′/H-4′′ and by the upfield ^{13}C NMR shift of the allylic C-2′′ (δ_C = 27.1) (Table 3). Generally, the chemical shifts of allylic carbons of linear olefins of Z-isomers resonate at ca 5 ppm higher fields (δ < 29) than those of *E*-isomers (δ > 31)[132]. Further HMBC correlation of H-1′′ with C-1 (δ_C 166.4) fixed the ester chain to the secondary amide group (Figure 53).

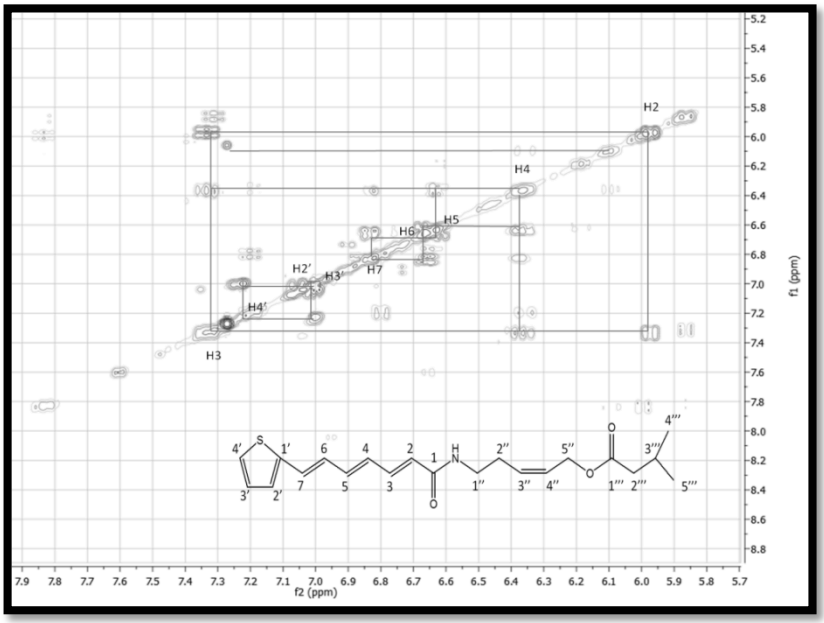

Figure 55. DQF-COSY (500 MHz) of **5**

DQF-COSY, HSQC and HMBC experiments (allowed the complete assignment of all signals and the identification of compound **5** as (2*Z*)-5-{[(2*E*,4*E*,6*E*)-7-(2-thienyl)-2,4,6-heptatrienoyl]amino}-2-pentenyl 3-methylbutanoate.

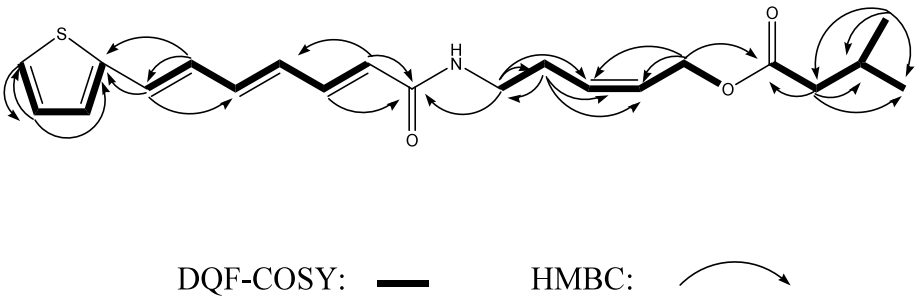

Figure 56. Main COSY and HMBC correlations of compound **5**

Table 3. ^{1}H (500 MHz) and ^{13}C (100 MHz) NMR spectral data of compounds **5** ($CDCl_3$, δ in ppm)

Position	δ_C, multiplicity[a]	δ_H, multiplicity[b]
1	166.4, s	
2	123.6, d	5.97, d (15.0)
3	140.3, d	7.32, dd (15.0, 10.0)
4	130.3, d	6.37, dd (15.0, 10.0)
5	138.8, d	6.62, dd (15.0, 10.0)
6	127.9, d	6.67, dd (15.0, 10.0)
7	128.3, d	6.83, d (15.0)
1′	142.3, s	
2′	127.0, d	7.04, d (3.5)
3′	127.8,	7.02, dd (5.0, 3.5)
4′	125.3, d	7.23, d (5.0)
1′′	38.9, t	3.45, q (6.0)
2′′	27.1, t	2.43, m
3′′	131.6, d	5.60, m
4′′	126.2, d	5.60, m
5′′	60.2, t	4.66, d (5.5)
1′′′	173.5, s	
2′′′	43.4, t	2.23, d (7.0)
3′′′	25.7, d	2.13, m
4′′′	22.4, q	1.00, d (6.5)
5′′′	22.4, q	1.00, d (6.5)
NH		6.16, br, s

[a]Multiplicity was determined by analysis of the APT spectrum. [b]J values (Hz) in parentheses

11.3.3 Strucure Elucidation of Compound 12

Compound **12** showed a pseudomolecular ion peak at *m/z* 441.1908 $[M + H]^+$ (calc. 441.1908) in HR-TOF-ESI mass spectrum (Figure 57), accounting for the elemental composition of $C_{25}H_{28}O_7$, possessing thirteen degrees of unsaturation

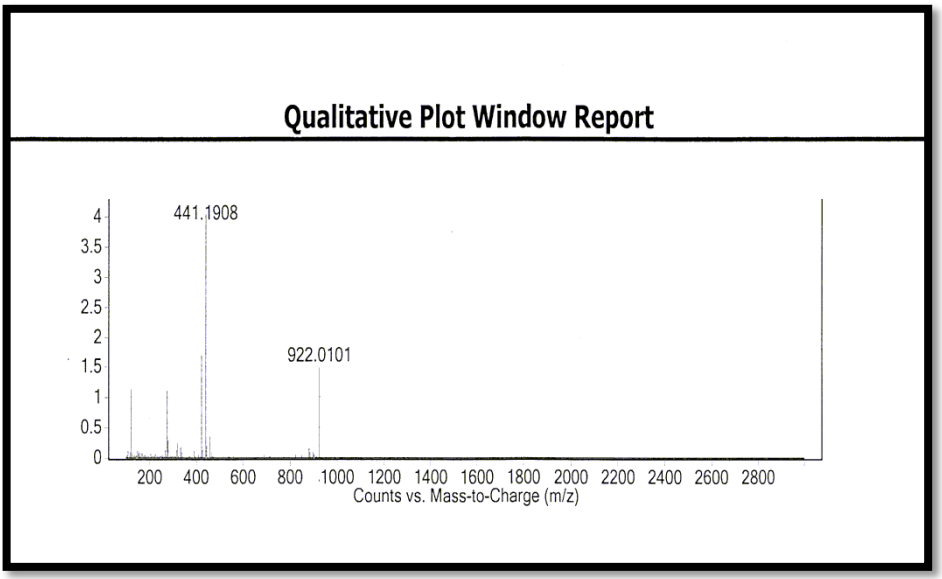

Figure 57. HR-TOF-ESIMS spectrum of **12**

Analysis of the ^{1}H, ^{13}C and APT NMR data (Figures 58-59) (Table 4) and the HSQC spectrum of **12** revealed the presence of three sp^3 methine, two sp^3 methylene, four methyl, eight sp^2 methine, and eight sp^2 quaternary carbons. The ^{1}H NMR spectrum of **12** (Table 4) revealed the presence of a dihydrobenzofuran-type lignan moiety [δ_H 5.55 (1H, d, *J* = 7.0 Hz, H-7), 3.82 (1H, m, H-8), 4.41 (2H, d, *J* = 6.0 Hz, H-9)], which was supported by resonances in the ^{13}C NMR spectrum (Table 4) [δ_C 89.4 (CH, C-7), 50.0 (CH, C-8), 64.6 (CH_2, C-9)].

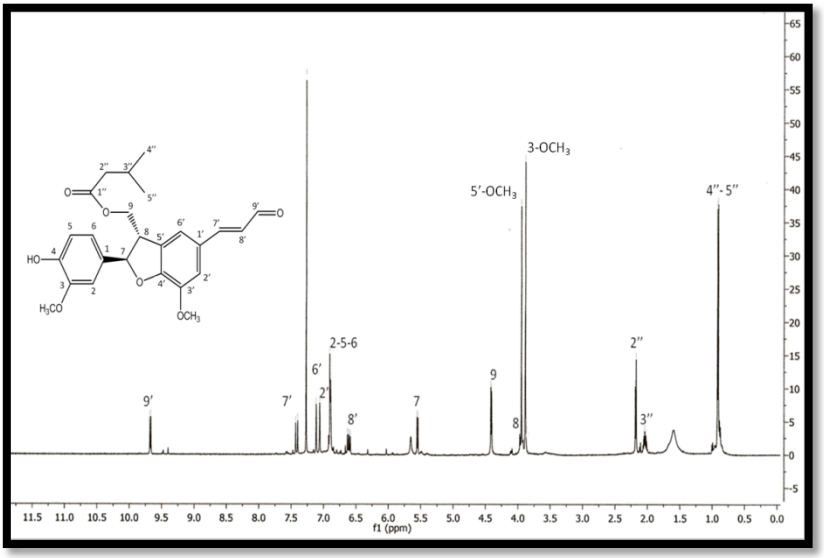

Figure 58. ^{1}H NMR spectrum (500 MHz) of compound **12** measured in $CDCl_3$

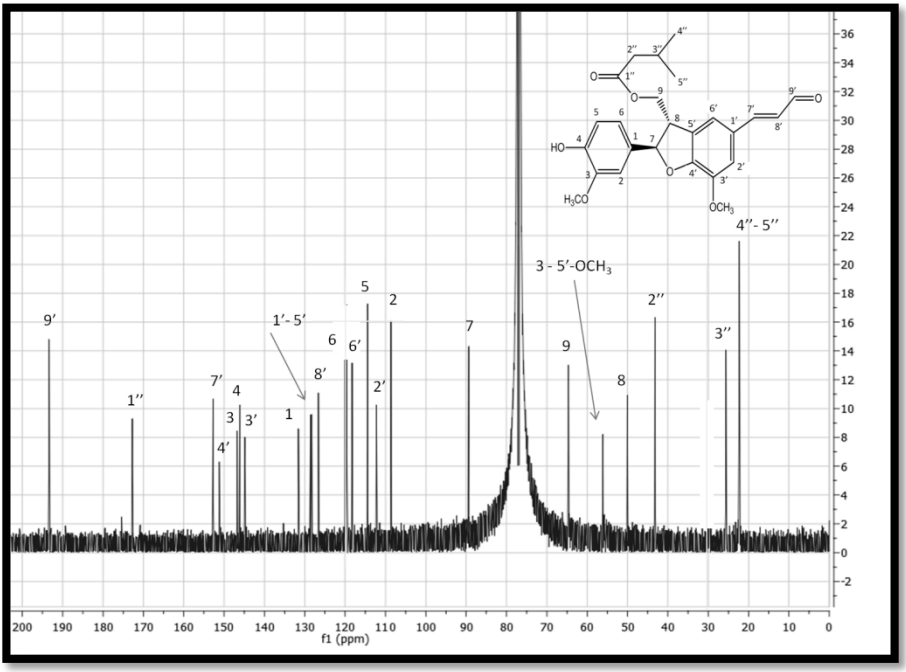

Figure 59.^{13}C NMR spectrum (500 MHz) of **12** measured in $CDCl_3$

Furthermore, a feruloyl aldehyde group [δ_H 9.67 (1H, d, *J* = 7.5 Hz, H-9′), 7.42 (1H, d, *J* = 15.5 Hz, H-7′), 7.11 (1H, s, H-6′), 7.06 (1H, s, H-2′), 6.61 (1H, dd, *J* = 15.5, 7.5 Hz, H-8′)] and a 3-metoxy-4-hydroxyphenyl moiety [δ_H 6.89 (1H, d, *J* = 1.5 Hz, H-2), 6.90 (1H, dd, *J* = 7.5, 1.5 Hz, H-6), 6.91 (1H, d, *J* = 7.5 Hz, H-5)] could be detected in the ^{1}H NMR spectrum (Figure 58).

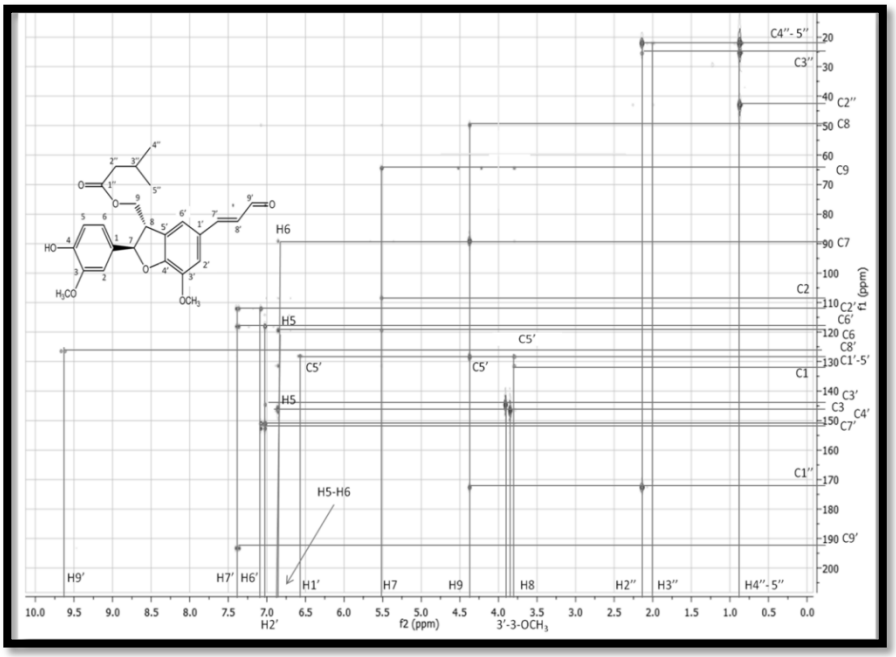

Figure 60. HSQC spectrum (500 MHz) of **12** measured in $CDCl_3$

According to HMBC (Figure 61) and COSY (Figure 62) cross-peaks, the above groups were connected to the dihydrofuran nucleus, highlighting the presence of a balanophonin derivative.[133]

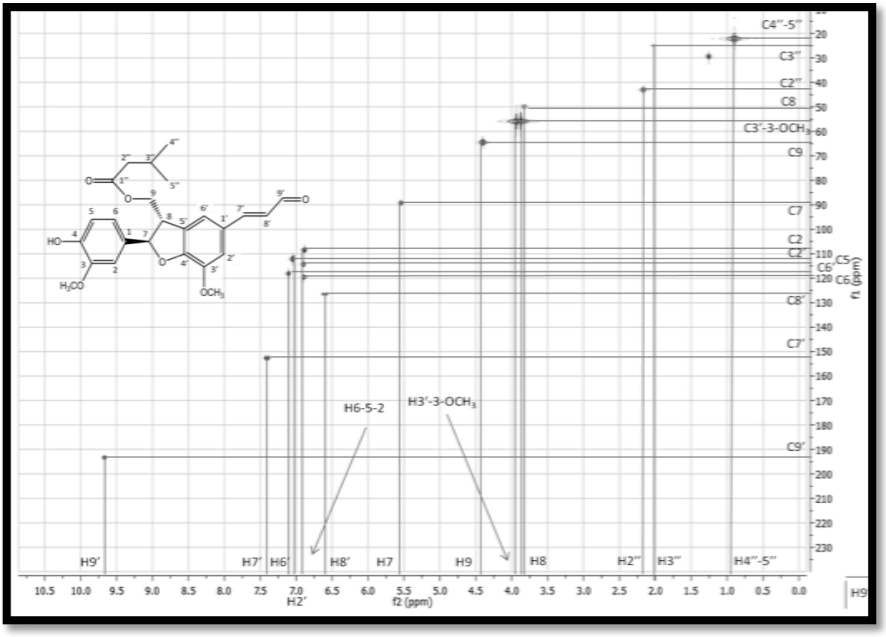

Figure 61. HMBC spectrum (500 Mhz) of **12** measured in $CDCl_3$

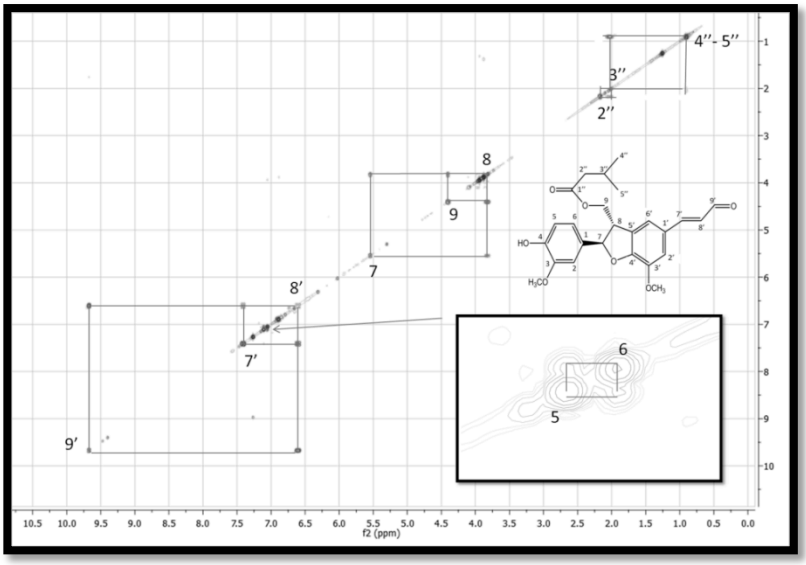

Figure 62. DQF-COSY (500 MHz) of **12** measured in $CDCl_3$

Moreover, the ^{1}H and ^{13}C NMR spectra showed a isovaleroyl group [δ_H 2.18 (2H, d, *J* = 7.0 Hz, H-2′′), 2.04 (1H, m, H-3′′), 0.91 (6H, d, *J* = 7.0 Hz, H-4′′, H-5′′) linked at C-9 (δ_C = 64.6), judged from the observed correlations in the HMBC spectrum (Figure 61) between the ester carbonyl carbon (δ_C 172.7) and H_2-9 and H-3′′ (δ_H = 2.04, m).

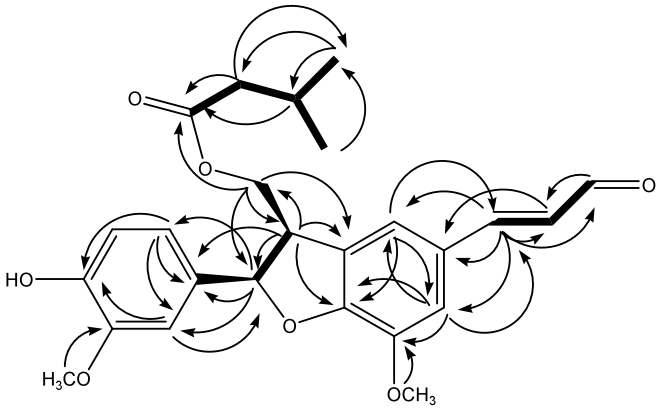

Figure 63. Main HMBC and DQF-COSY correlations of **12**

The relative configuration of C-7 and C-8 was determined by ROESY experiments and analyzing scalar ($^3J_{HH}$) coupling of the protons. Namely, since the coupling constant of H-7 was 7.0 Hz, the relative configuration of C-7 and C-8 was assigned as *trans*.

This observation was supported on the basis of the ROESY spectrum, which showed correlations between H-7 and H-9, and between H-8 and H-2 and H-6 (Figure 64). The absolute configuration of **12** could not be determined due to the fact that a crystalline derivative suitable for an X-ray structure determination could not be obtained from the compound isolated.

Consequently, the structure of compound **12** was established as, 9-isovaleroxy balanophonin (Figure 65).

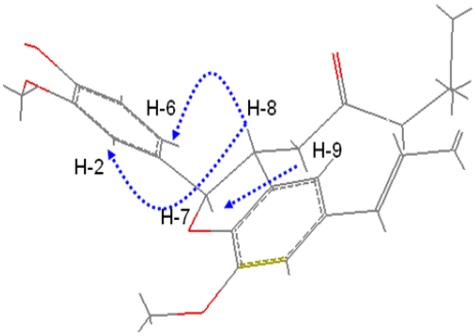

Figure 64. Key ROE correlations observed for compound **12**

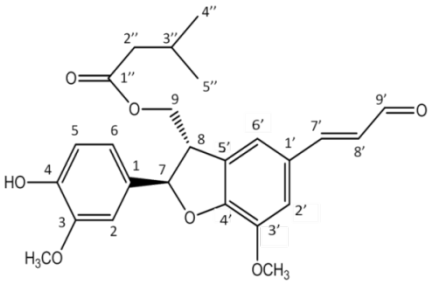

Figure 65. Structure of 9-isovaleroxy balanophonin (**12**)

Table 4. ^{1}H (500 MHz) and ^{13}C (100 MHz) NMR spectral data of compound **12** ($CDCl_3$, δ in ppm)

Position	δ_C, multiplicity[a]	δ_H, multiplicity[b]
1	131.6, s	
2	108.6, d	6.89, d (1.5)
3	146.8, s	
4	146.1, s	
5	114.5, d	6.91, d (7.5)
6	119.6, d	6.90, dd (7.5, 1.5)
7	89.4, d	5.55, d (7.0)
8	50.0, d	3.82, m
9	64.6, t	4.41, d (6.0)
1′	128.6, s	
2′	112.2, d	7.06, s
3′	144.8, s	
4′	151.2, s	
5′	128.3, s	
6′	118.3, d	7.11, s
7′	152.6, d	7.42, d (15.5)
8′	126.6, d	6.61, dd (15.5, 7.5)
9′	193.4, d	9.67, d (7.5)
1′′	172.7, s	
2′′	43.2, t	2.18, d (7.0)
3′′	25.6, d	2.04, m
4′′	22.3, q	0.91, d (7.0)
5′′	22.3, q	0.91, d (7.0)
3-OCH_3	56.0	3.89, s
3′-OCH_3	56.1	3.95, s

[a]Multiplicity was determined by analysis of the APT spectrum.
[b]J values (Hz) in parentheses.

11.3.4 In Silico Modelling Study

Up to now, it is believed that, for a high affinity to CB2 receptors, alkylamides should be N-substituted with an isobutyl or dimethylbutyl group and represented by a secondary alkylamide as the amide proton seems to be involved in the CB2 receptor interaction.[134] Our findings are somewhat surprising because among all tested compounds the most potent and selective alkylamide resulted the tertiary amide 1-[(2E,4E,8Z)-tetradecatrienoyl]piperidine (**10**) which contain a piperidinyl moiety linked to a C14 acyl chain (see biological section, 12.1,p.196). Compound **10** showed CB2 affinity higher than that of dodeca-2E,4E-dienoic acid isobutylamide **6**, that is one of the active principles of *Echinacea* species. In our hands, compound **6** displayed a K_iCB2 value of 0.9 μM that is higher than that reported by Raduner et al.[5] (K_iCB2 = 0.06 μM) but lower in respect to that measured by Woelkart et al.[71] (KiCB2 = 9.694 μM). As reported in a previous work,[5] the discrepancy between the K_i values could be due to the different source of CB2 receptors, as well as experimental condition.[135]

Until now, the presence of secondary amide group was described to be essential for the activity of alkylamides isolated from *Echinacea.*[5] In order to explore the nature of the ligand-receptor interactions, we have carried out docking experiments into CB2 receptor by means of GlideXP.[136]

We focused on the compound **6** and **10**, which show interesting activity but differ for the presence of secondary and tertiary amide moiety respectively. 3D models of CB2 human receptor has been generated by homology modeling using as template the X-ray structure of the human A2A adenosine receptor with UK-432097 (PDB:3QAK)[137] as reported by Ruhl et al.[138] The obtained complexes were optimized by energy minimization and successive interaction energies calculation applying molecular mechanics and continuum solvation models using the molecular mechanics generalized Born/surface area (MM-GBSA) method.[139] According to the available literature information, we validated our simulation protocol by docking the compound WIN55212-2 in both wild type and mutated F5.46(197)V receptor. In fact a decreased ligand affinity for the mutated CB2 was disclosed.[140]

The applied protocol confirmed the importance of F197 residue. The complex is stabilized by tilted T-shaped edge-to-face aromatic

interaction between the indole ring of the ligand and F5.46(197), by π-π stacking with F3.36(117) and cation- π with K3.28(109) (Figure 66 and Table 5). The same experiment with the mutated F5.46(197)V, produced a loss of the stability of the complex as reported in Table 5 confirming the experimental data.

Table 5. ΔTotal Interaction Energy (IE) Term expressed in kcal/mol per complex

CB2 receptor	Ligand	DTotal-IE
wt	WIN55212-2	-28.24
F197V	WIN55212-2	-24.44
wt	**6**	-27.93
wt	**10**	-29.48

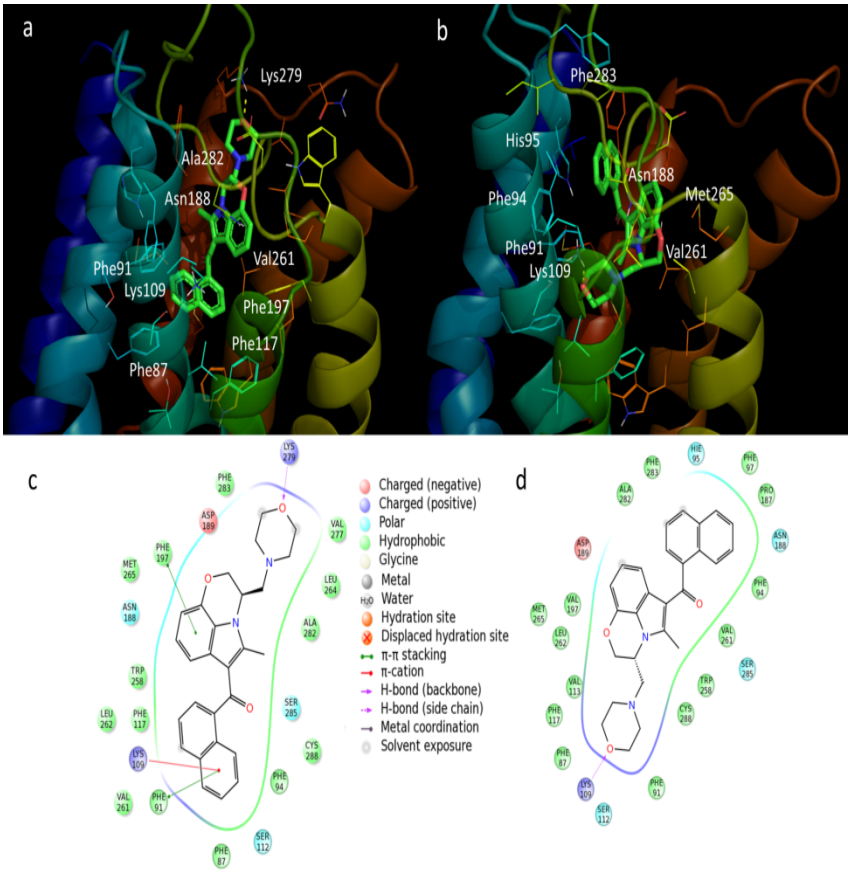

Figure 66. Optimized docked poses of complexes CB2-Ligand: a) wt-WIN55212-2; b) F197Vmut-WIN55212-2; c-d) 2D visualization of interactions of putative binding mode

Consecutively, the analysis of the putative binding modes of compounds **6** and **10** (Figure 67) highlighted the accommodation of the amide group in a hydrophilic area, enclosed by polar residues (e.g. Asn 188, Asp-189, Gln-276 and Lys 279), and of the alkyl tail into a hydrophobic cleft, surrounded by aromatic and hydrophobic residues (e.g. Phe-87-91-94-117-197, Trp-258 and Val261, Leu264, Leu262 respectively).

Both compounds **6** and **10** are able to establish a strong hydrogen bond with Asn188: in the former compound the amide group behaves as a donor, while in the latter as an acceptor. Therefore, the presence of the secondary amide as donor group is not critical for activity. Furthermore the docking of compound **10** confirms the importance of double bond with *Z* configuration at C8 position. This diasteroisomer can adopt an U shape conformation which perfectly fit into the binding pocket and increases the number of good contacts between ligand-receptor (Figure 67). This particular feature was already reported as important in other compounds.[141]

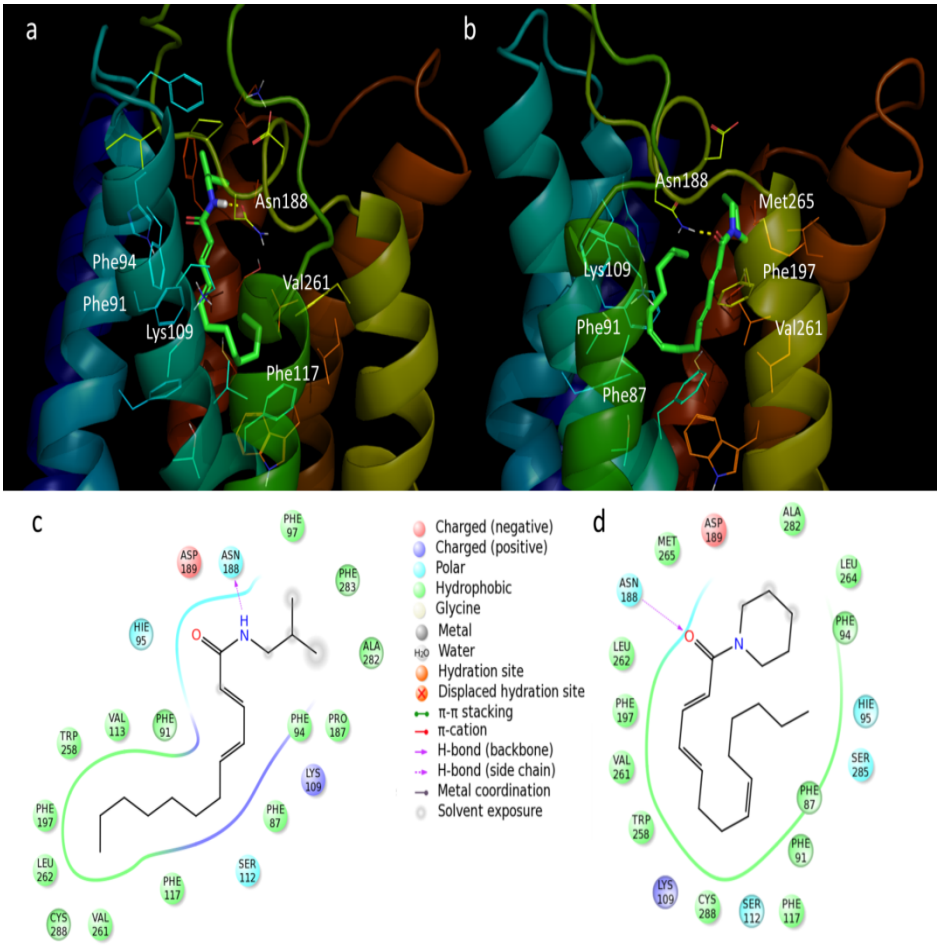

Figure 67. Optimized docked poses of complexes CB2-Ligand: a) CB2wt-6; b) CB2wt-10; c-d) 2D visualization of interactions of putative binding mode of each compound examined

11.3.5 Structure Elucidation of Known Compounds

The structure of the known metabolites were deduced from NMR spectroscopy and mass spectrometry and confirmed by comparison with data reported in the literature.

(2*E*,4*E*,6*E*)-N-isobutyl-7-(2-thienyl)-2,4,6-heptatrienamide (2)

(2*E*,4*E*,6*E*)-N-isobutyl-7-(2-thienyl)-2,4,6-heptatrienamide (**2**) was identified by comparison of the ^{1}H (Figure 69) and ^{13}C (Figure 70) NMR chemical shifts and ESI-MS(Figure 68) data with literature values.[142]

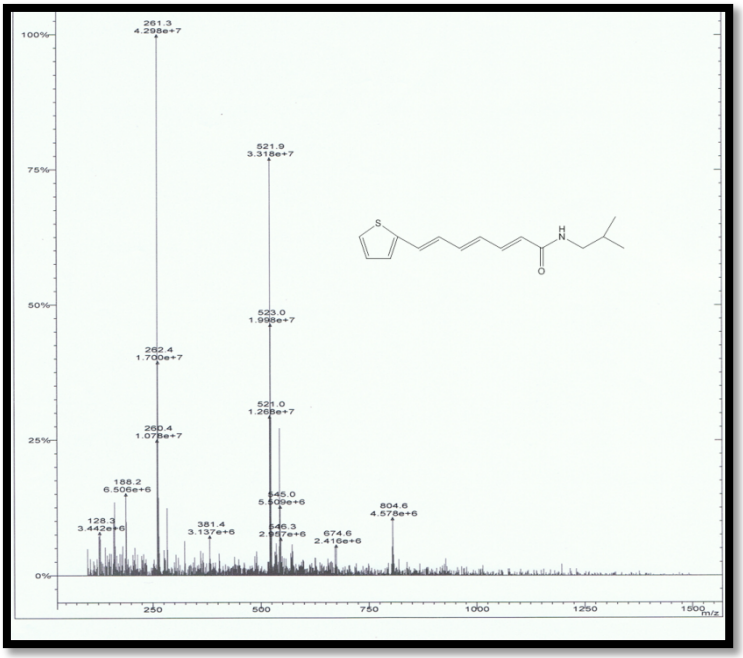

Figure 68. ESI mass spectrum ofcompound **2**

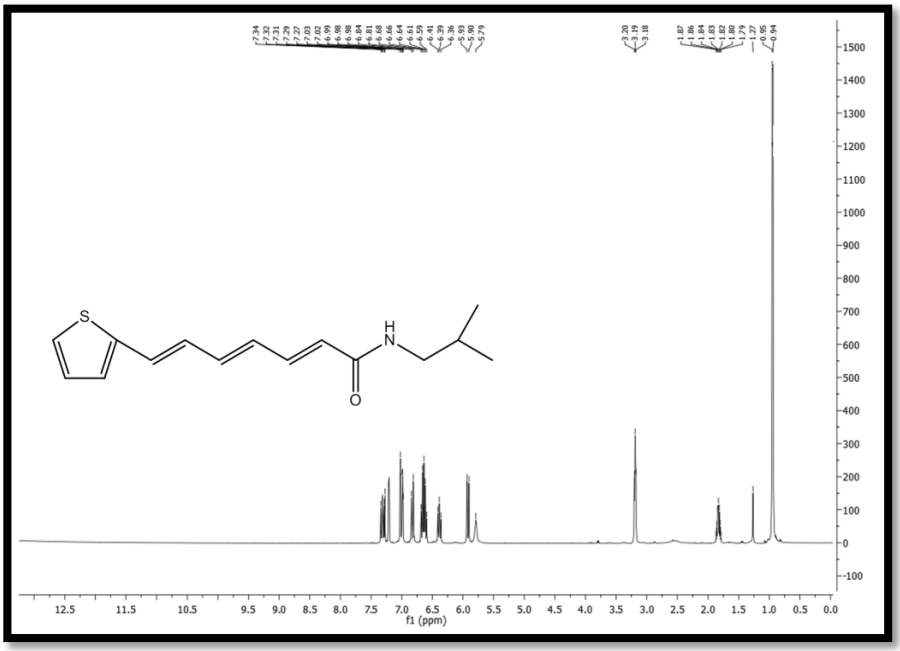

Figure 69. ^{1}H NMR spectrum (500 MHz) of compound **2** measured in $CDCl_3$

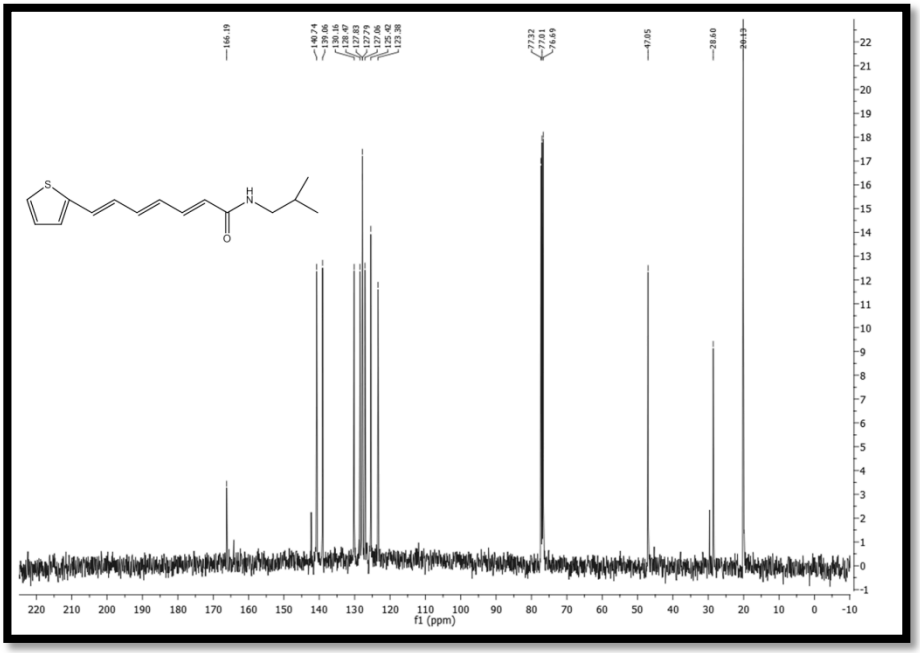

Figure 70. ^{13}C NMR spectrum(100 Mhz)of compound **2** measured in $CDCl_3$

1-[(2*E*,4*E*,6*E*)-7-(2-thienyl)-2,4,6-heptatrienoyl]piperidine (3)

1-[(2*E*,4*E*,6*E*)-7-(2-thienyl)-2,4,6-heptatrienoyl]piperidine (**3**) was identified by comparison of the ^{1}H (Figure 72) and APT (Figure 73) NMR chemical shifts and ESI-MS(Figure 71) data with literature values.[142]

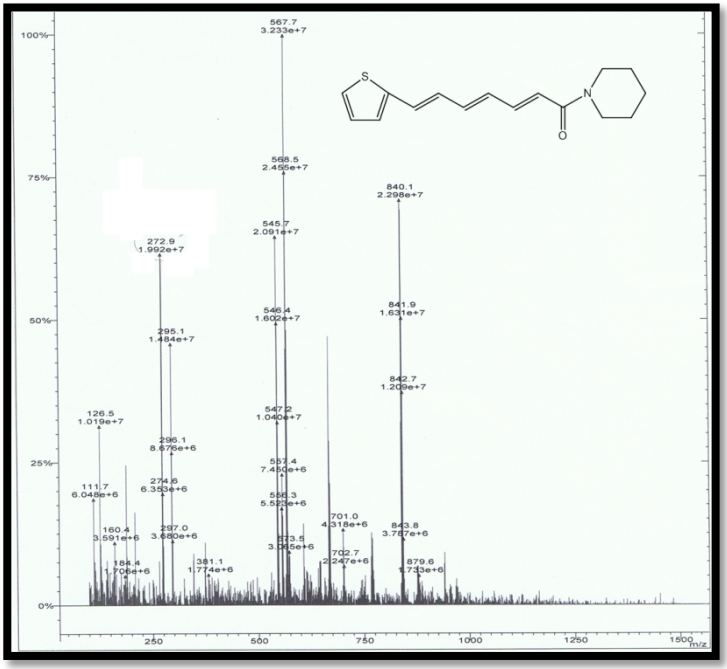

Figure 71. ESI mass spectrum ofcompound **3**

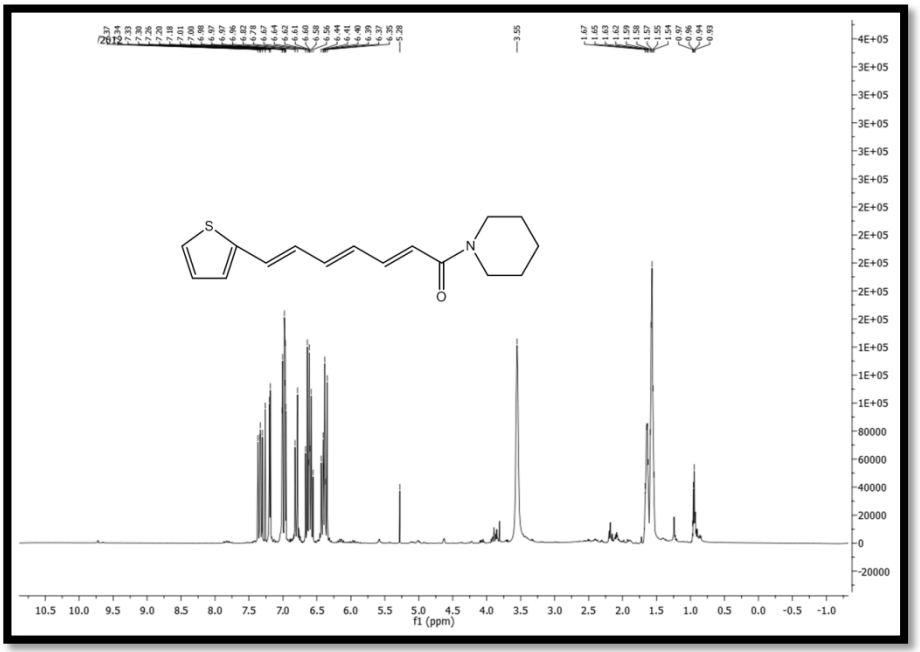

Figure 72. ^{1}H NMR spectrum (500 MHz) of compound **3** measured in $CDCl_3$

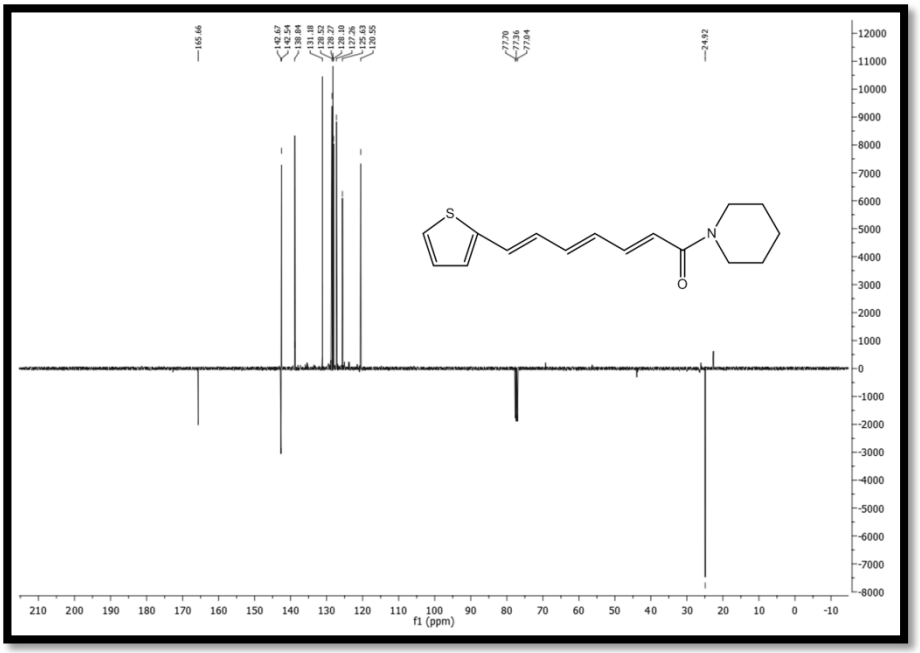

Figure 73. APT NMR spectrum (100 Mhz) of compound **3** measured in $CDCl_3$

1-[(2*E*,4*E*,6*E*)-7-(2-thienyl)-2,4,6-heptatrienoyl]2,3-dehydropiperidine (4)

1-[(2*E*,4*E*,6*E*)-7-(2-thienyl)-2,4,6-heptatrienoyl]2,3 dehydropiperidine (**4**) was identified by comparison of the ^{1}H (Figure 75) and ^{13}C (Figure 76) NMR chemical shifts and ESI-MS (Figure 74) data with literature values.[65]

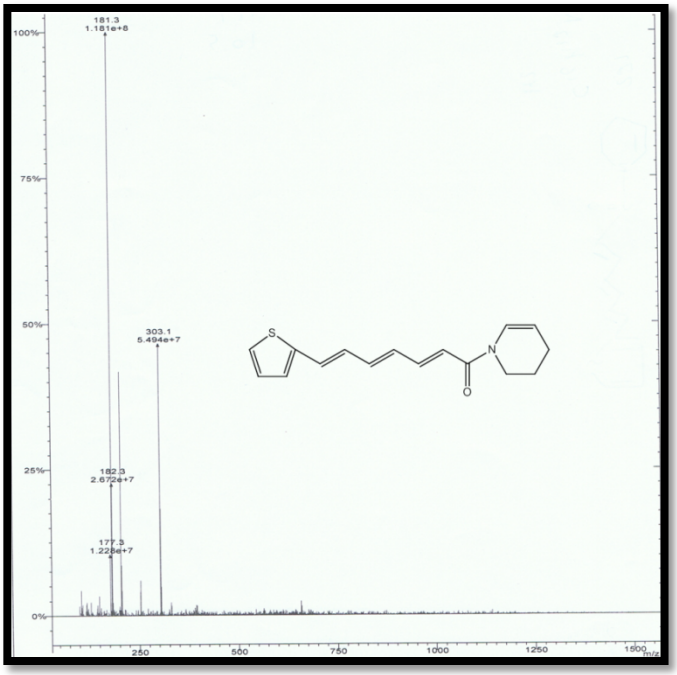

Figure 74. ESI mass spectrum ofcompound 4

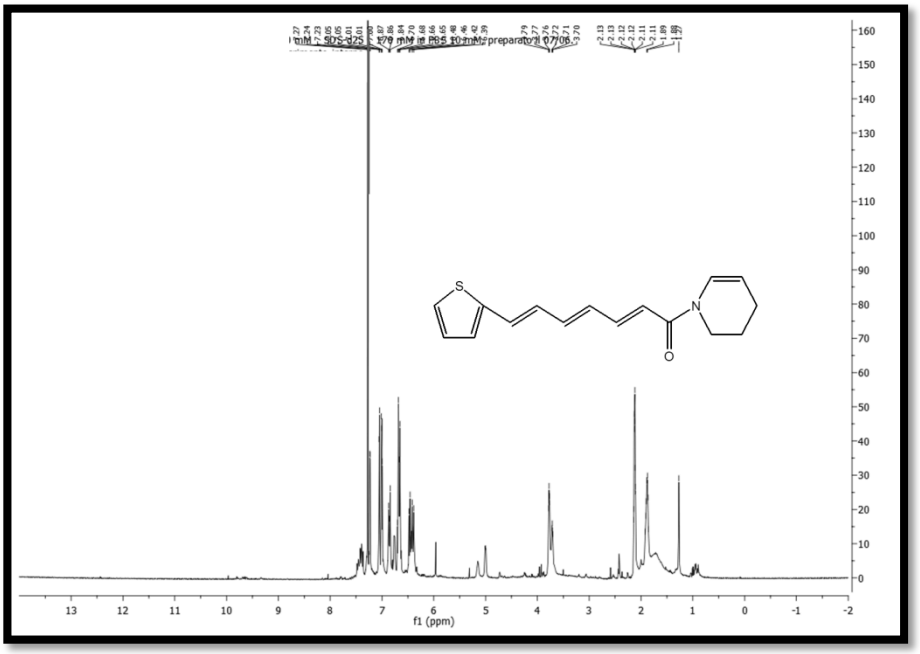

Figure 75. ^{1}H NMR spectrum (500 MHz) of compound **4** measured in $CDCl_3$

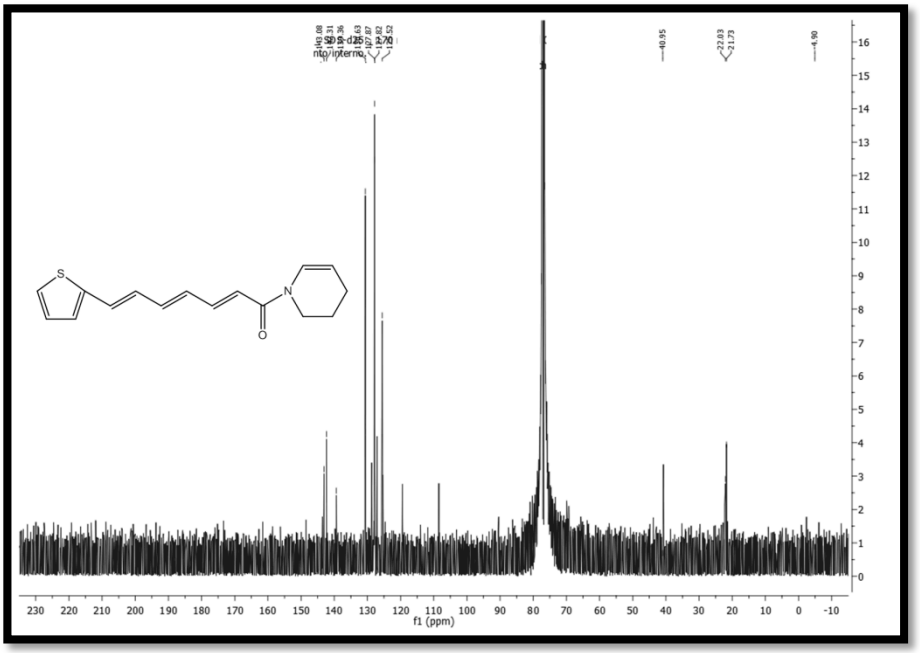

Figure 76. ^{13}C NMR spectrum (100 MHz) of compound **4** measured in $CDCl_3$

Dodeca-2*E*,4*E*-dienoic acid isobutylamide (6)

dodeca-2*E*,4*E*-dienoic acid isobutylamide (**6**) was identified by comparison of the ^{1}H (Figure 78) and ^{13}C (Figure 79) NMR chemical shifts and ESI-MS(Figure 77) data with literature values.[143]

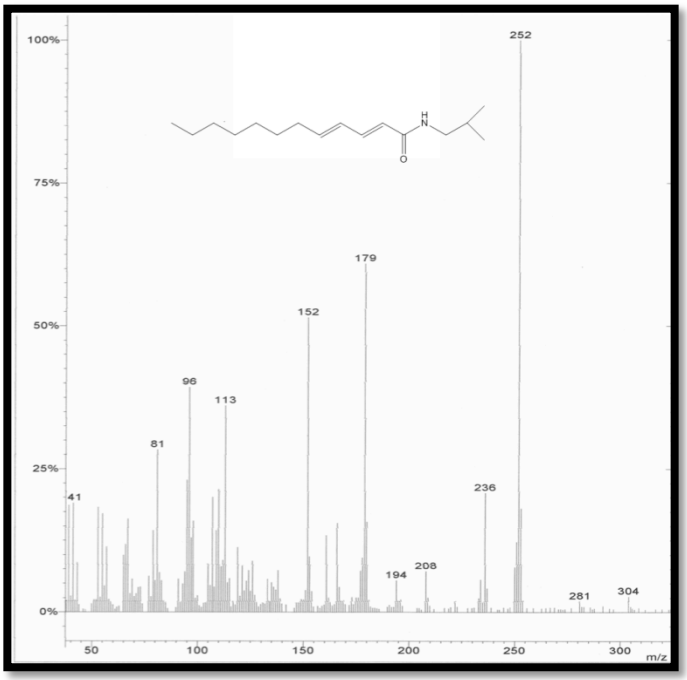

Figure 77. ESI mass spectrum of compound **6**

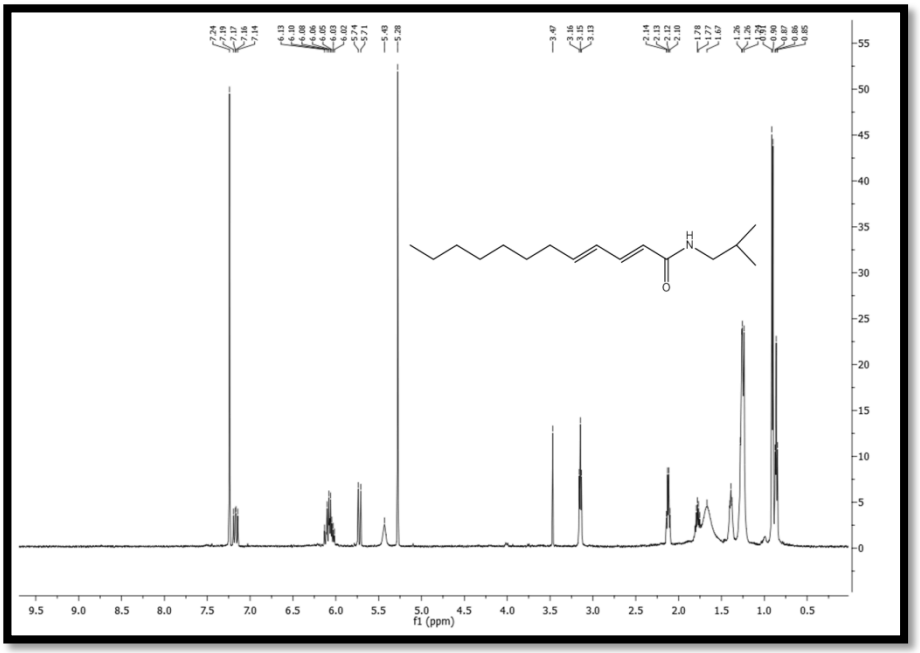

Figure 78. ^{1}H NMR spectrum (500 MHz) of compound **6** measured in $CDCl_3$

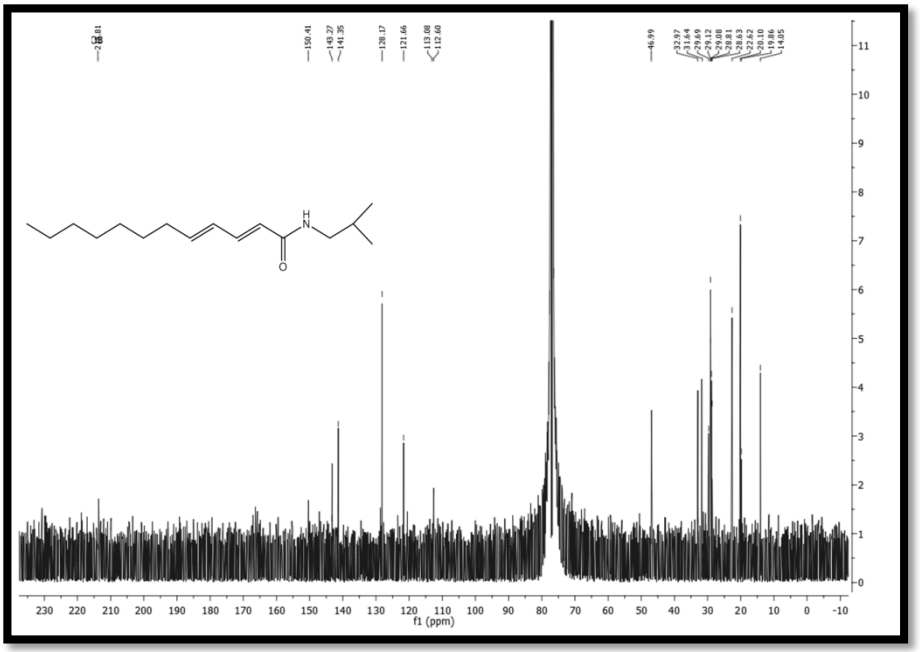

Figure 79. ^{13}C NMR spectrum (100 MHz) of compound **6** measured in $CDCl_3$

Tetradeca-2*E*,4*E*-dienoic acid isobutylamide (7)

Tetradeca-2*E*,4*E*-dienoic acid isobutylamide (**7**) was identified by comparison of the ^{1}H (Figure 80) and ^{13}C (Figure 81) NMR chemical shifts data with literature values.[144]

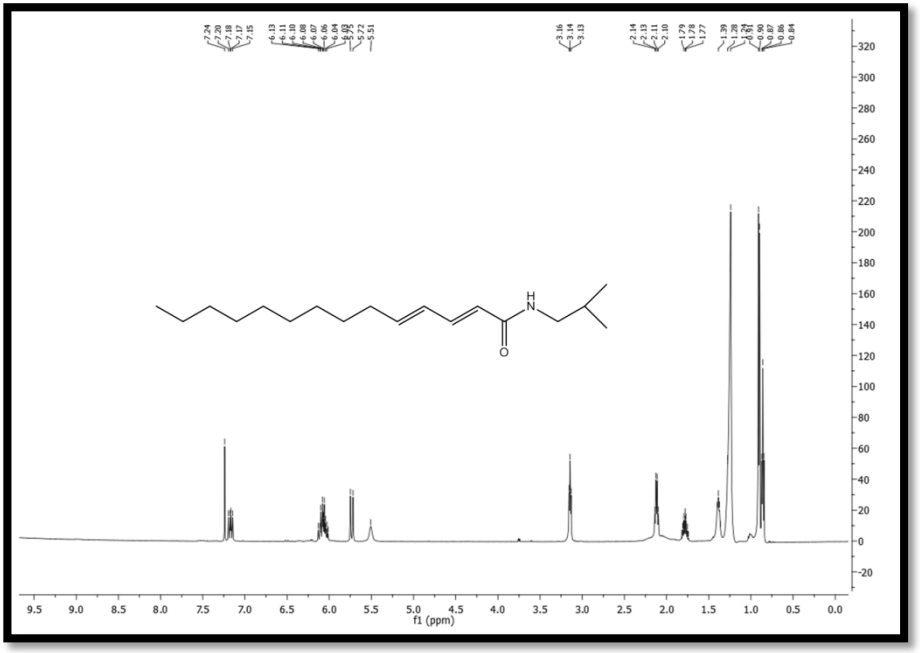

Figure 80. ^{1}H NMR spectrum (500 MHz) of compound **7** measured in $CDCl_3$

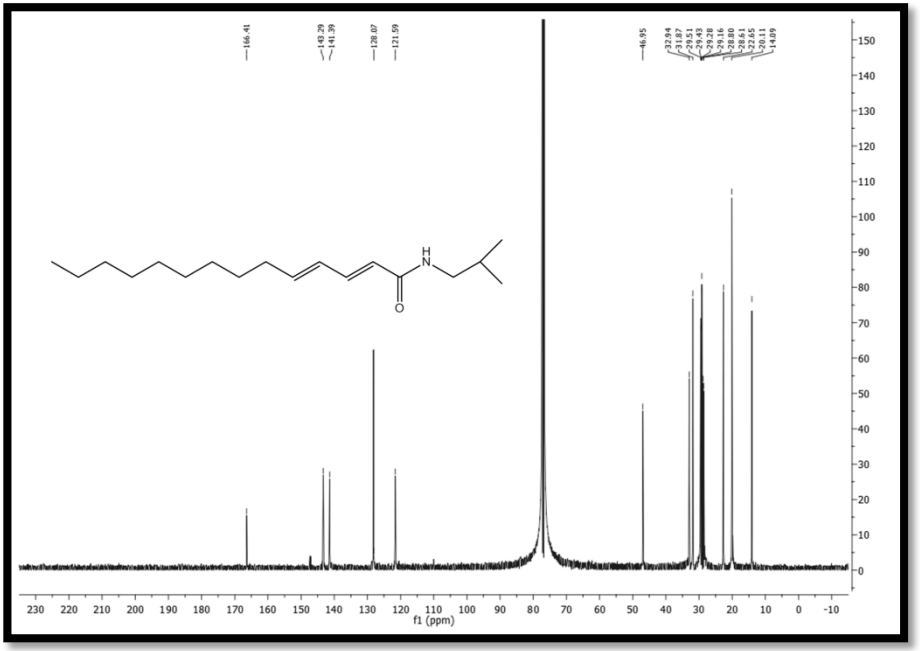

Figure 81. ^{13}C NMR spectrum (100 MHz) of compound **7** measured in $CDCl_3$

Tetradeca-2*E*,4*E*,8*Z*-trienoic acid isobutylamide (8)

Tetradeca-2*E*,4*E*,8*Z*-trienoic acid isobutylamide (**8**) was identified by comparison of the ^{1}H (Figure 82) NMR chemical shifts data with literature values.[145,146]

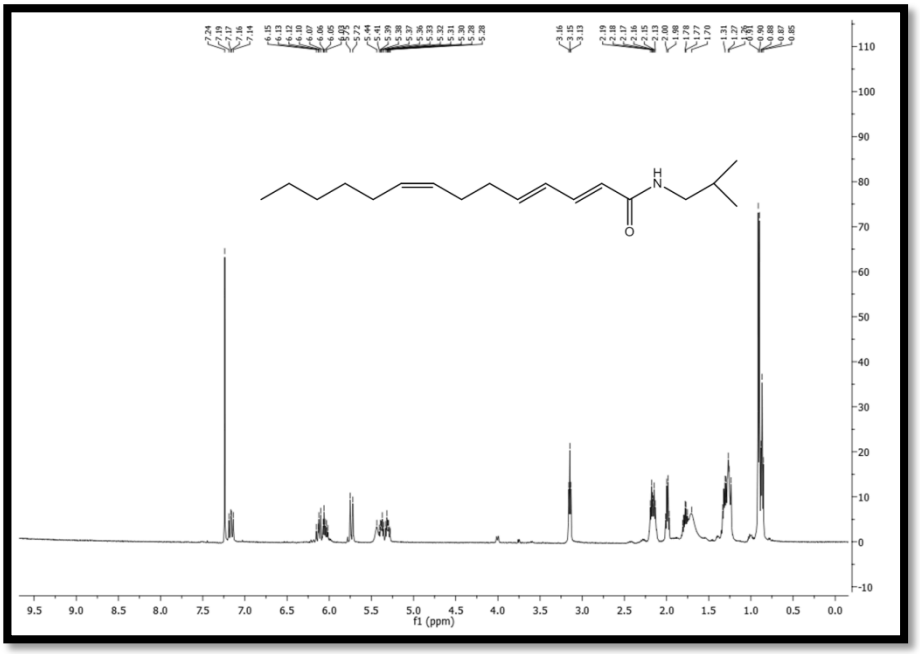

Figure 82. ^{1}H NMR spectrum (500 MHz) of compound **8** measured in $CDCl_3$

1-[(2*E*,4*E*)-tetradecadienoyl]piperidine (9)

1-[(2*E*,4*E*)-tetradecadienoyl]piperidine (**9**) was identified by comparison of the ^{1}H (Figure 83) and ^{13}C (Figure 84) NMR chemical shifts with literature values.[144]

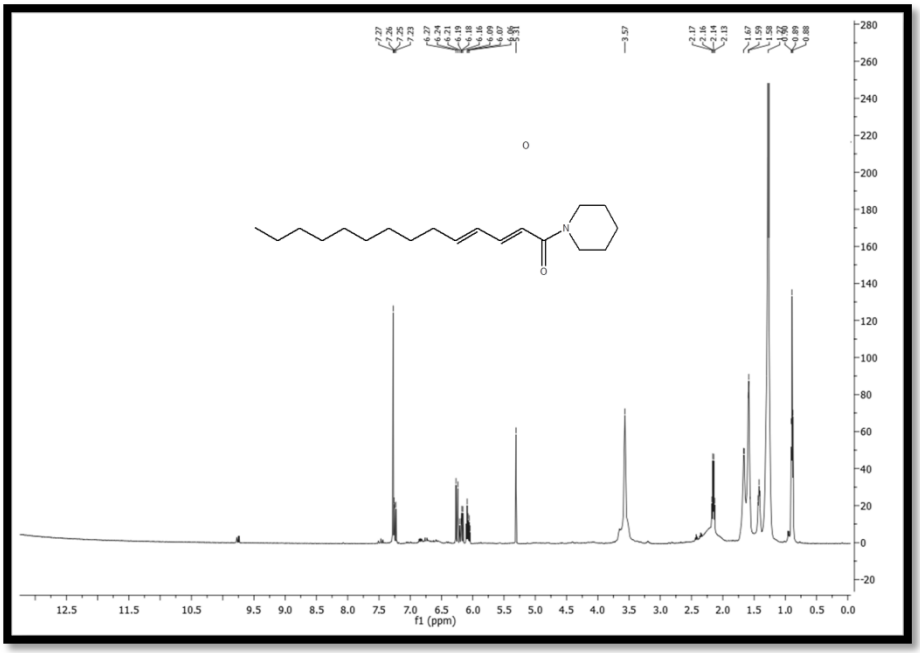

Figure 83. ^{1}H NMR spectrum (500 MHz) of compound **9** measured in $CDCl_3$

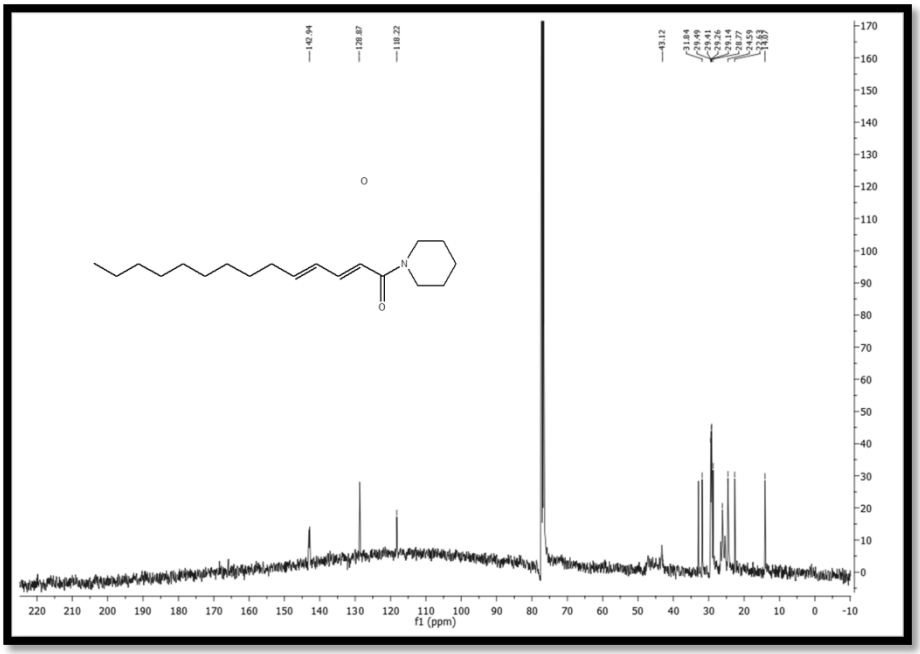

Figure 84. ^{13}C NMR spectrum (100 MHz) of compound **9** measured in $CDCl_3$

1-[(2*E*,4*E*,8*Z*)-tetradecatrienoyl]piperidine (10)

1-[(2*E*,4*E*,8*Z*)-tetradecatrienoyl]piperidine (**10**) was identified by comparison of the ^{1}H (Figure 85) NMR chemical shifts and ESI-MS (Figure 86) data with literature values.[67]

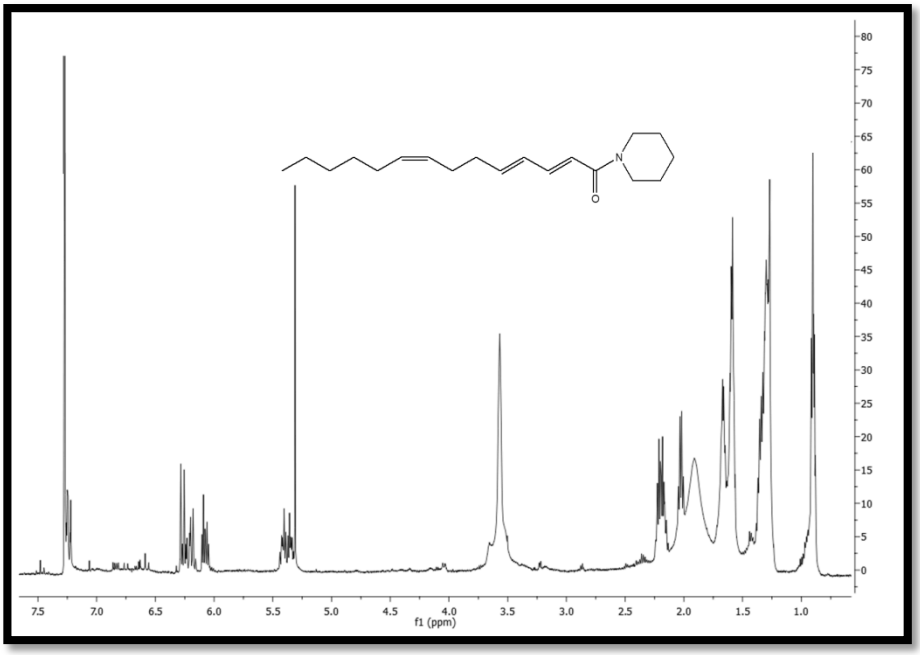

Figure 85. ^{1}H NMR spectrum (500 MHz) of compound **10** measured in $CDCl_3$

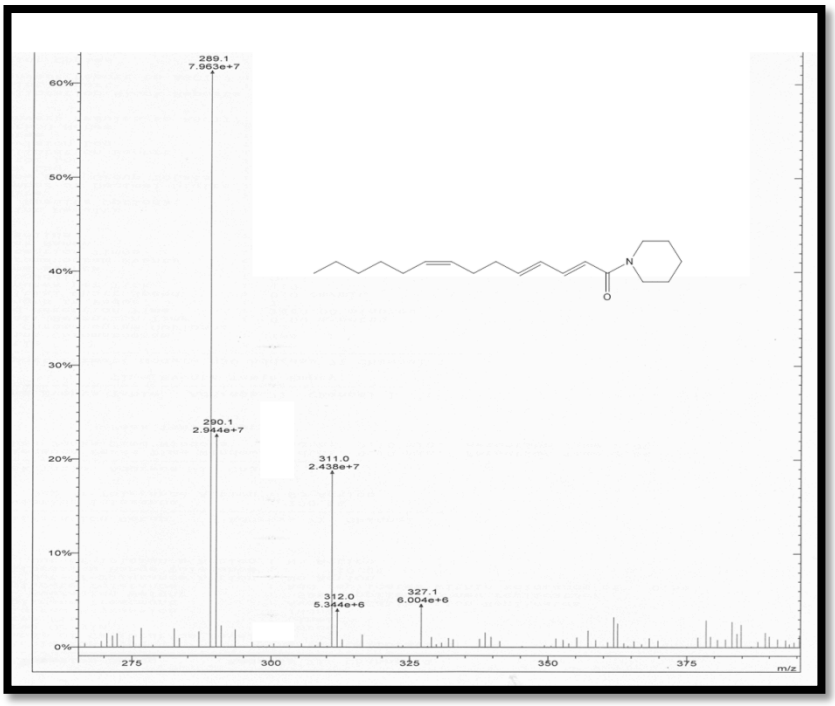

Figure 86. ESI mass spectrum of compound **6**

Pontica epoxide (11)

Pontica epoxide (**11**) was identified by comparison of the ^{1}H NMR (Figure 87) chemical shifts data with literature values.[65]

^{13}C NMR assignments for compound **11** (Figure 88), which are lacking in the literature, are also reported (Table 6).

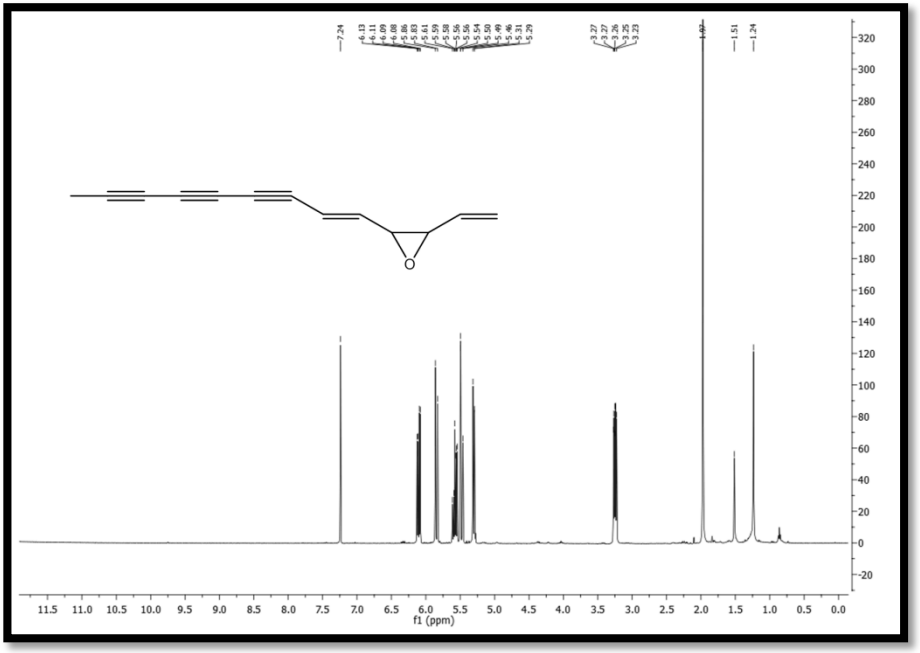

Figure 87. ^{1}H NMR spectrum (500 MHz) of compound **11** measured in $CDCl_3$

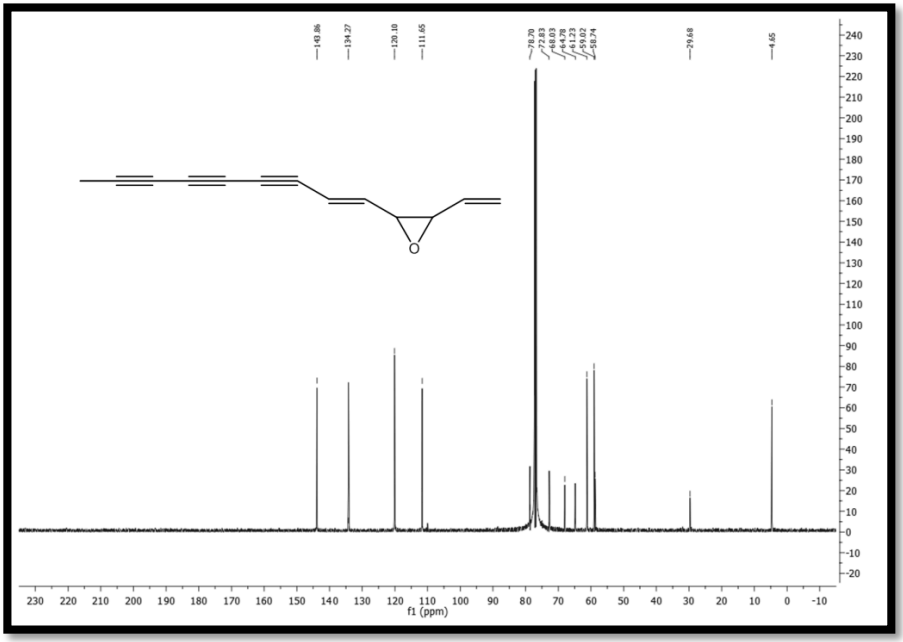

Figure 88. ^{13}C NMR spectrum (100 MHz) of compound **11** measured in $CDCl_3$

Table 6. ^{13}C (100 MHz) NMR spectral data of compound **11** ($CDCl_3$, δ in ppm)

Position	δ_C, multiplicity[a]
1	
2	143.9
3	59.0
4	61.2
5	134.2
6	111.7
7	76.6
8	68.0
9	58.7
10	72.8
11	64.8
12	78.7
13	4.7

Sesamin (13)

Sesamin (**13**) was identified by comparison of the ^{1}H (Figure 89) and ^{13}C (Figure 90) NMR chemical shifts data with literature values.[147]

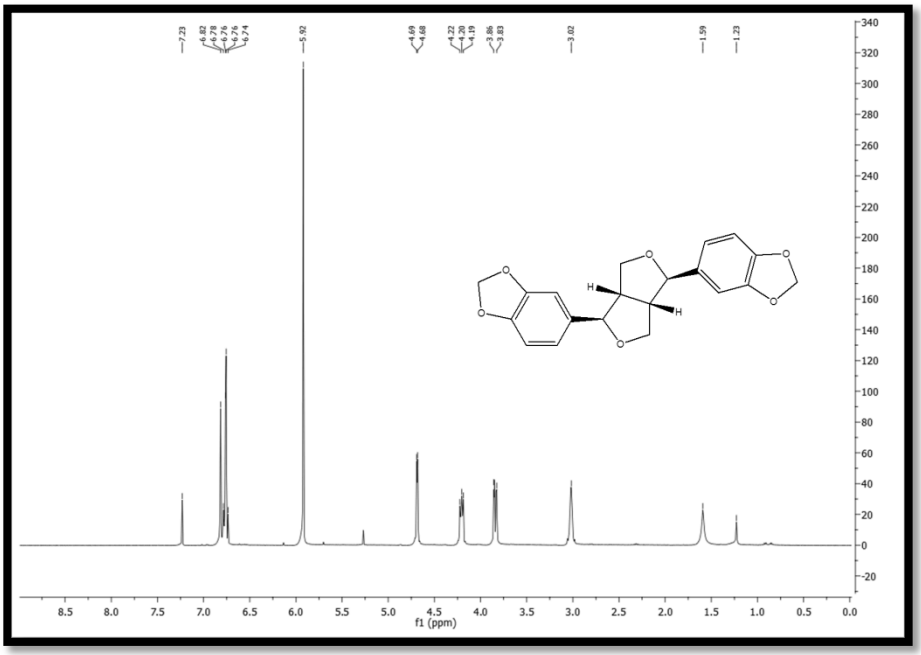

Figure 89. ^{1}H NMR spectrum (500 MHz) of compound **13** measured in $CDCl_3$

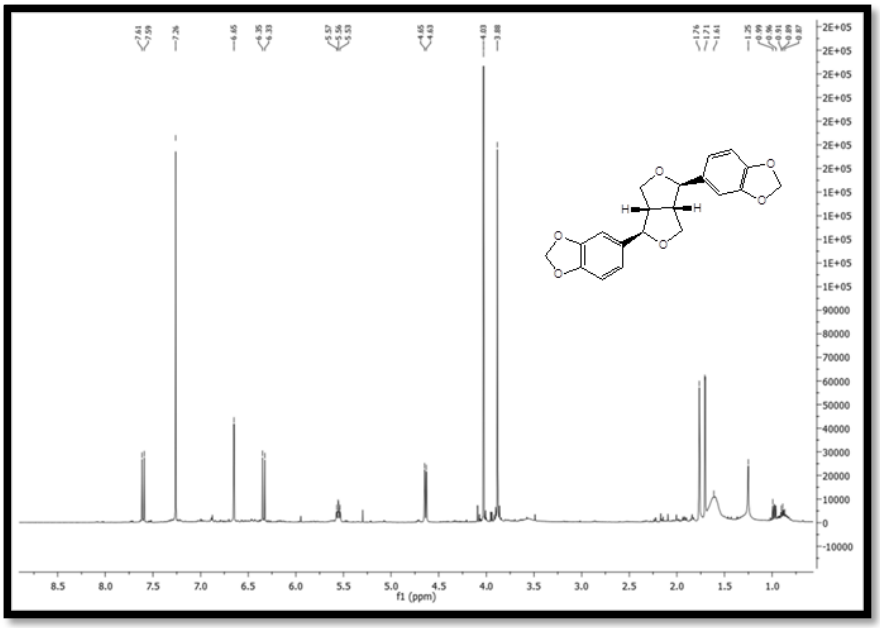

Figure 90. ^{13}C NMR spectrum (100 MHz) of compound **13** measured in $CDCl_3$

Puberulin (14)

Puberulin (**14**) was identified by comparison of the ^{1}H (Figure 91) and APT (Figure 92) NMR chemical shifts with literature values.[148]

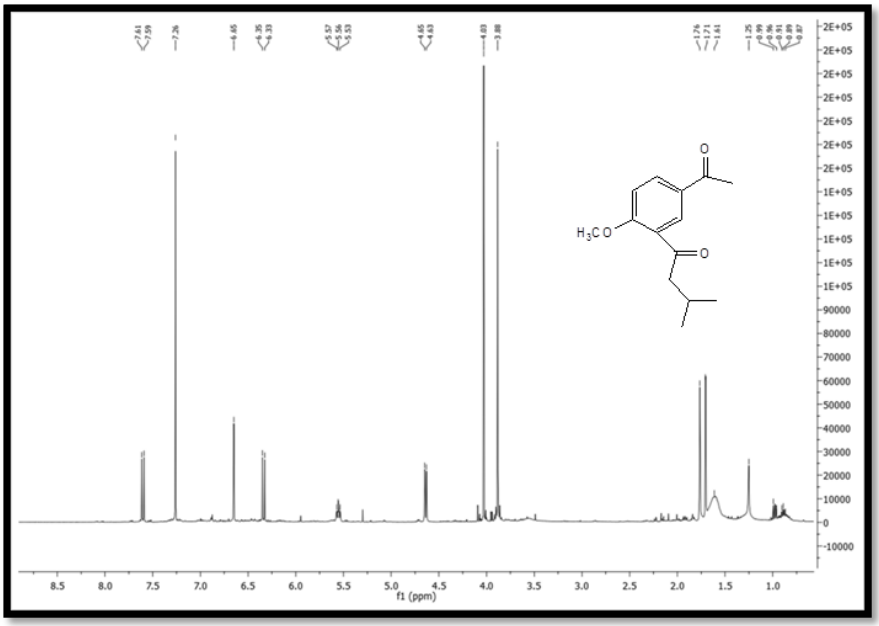

Figure 91. ^{1}H NMR spectrum (500 MHz) of compound **14** measured in $CDCl_3$

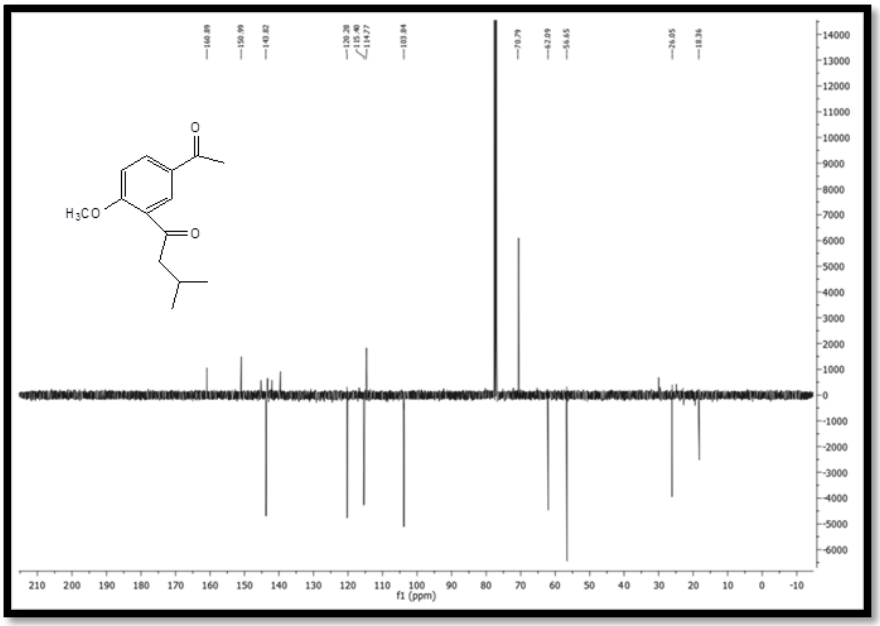

Figure 92. APT NMR spectrum (100 MHz) of compound **14** measured in $CDCl_3$

Espeletone (15)

Espeletone (**15**) was identified by comparison of the ^{1}H (Figure 93) and ^{13}C (Figure 94) NMR chemical shifts data with literature values.[149]

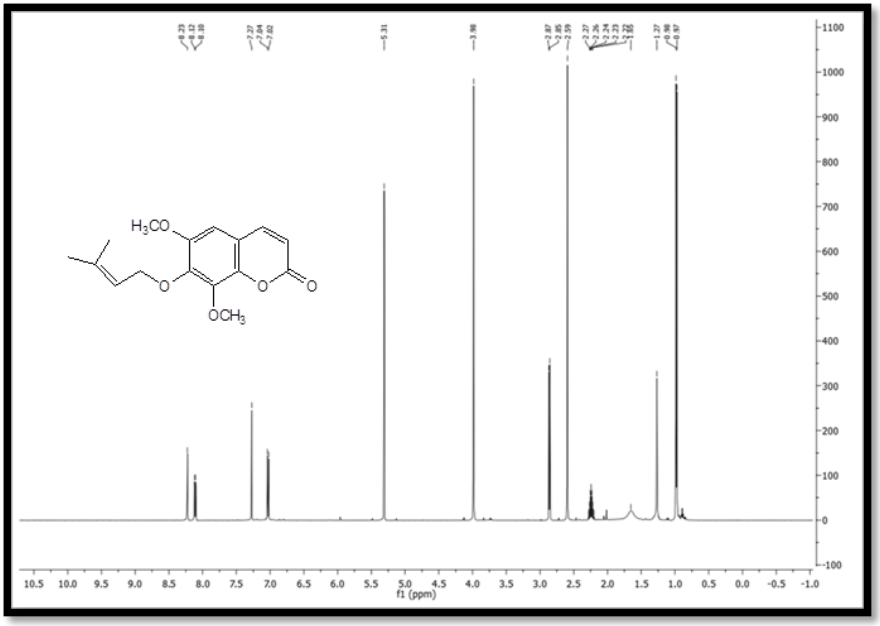

Figure 93. ^{1}H NMR spectrum (500 MHz) of compound **15** measured in $CDCl_3$

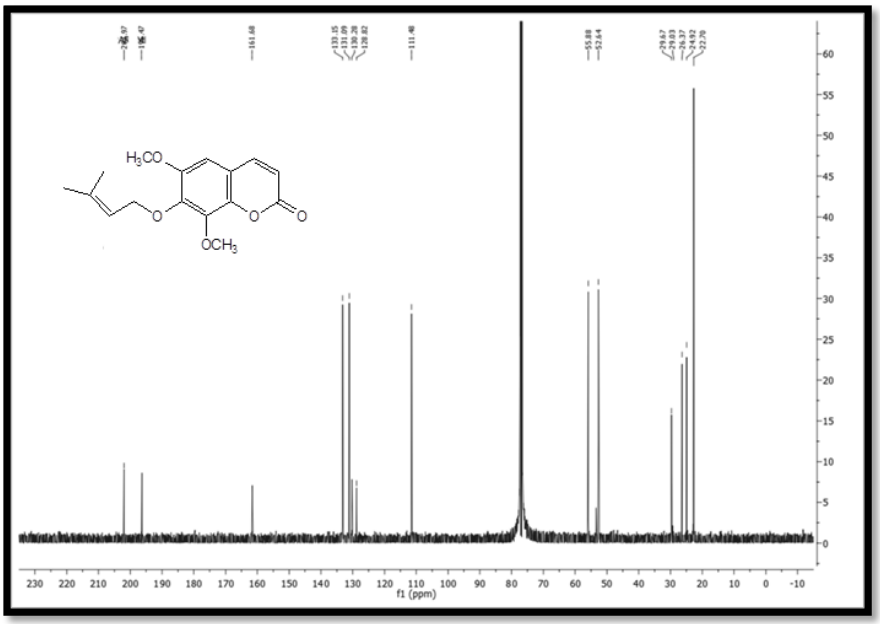

Figure 94. ^{13}C NMR spectrum (100 MHz) of compound **15** measured in $CDCl_3$

(2*Z*,6*E*,10*E*)-geranylgeraniol (16)

(2*Z*,6*E*,10*E*)-geranylgeraniol (16) was identified by comparison of the ^{1}H (Figure 95) and ^{13}C (Figure 96) NMR chemical shifts data with literature values.[150]

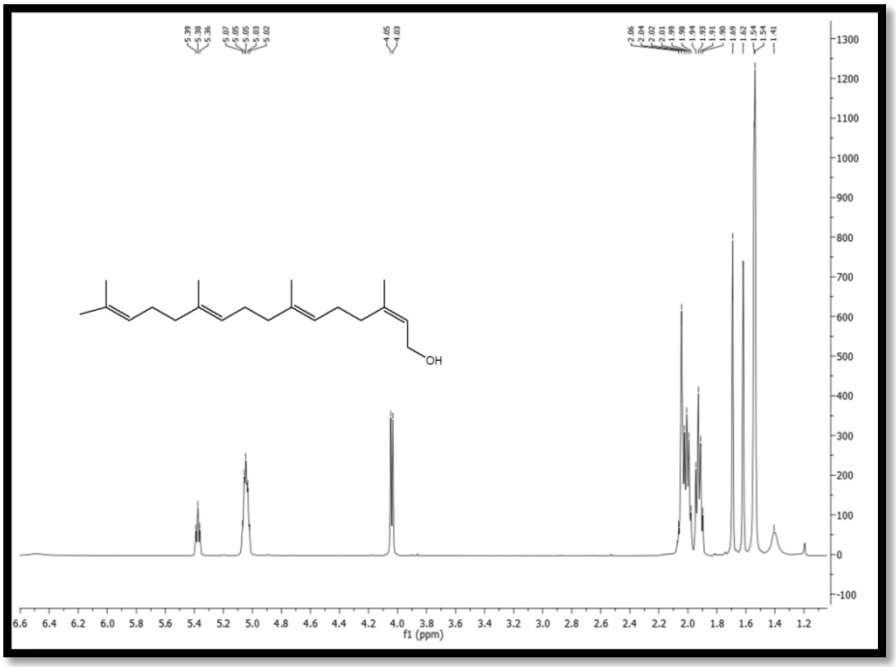

Figure 95. ^{1}H NMR spectrum (500 MHz) of compound **16** measured in $CDCl_3$

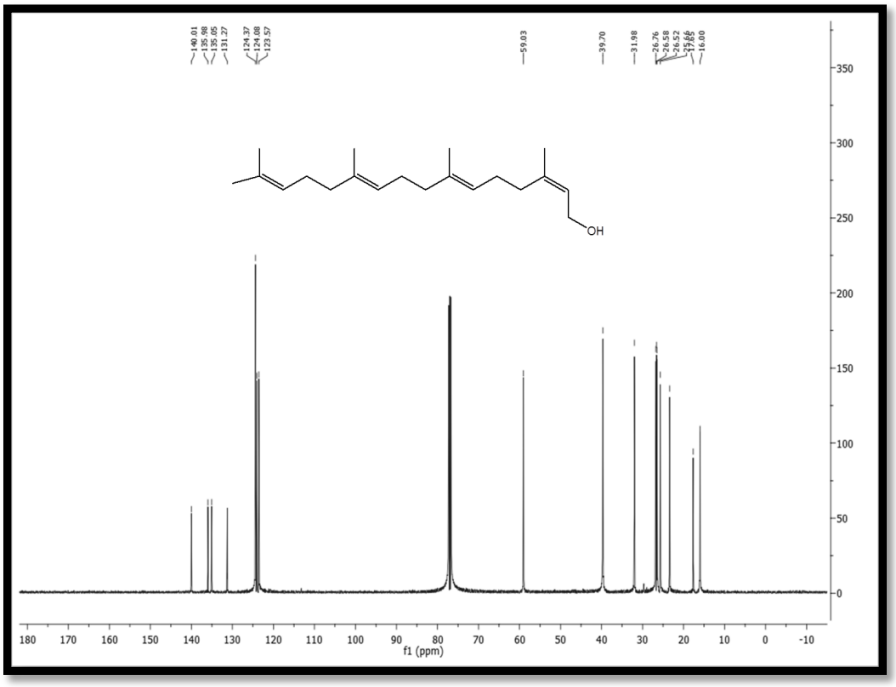

Figure 96. ^{13}C NMR spectrum (100 MHz) of compound **16** measured in $CDCl_3$

11.4 Extraction of *S. glutinosa* Aerial Parts

The powered dried aerial parts of *S. glutinosa* (548 g) were succesively extracted with DCM and MeOH yielding 52.4 g and 110 g, respectively. The extraction was carried out by percolation during the day and at night the roots were left to maceration.

11.5 Isolation of Metabolites from *S. glutinosa*

The DCM extract exhibited good binding affinity to μ and δ opioid receptors (Table 1) and was therefore subjected to fractionation by silica gel vacuum-liquid chromatography (VLC) and column chromatography (silica gel and Sephadex LH 20) to give four known flavones (**17**, **18**, **19**, **20**), one known *neo*-clerodane (**21**) and one new *neo*-clerodane (**22**) (Figure 97).

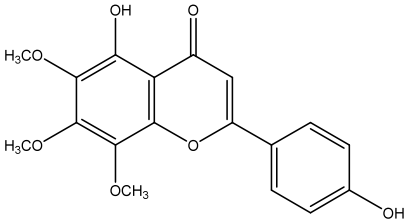

xanthomicrol (**17**)

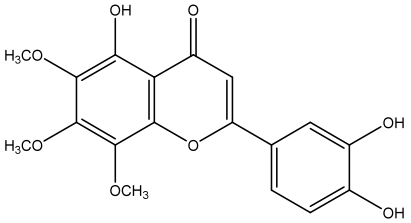

sideritoflavone (**18**)

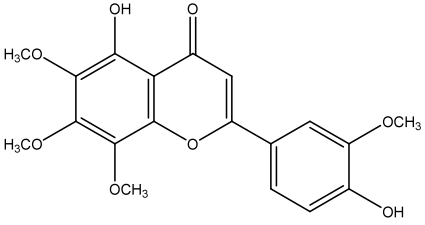

8-methoxycirsilineol (**19**)

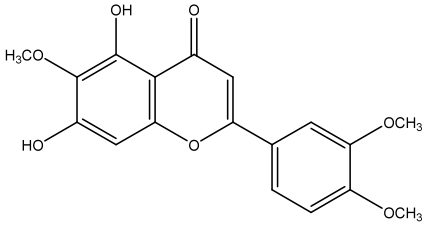

eupatilin (**20**)

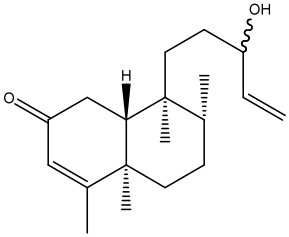

roseostachenone (**21**)

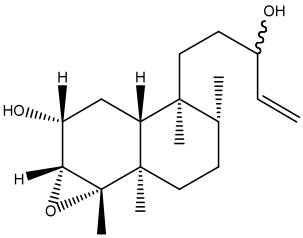

3,4alfa-epoxy roseostachenol (**22**)

Figure 97. Structures of the compounds isolated from *S. glutinosa*

11.6 Semi-Synthesis of 5-demethyltangeretin and Tangeretin

In order to find a structure-activity relationship, two key derivatives, 5-demethyltangeretin (**23**)[150] and tangeretin (**24**)[151,152] were also prepared by methylation with dimethyl sulfate of compound **17** (Figure 98).

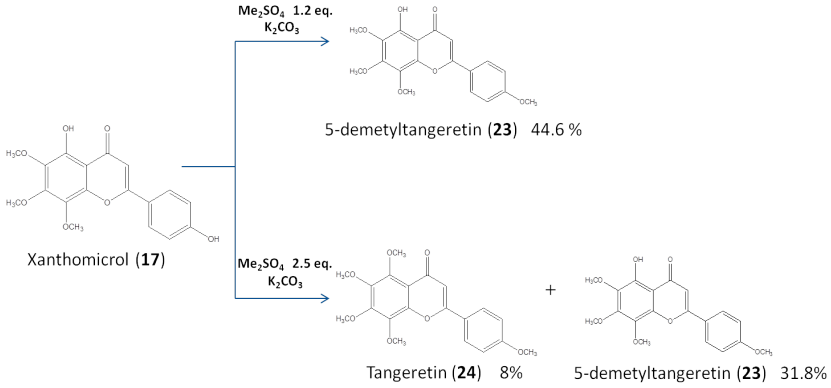

Figure 98. Synthesis of compounds **23** and **24**

11.7 STRUCTURE ELUCIDATION OF SECONDARY METABOLITES FROM *S. GLUTINOSA*

11.7.1 Structure Elucidation of Compound 22

Compound **22** was obtained as white amorphous solid. The ^{13}C NMR spectrum of compound **22** (Figure 100) exhibited 20 carbon signals, which were sorted by APT NMR (Figure 101) into five CH_3, six CH_2, five CH, and four quaternary carbons (Table 7). This corresponded to the molecular formula $C_{20}H_{34}O_3$, in agreement with a pseudomolecular ion at *m/z* 345.2418 $[M + Na]^+$ (calc. 345.2406) in HR-TOF-ESI mass spectrum (Figure 99).

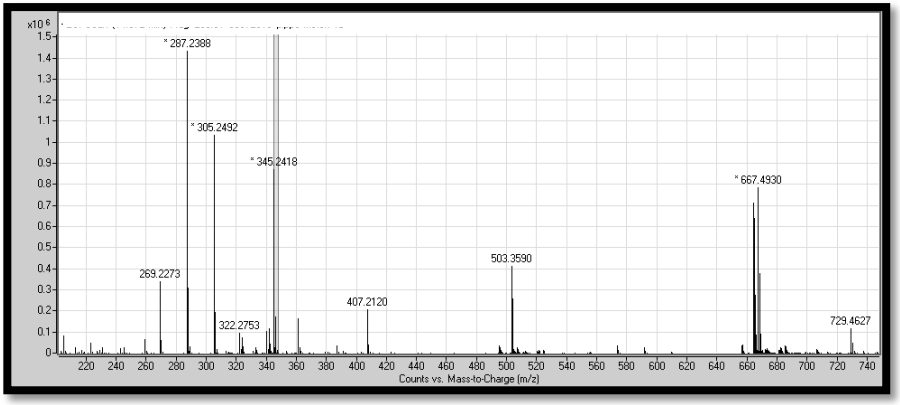

Figure 99. HR-TOF-ESIMS spectrum of **22**

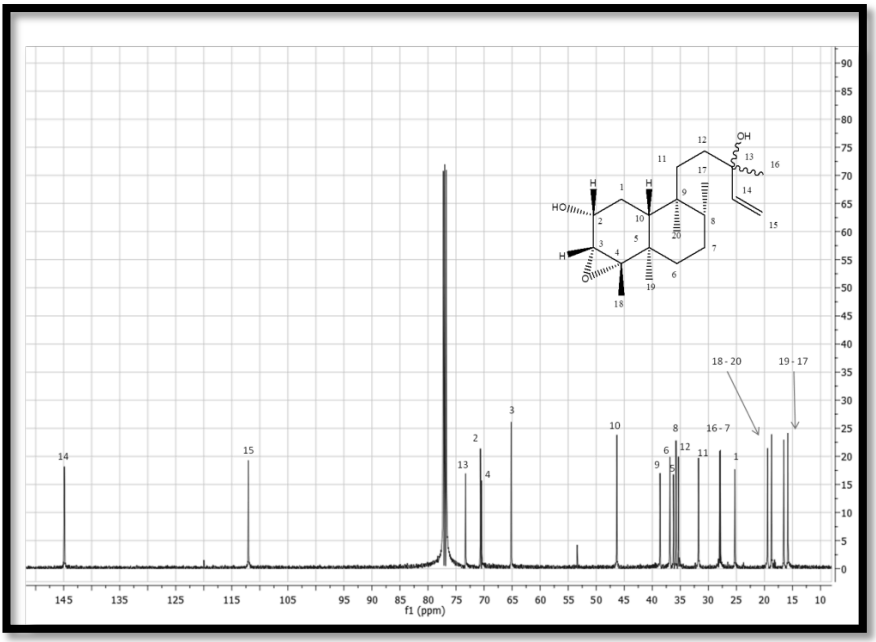

Figure 100. ^{13}C NMR spectrum (100 MHz) of compound **22** measured in $CDCl_3$

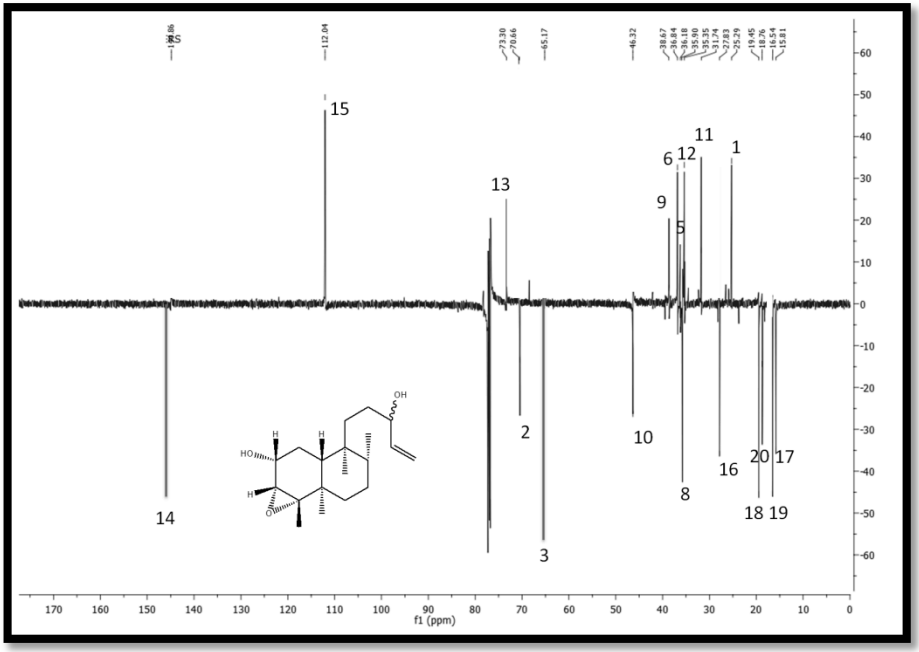

Figure 101. APT NMR spectrum (100 MHz) of compound **22** measured in $CDCl_3$

The ^{1}H NMR spectrum of **22** (Figure 102) (Table 7) exhibited four methyl groups at δ_H 0.66 (3H, s, H_3-20), 1.04 (3H, s, H_3-19), 1.20 (3H, s, H_3-18), and 1.28 (3H, s, H_3-16), one secondary methyl group at δ_H 0.76 (3H, d, J = 6.5 Hz, H_3-17), a vinyl system (δ_H 5.08, 1H, dd, J = 1, 10.8 Hz, H-15A; 5.21, 1H, dd, J = 1, 17.2 Hz, H-15B; 5.88, 1H, dd, J = 10.8, 17.2 Hz, H-14), two oxygenated methine protons at δ_H 3.06 (1H, br s, H-3), and 3.90 (1H, ddd, J = 2.0, 6.0 Hz, H-2), two methines at δ_H 0.88 (1H, bd , J = 11.5 Hz), and 1.42 (1H, m, H-8), and partially overlapped resonances due to five methylenes from δ_H 1.16 to δ_H

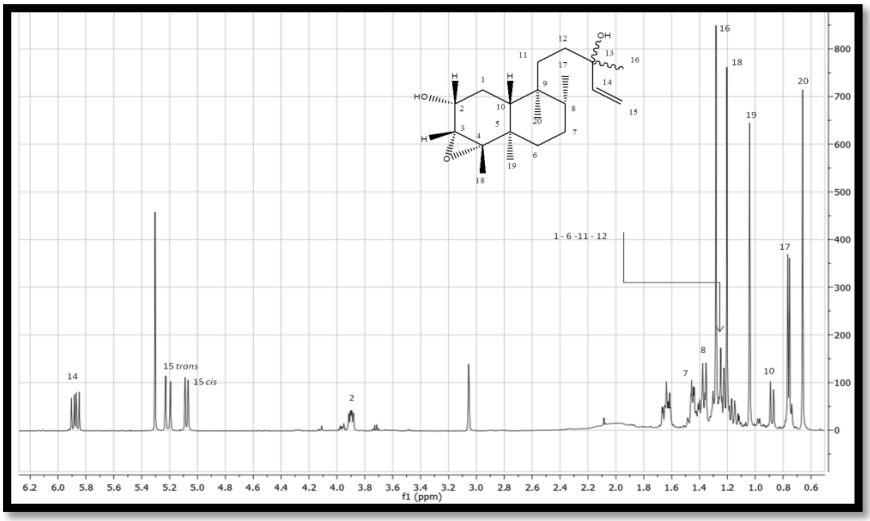

1.65.

Figure 102. ^{1}H NMR spectrum (500 MHz) of compound **22** measured in $CDCl_3$

The ^{1}H and ^{13}C NMR spectra (Table 7) of **22** were very similar to those of the *neo*-clerodane diterpene **21**, roseostachenone, and the main differences between the two compounds were the presence of two oxy-methines at δ_H 3.90 (δ_C 70.7) and δ_H 3.06 (δ_C 65.2) instead of a ketone group (δ_C 200.5) and of an olefinic proton signal at δ_H 5.67 (δ 125.5) in roseostachenone.

The observed HMBC correlations of the oxy-methine at δ_H 3.06 with C-1 (δ_C 25.3), C-2 (δ_C 70.7), C-4 (δ_C 70.4), C-18 (δ_C 19.4), and of the further oxy-methine at δ_H 3.90 with C-1 and C-3 (δ_C 65.2), and of methylene protons at δ_H 1.63 and 1.16 with C-2, C-3, C-5 (δ_C 36.2), and C-10 (δ_C 46.3) (Figure 104-105), suggested that the two oxy-methine protons at δ_H 3.90 and δ_H 3.06 were attached to C-2 and C-3, respectively.

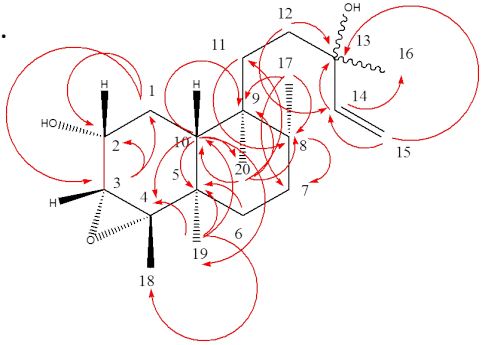

Figure 103.Main HMBC correlations of compound **22**

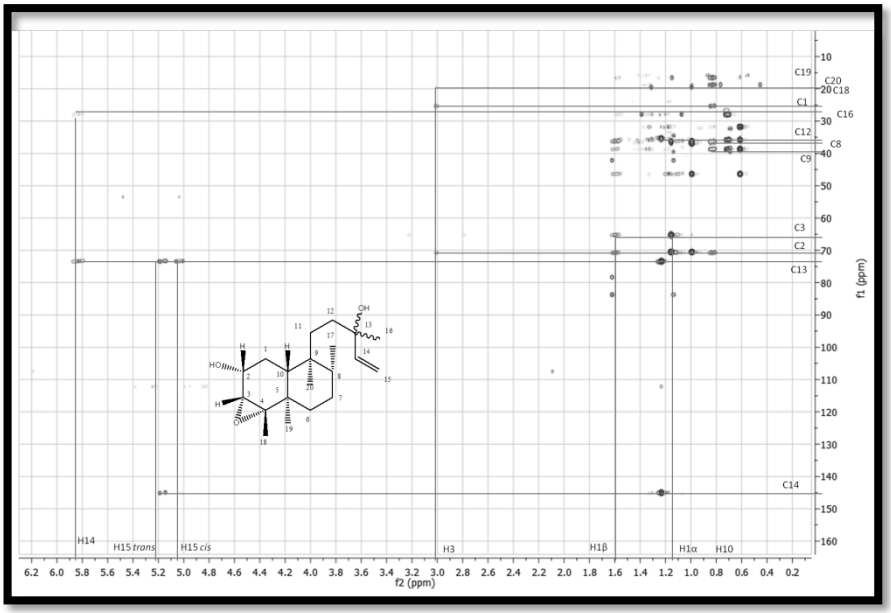

Figure 104. HMBC spectrum (500 Mhz) of compound **22** measured in $CDCl_3$

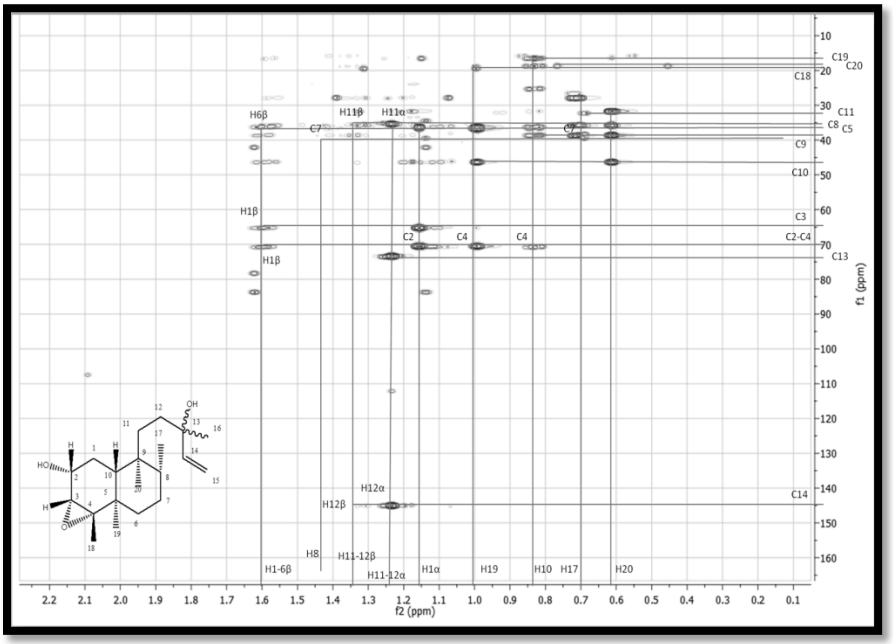

Figure 105. HMBC spectrum (500 Mhz) of compound **22** measured in $CDCl_3$

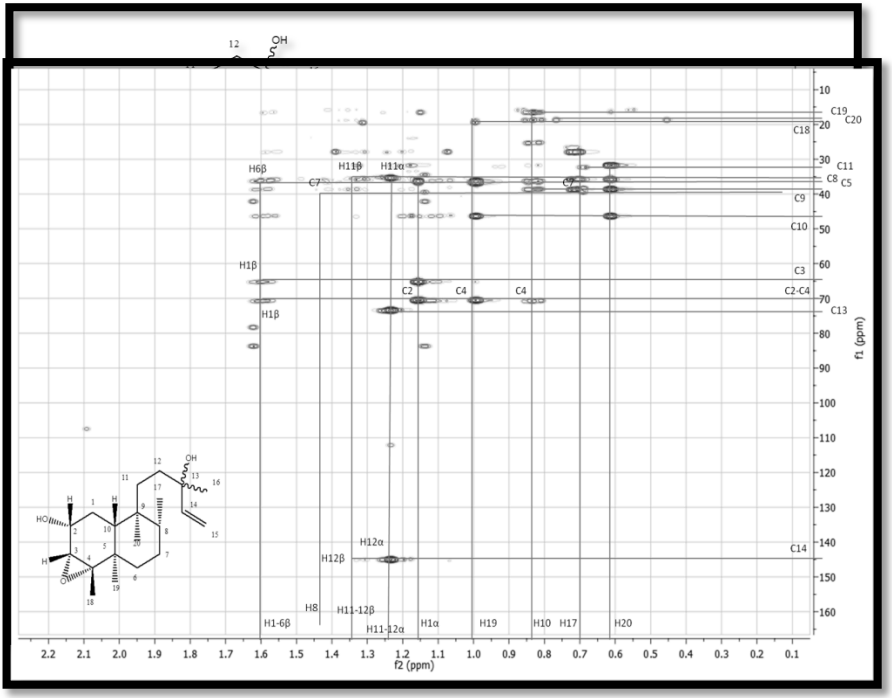

Figure 106. HSQC spectrum (500 Mhz) of compound **22** measured in $CDCl_3$

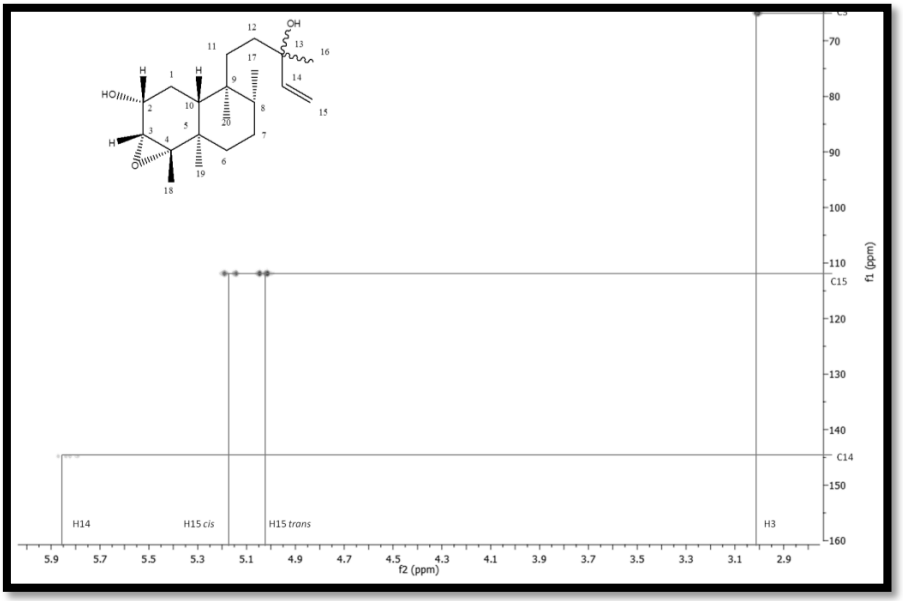

Figure 107.HSQC spectrum (500 Mhz) of compound **22** measured in $CDCl_3$

The location of the above mentioned protons were confirmed by DQF-COSY experiments. In fact, in the COSY spectrum the proton at δ_H 3.90 correlated with the methine at δ_H 3.06 and with the methylene protons at δ_H 1.63 and 1.16 while the methine at 3.06 ppm showed cross-peaks with the proton at 3.90 but not with those

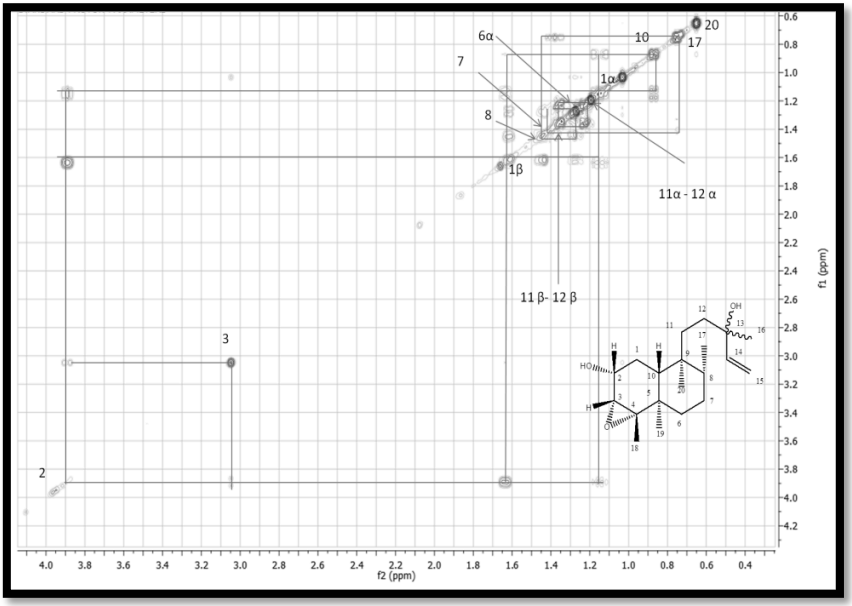

at 1.63 and 1.16 ppm (Figure 108-109).

Figure 108. DQF-COSY (500 MHz) of compound **22**

Since compound **22** has 4° of unsaturation, **22** may also contain one epoxide ring. This proposal was confirmed by a broad singlet at δ_H 3.06 (H-3) in the ^{1}H NMR spectrum, indicating a 3,4-epoxy group.

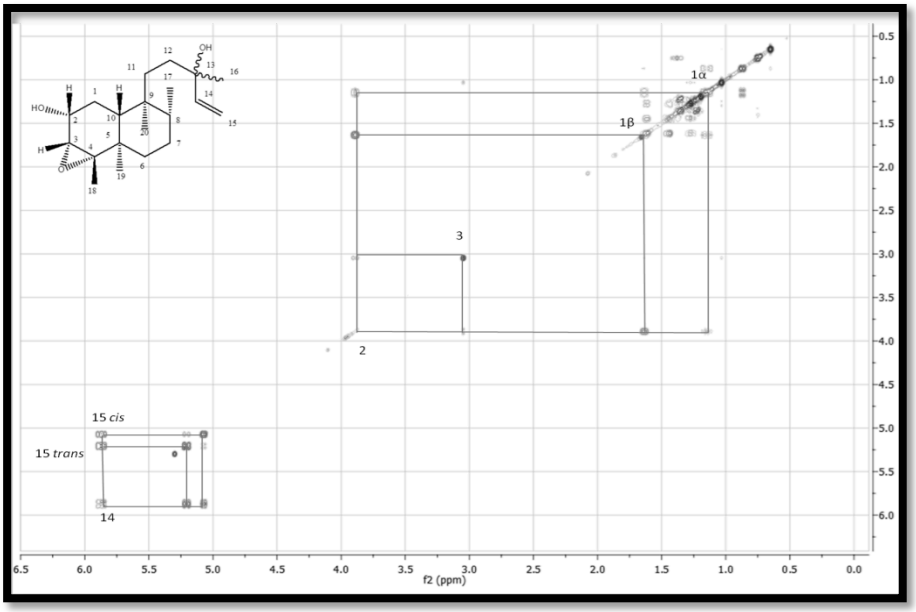

Figure 109. DQF-COSY (500 MHz) of compound **22**

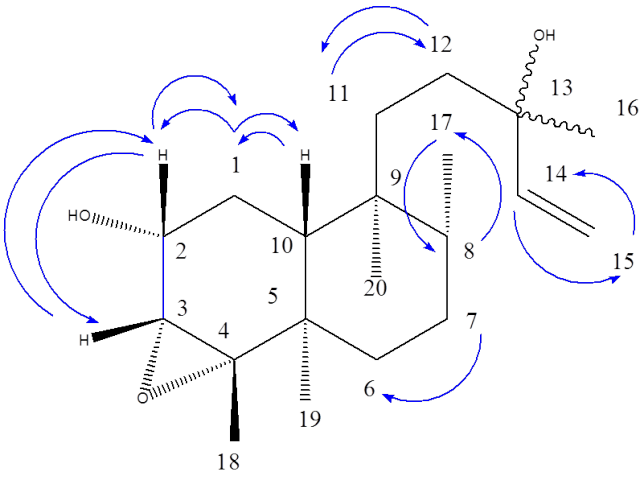

Figure 110. Main COSY correlations of compound **22**

The relative configuration of **22** was elucidated analyzing the ^{13}C NMR values and by ROESY experiment. The chemical shifts of C-19 and C-20 clearly indicated a *trans*-AB ring junction.[153] ROESY cross-peaks of H-2/H-10, H-1β/H-2, and H-2/H-3 were congruent with a α-orientation both for the C-2 hydroxyl group and 3,4-epoxy group (Figure 111-112). Thus, compound **22** is 3,4α-epoxy roseostachenol.

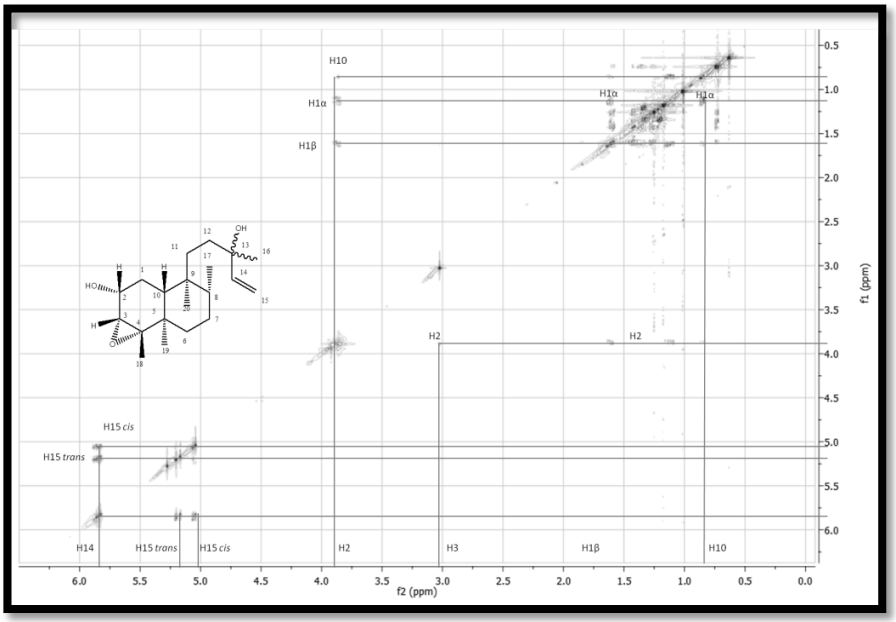

Figure 111. ROESY spectrum (500 MHz) of compound **22** measured in $CDCl_3$

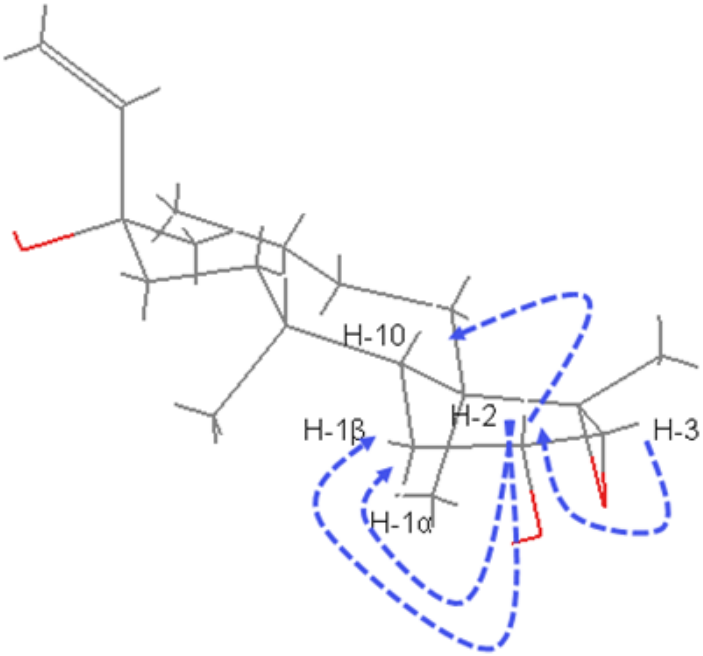

Figure 112. KEY ROE correlations observed for compound **22**

Table 7. ^{1}H (500 MHz) and ^{13}C (100 MHz) NMR spectral data of compounds **4** ($CDCl_3$, δ in ppm)

Position	**δ_C, multiplicity**[a]	**δ_H, multiplicity**[b]
1	25.3, t	α 1.16,m ; β 1.63, m
2	70.7, d	3.90, m
3	65.2, d	3.06,d,br
4	70.4, s	
5	36.2, s	
6	36.8, t	α 1.25,m ; β 1.65, m
7	27.9, t	1.45, m
8	35.8, d	1.42, m
9	38.6, s	
10	46.3, d	0.88, d,br
11	31.8, t	α 1.24,m ; β 1.36, m
12	35.3, t	α 1.23,m ; β 1.37, m
13	73.3, s	
14	144.9, d	5.88, dd
15	112.0, t	*cis* 5.08, dd *trans* 5.21, dd
16	27.8, q	1.28, s
17	15.8, q	0.76, d
18	19.4, q	1.20, s
19	16.5, q	1.04, s
20	18.7, q	0.66, s

[a]Multiplicity was determined by analysis of the APT spectrum. [b]J values (Hz) in parentheses.

11.7.2 Structure Elucidation of Known Compounds

The following known compounds were also identified: xanthomicrol (**17**), sideritoflavone (**18**), 8-methoxycirsilineol (**19**), eupatilin (**20**), roseostachenone (**21**), 5-demethyltangeretin (**23**) and tangeretin (**24**). They were confirmed by comparison of physical and spectroscopic data (UV, ^{1}H and ^{13}C NMR, and MS) with literature values.

Xanthomicrol (17)

Xanthomicrol (**17**) was identified by comparison of the ^{1}H (Figure 113) and ^{13}C (Figure 114) NMR chemical shifts data with literature values.[154]

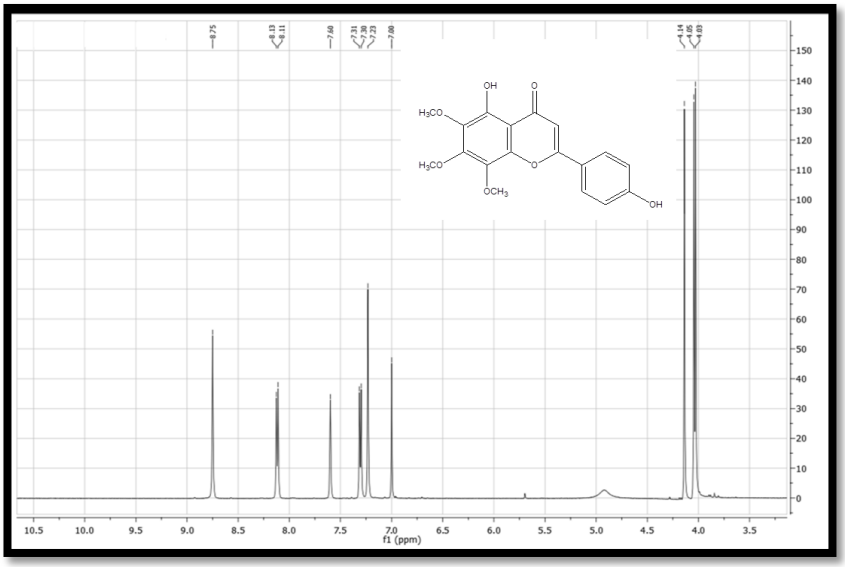

Figure 113. ^{1}H NMR spectrum (500 MHz) of compound **17** measured in $CDCl_3$

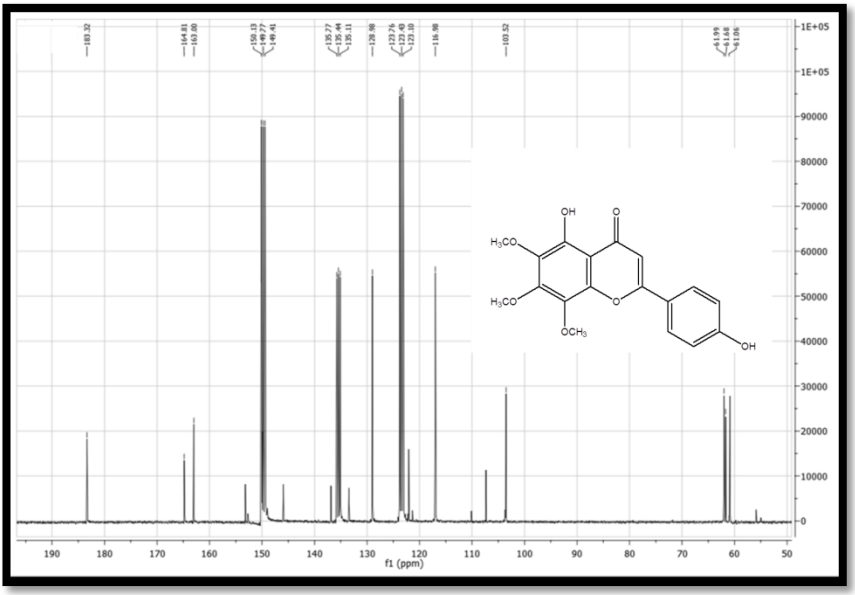

Figure 114. ^{13}C NMR spectrum (100 MHz) of compound **17** measured in $CDCl_3$

Sideritoflavone (18)

Sideritoflavone (**18**) was identified by comparison of the ^{1}H (Figure 115) and ^{13}C (Figure 116) NMR chemical shifts data with literature values.[155]

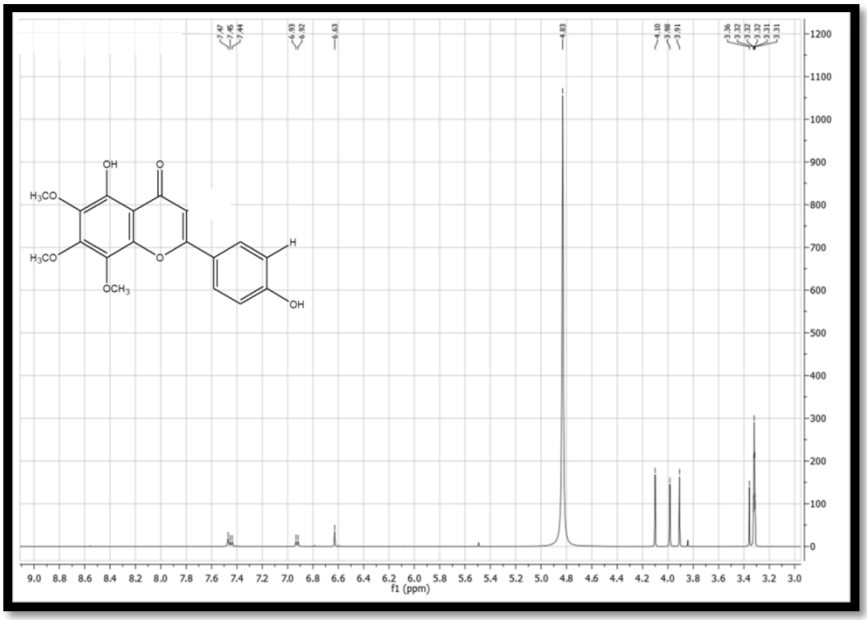

Figure 115. ^{1}H NMR spectrum (500 MHz) of compound **18** measured in $CDCl_3$

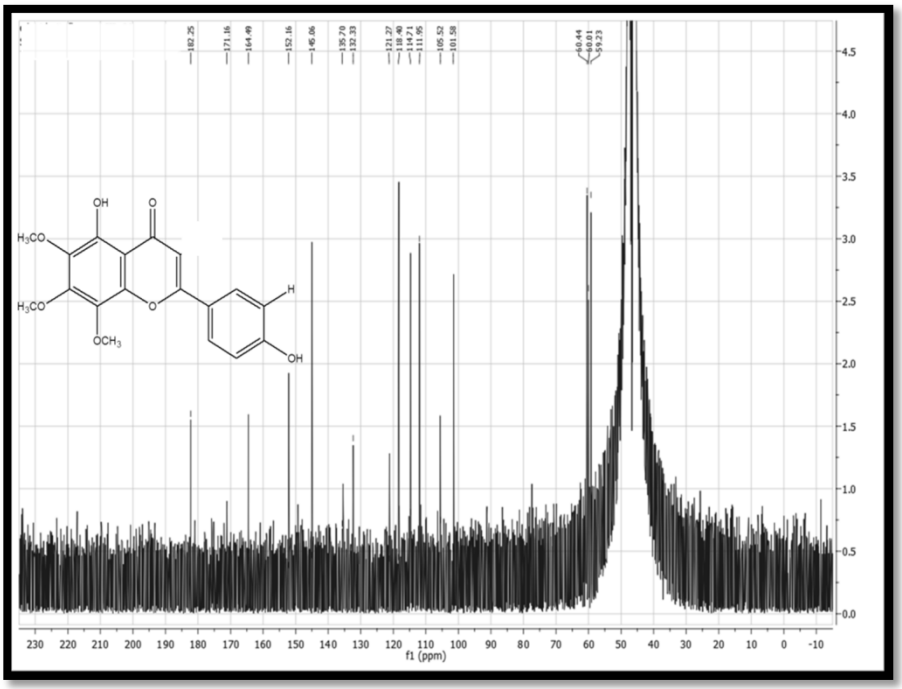

Figure 116. ^{13}C NMR spectrum (100 MHz) of compound **18** measured in $CDCl_3$

8-methoxycirsilineol (19)

8-methoxycirsilineol (19) was identified by comparison of the ^{1}H (Figure 117) and ^{13}C (Figure 118) NMR chemical shifts data with literature values.[156]

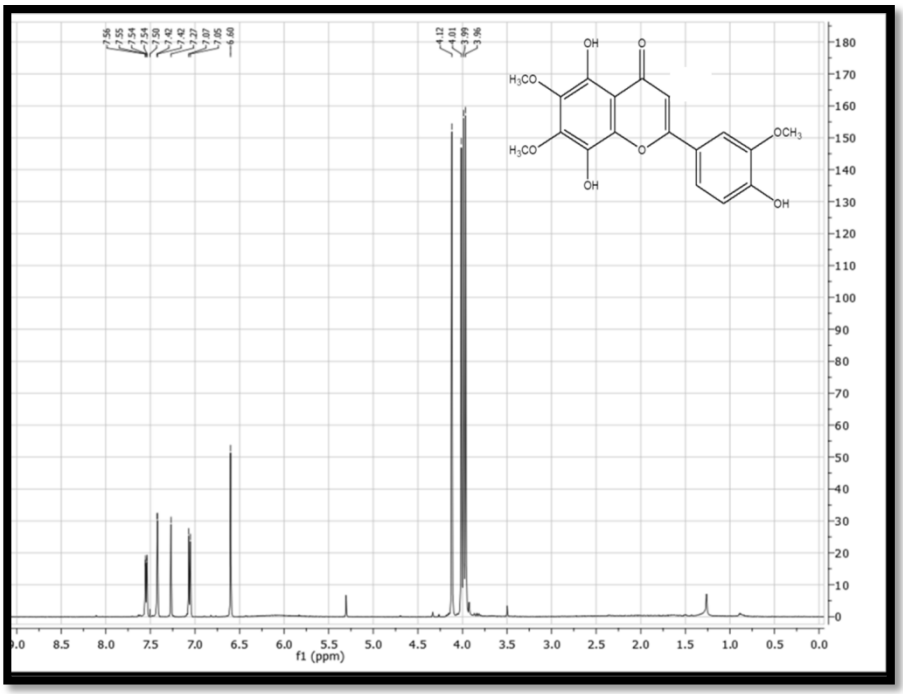

Figure 117. ^{1}H NMR spectrum (500 MHz) of compound **19** measured in $CDCl_3$

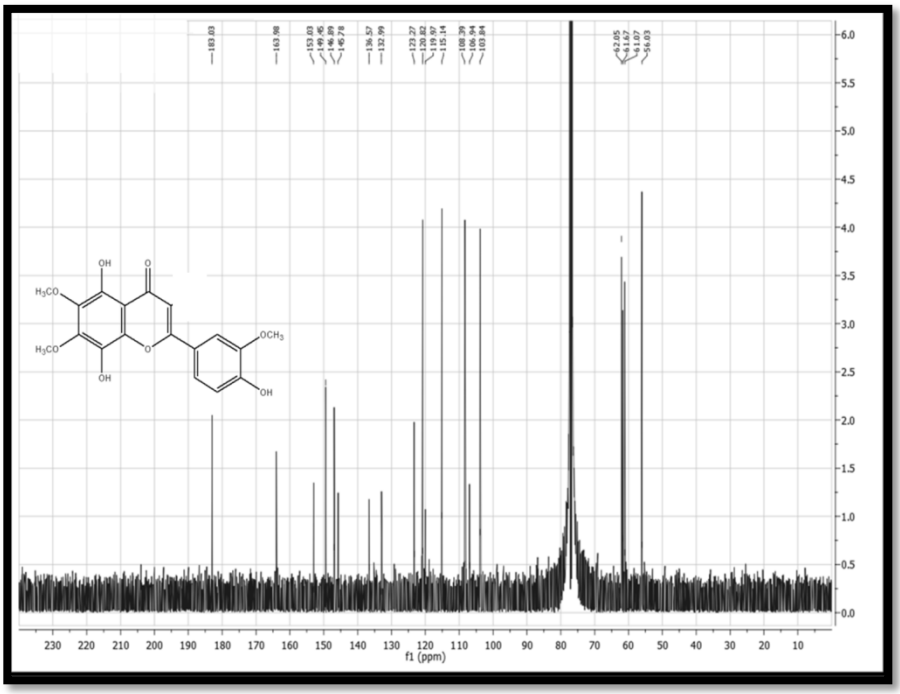

Figure 118. ^{13}C NMR spectrum (100 MHz) of compound **19** measured in $CDCl_3$

Eupatilin (20)

Eupatilin (**20**) was identified by comparison of the ^{1}H (Figure 120) and ^{13}C (Figure 121) NMR chemical shifts and EI-MS (Figure 119) data with literature values.[157]

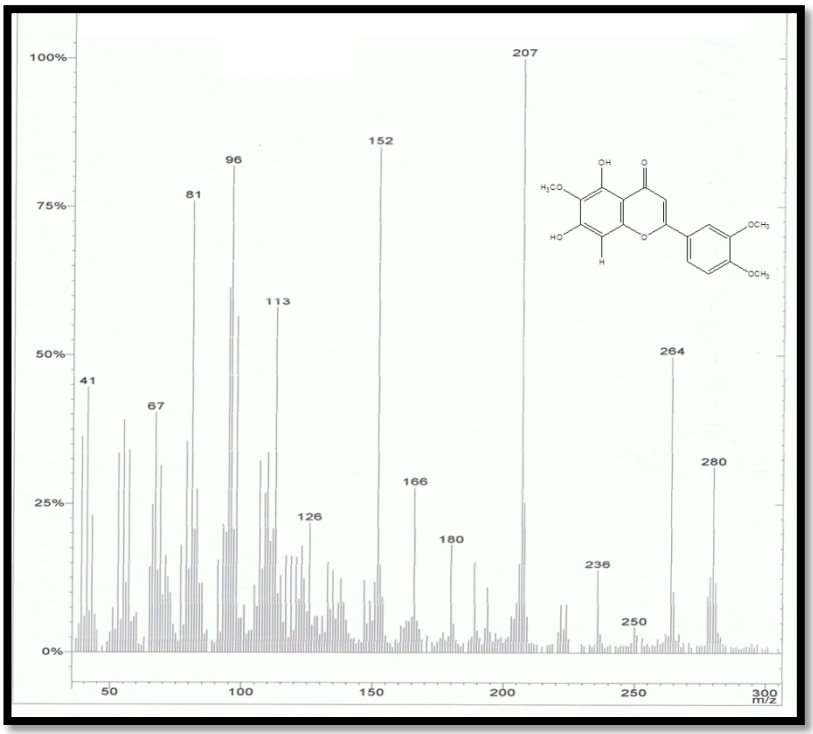

Figure 119. EI mass spectrum of compound **20**

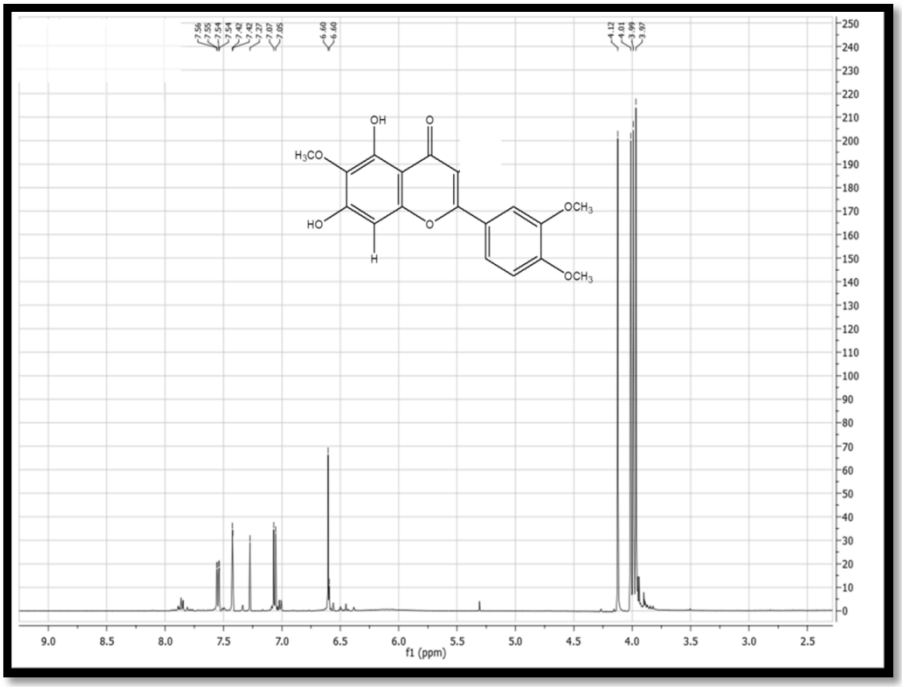

Figure 120. ^{1}H NMR spectrum (500 MHz) of compound **20** measured in $CDCl_3$

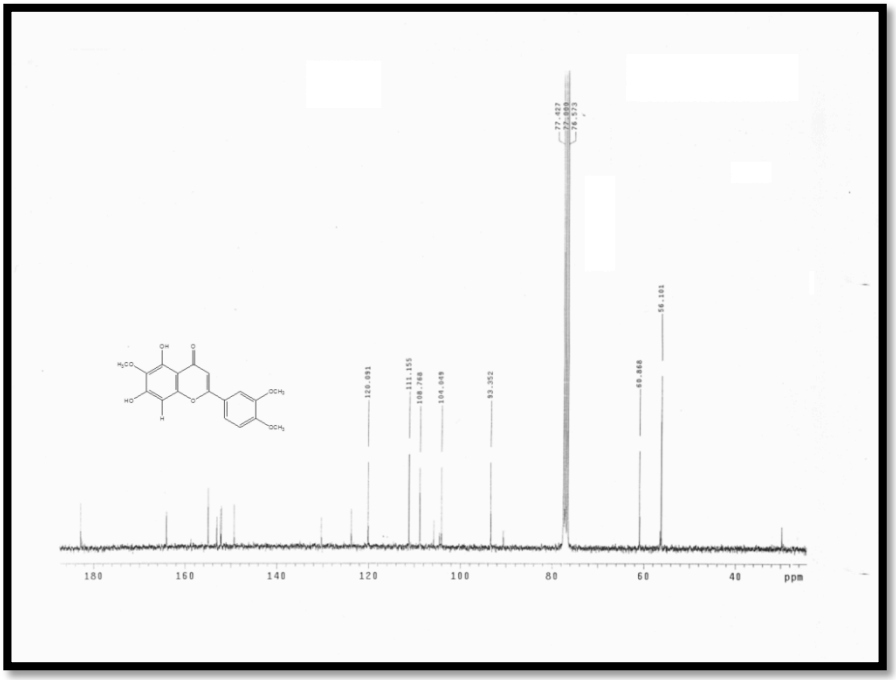

Figure 121. ^{13}C NMR spectrum (100 MHz) of compound **20** measured in $CDCl_3$

Roseostachenone (21)

Roseostachenone (**21**) was identified by comparison of the ^{1}H (Figure 122) and ^{13}C (Figure 123) NMR chemical shifts data with literature values.[97]

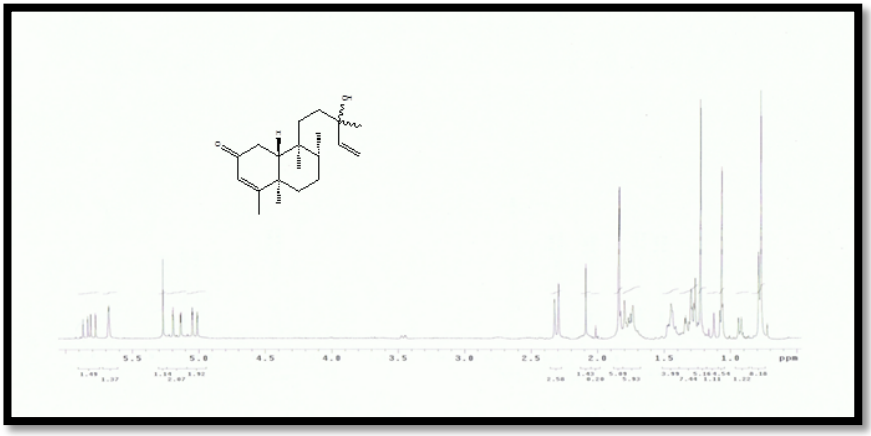

Figure 122. ^{1}H NMR spectrum (400 MHz) of compound **21** measured in $CDCl_3$

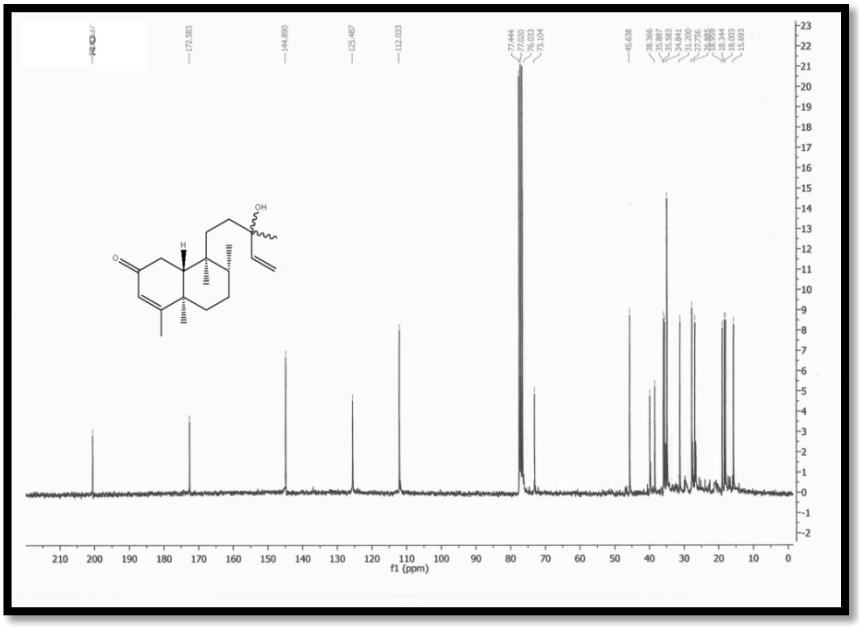

Figure 123. ^{13}C NMR spectrum (100 MHz) of compound **21** measured in $CDCl_3$

5-demethyltangeretin (23)

5-demethyltangeretin (**23**) was identified by comparison of the ^{1}H (Figure 124) and ^{13}C (Figure 125) NMR chemical shifts data with literature values.[150]

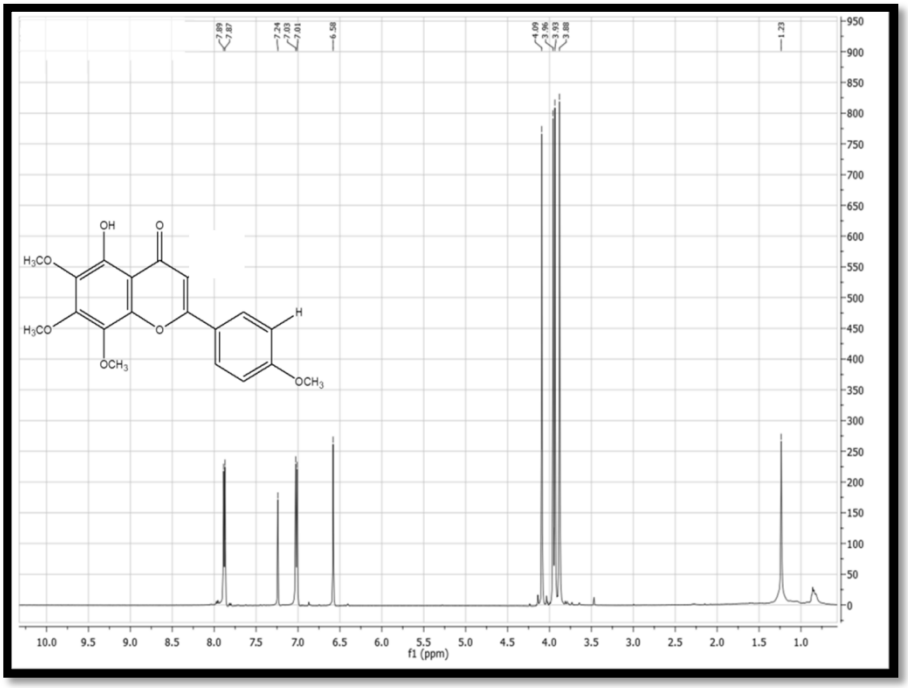

Figure 124. ^{1}H NMR spectrum (500 MHz) of compound **23** measured in $CDCl_3$

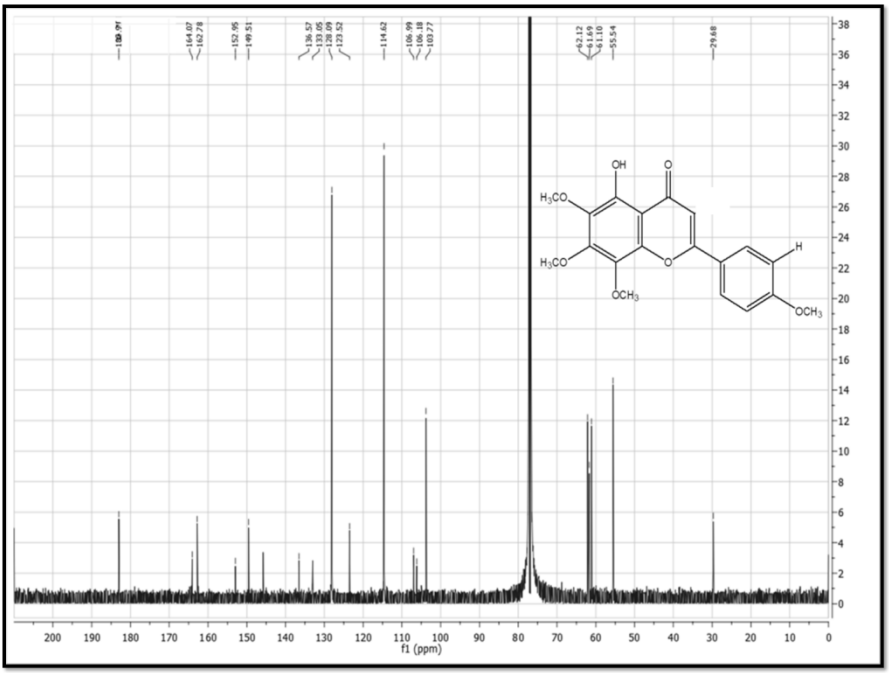

Figure 125. ^{13}C NMR spectrum (100 MHz) of compound **23** measured in $CDCl_3$

Tangeretin (24)

Tangeretin (**24**) was identified by comparison of the ^{1}H (Figure 126) NMR chemical shifts data with literature values.[151,152]

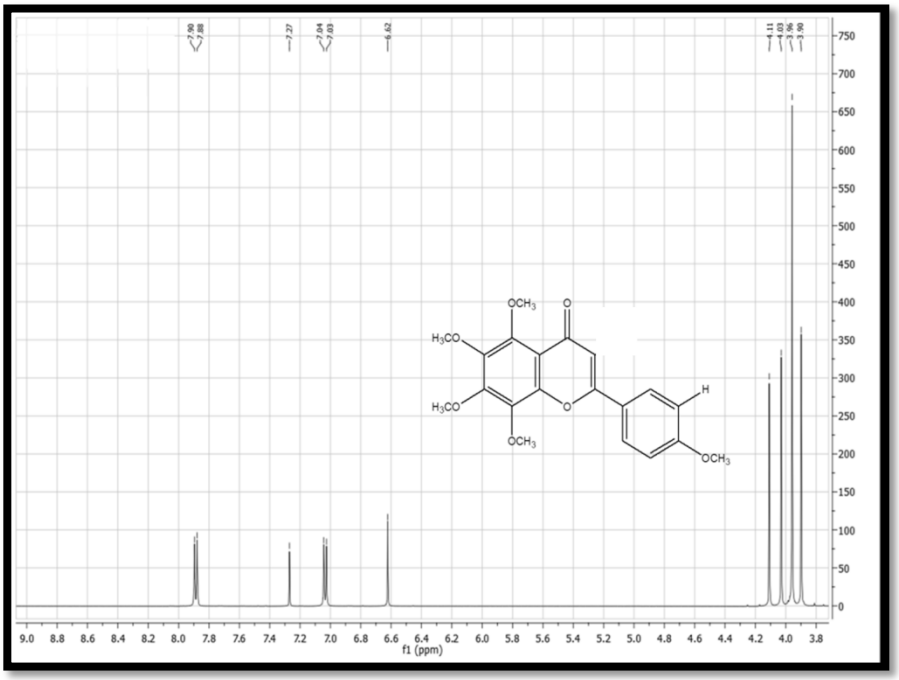

Figure 126. ^{1}H NMR spectrum (500 MHz) of compound **24** measured in $CDCl_3$

11.8 Isolation of Metabolites from *W. somnifera*

The commercial MeOH extract of *W. somnifera* (WSE) (Natural Remedies Pvt. Ltd., Bangalore, India) showed an interesting affinity to $GABA_A$ and a very low affinty to CB and opioid receptors whereas the alcaloid fraction of WSE (WSAE), obtained by liquid-liquid partition of WSE, besides the good affinity towards $GABA_A$, displayed an appreciable affinity to CB, μ and δ opioid receptors (Table 1). As a consequence, WSE and WSAE were subjected to chromatographic techinques to give withanolide A (**30**), withanone (**31**,) and withaferin A (**32**,) (Figure 127) from the first and (+)-sedridine (**25**), anaferine (**26**), tropine (**27**), choline (**28**) and ferulic acid methyl ester (**29**), from the latter (Figure 128).

As far as we know, (+)-sedridine has been isolated from *W. somnifera* for the first time.

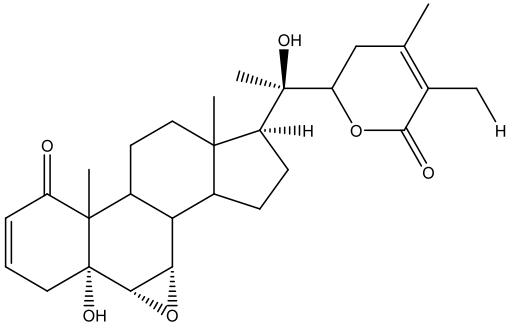

Withanolide A (**30**)

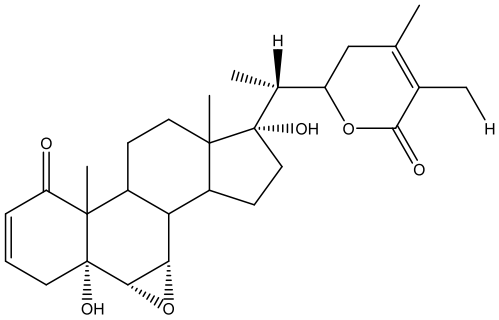

Withanone (**31**)

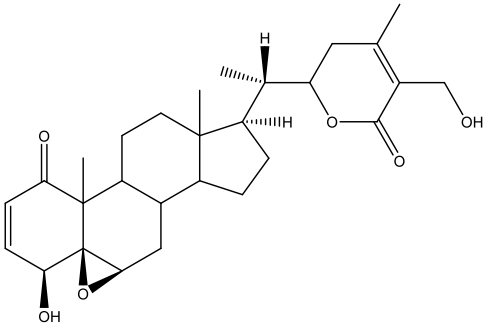

Withaferin A (**32**)

Figure 127. Structure of compounds **30**-**32** isolated from *W. somnifera*

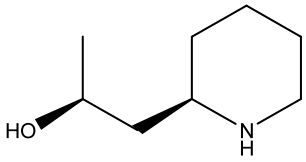

(+)-Sedridine (**25**)

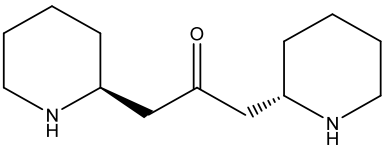

Anaferine (**26**)

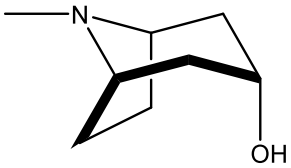

Tropine (**27**)

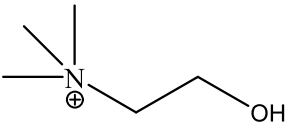

Choline (**28**)

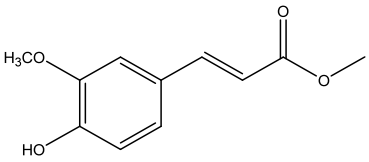

Ferulic acid methyl ester (**29**)

Figure 128. Structure of compounds **25-29** isolated from *W. somnifera*

11.8.1 Structure Elucidation of Known Compounds

The structure of the known metabolites were deduced from NMR spectroscopy, mass spectrometry and optical rotation and confirmed by comparison either with reference compounds (Choline) or with data reported in the literature.

(+)-Sedridine(25)

The structure of (+)-sedridine was confirmed by comparing the MS, ^{1}H, ^{13}C NMR (Figure 129-131) data and optical rotation with those of authentic sample.

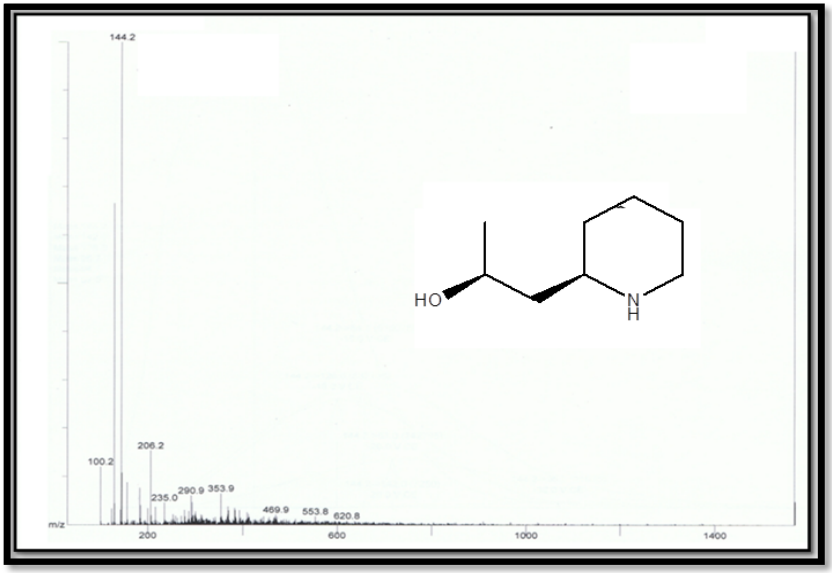

Figure 129. ESI mass spectrum of compound **25**

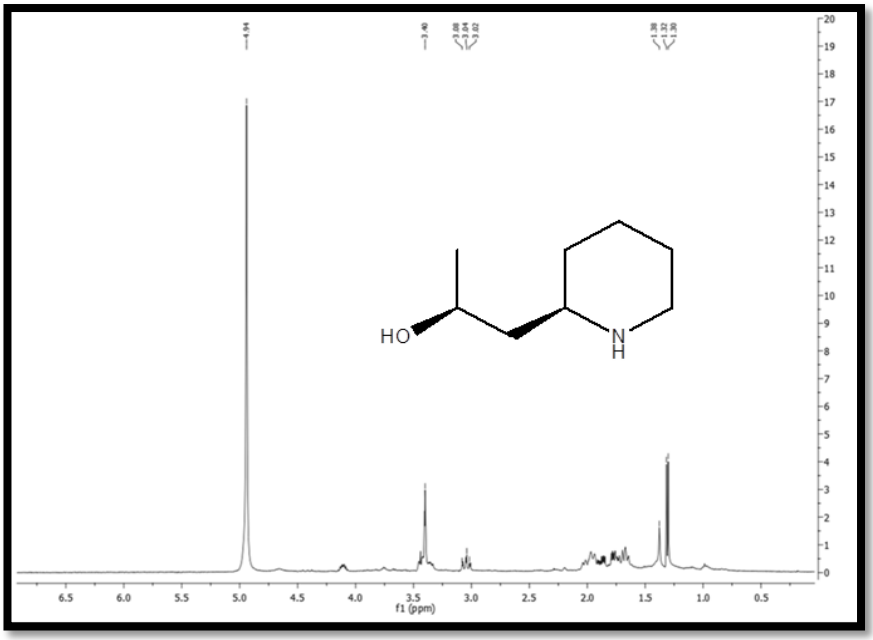

Figure 130. ^{1}H NMR spectrum (500 MHz) of compound **25** measured in $CDCl_3$

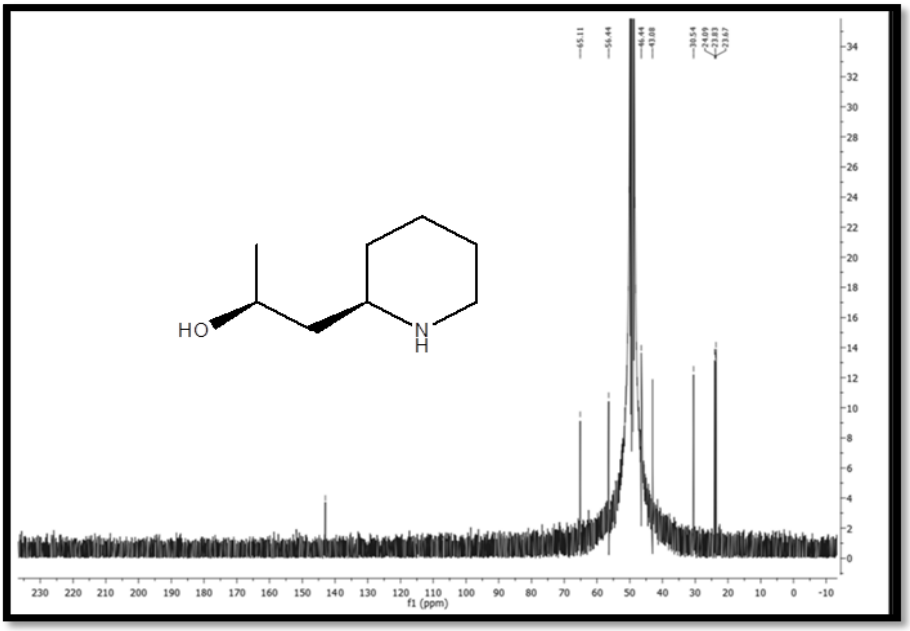

Figure 131. ^{13}C NMR spectrum (100 MHz) of compound **25** measured in $CDCl_3$

Anaferine (26)

Anaferine (**26**) was identified by comparison of the ^{1}H (Figure 133) and ^{13}C (Figure 134) NMR chemical shifts and ESI-MS (Figure132) data with literature values.[120,159]

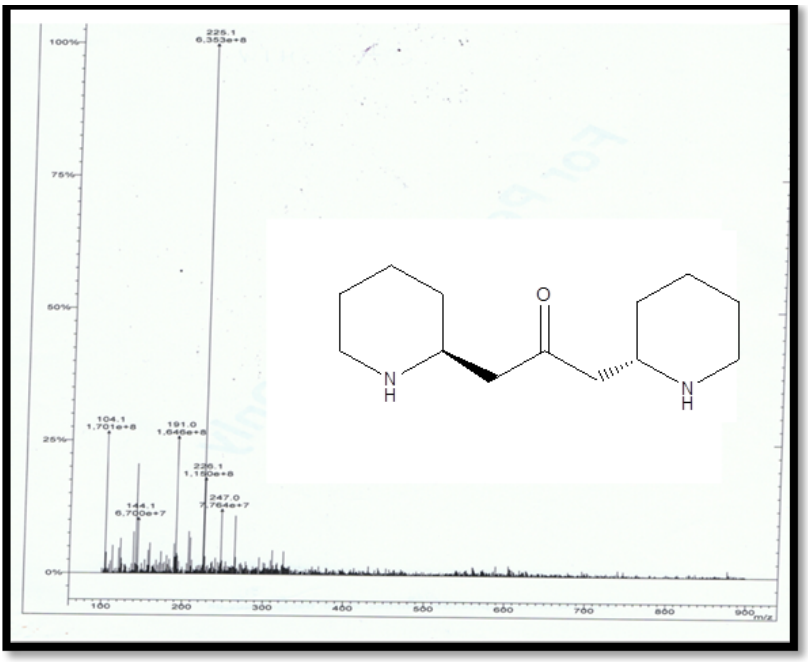

Figure 132. ESI mass spectrum of compound **26**

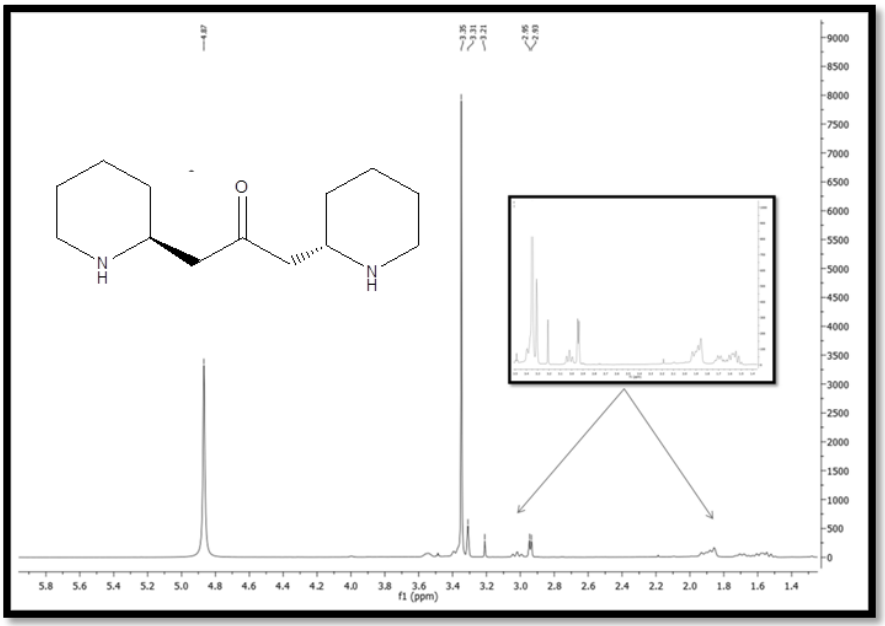

Figure 133. ^{1}H NMR spectrum (500 MHz) of compound **26** measured in $CDCl_3$

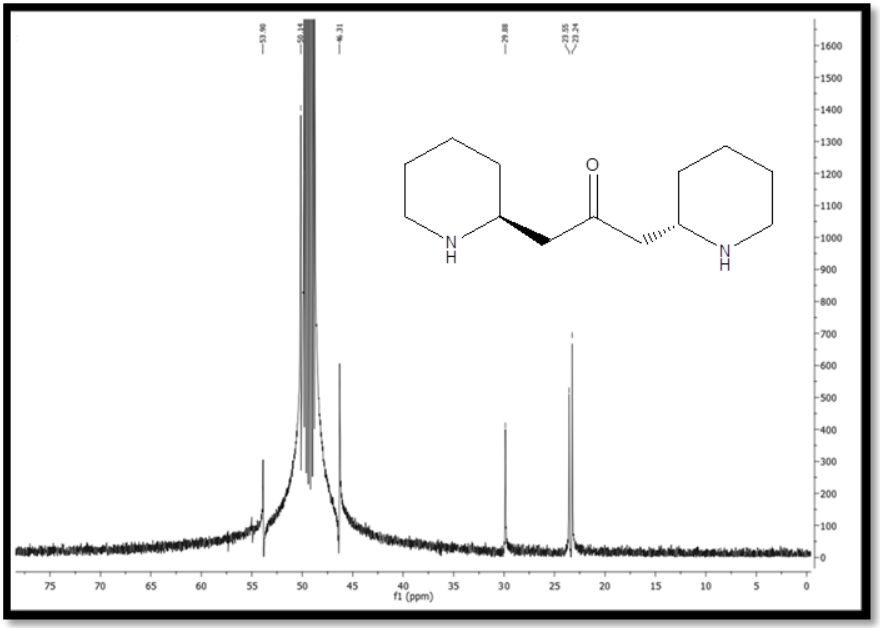

Figure 134. ^{13}C NMR spectrum (100 MHz) of compound 26 measured in $CDCl_3$

Tropine (27)

Tropine (**27**) was identified by comparison of the ^{13}C NMR (Figure 135) chemical shifts data with literature values.[160]

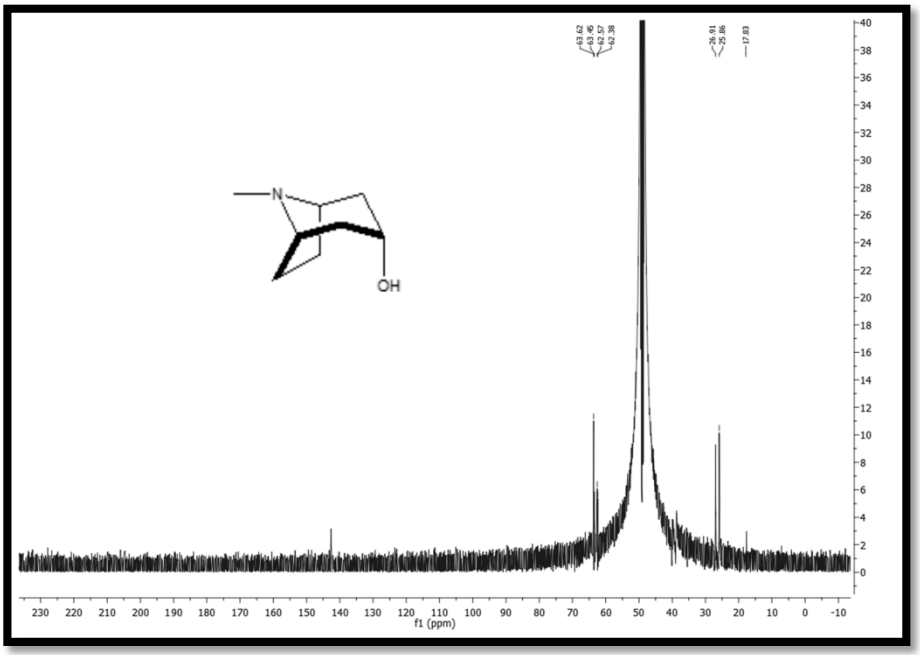

Figure 135. ^{13}C NMR spectrum (100 MHz) of compound **27** measured in $CDCl_3$

Choline (28)

Choline (**28**) was identified by comparison of the ^{1}H (Figure 136) and ^{13}C (Figure 137) NMR chemical shifts data with literature values.[160]

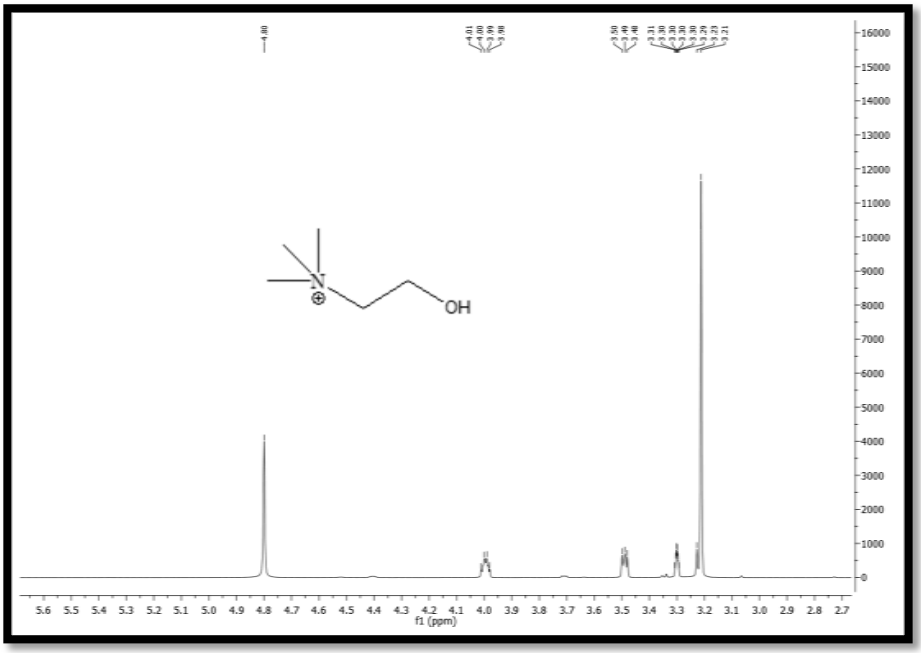

Figure 136. ^{1}H NMR spectrum (500 MHz) of compound **28** measured in $CDCl_3$

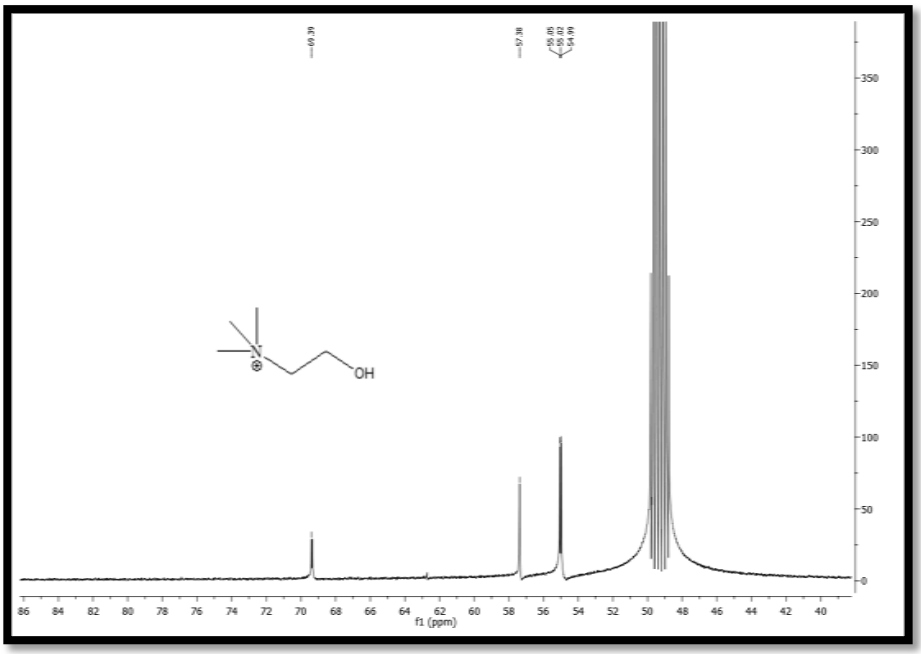

Figure 137. ^{13}C NMR spectrum (100 MHz) of compound **28** measured in $CDCl_3$

Ferulic acid methyl ester (29)

Ferulic acid methyl ester (**29**) was identified by comparison of the ^{1}H (Figure 139) and ^{13}C (Figure 140) NMR chemical shifts and ESI-MS(Figure 138) data with literature values.[161]

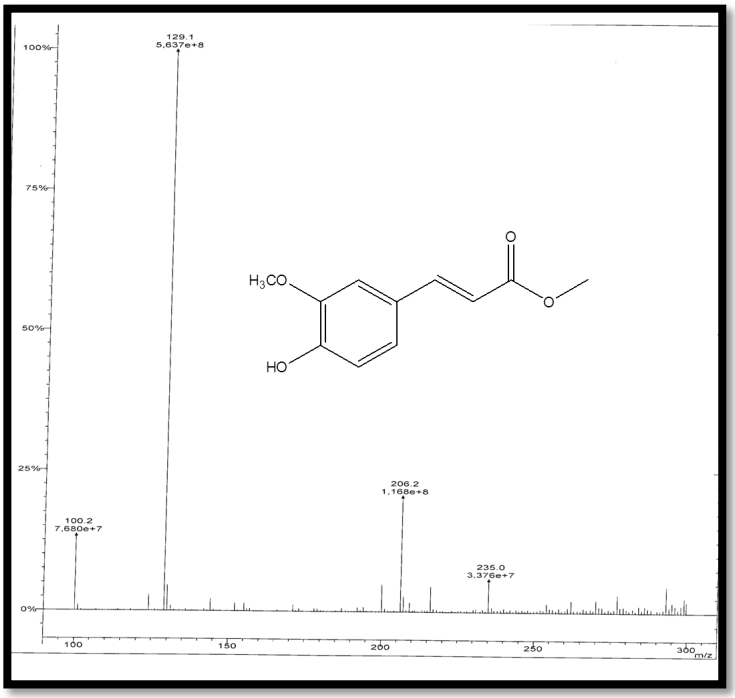

Figure 138. ESI mass spectrum of compound **29**

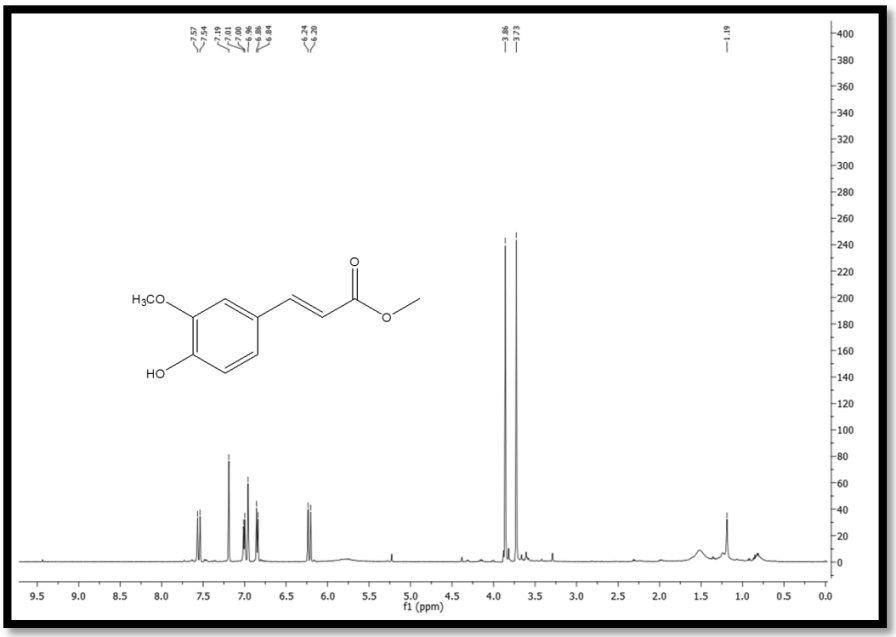

Figure 139. ^{1}H NMR spectrum (500 MHz) of compound **29** measured in $CDCl_3$

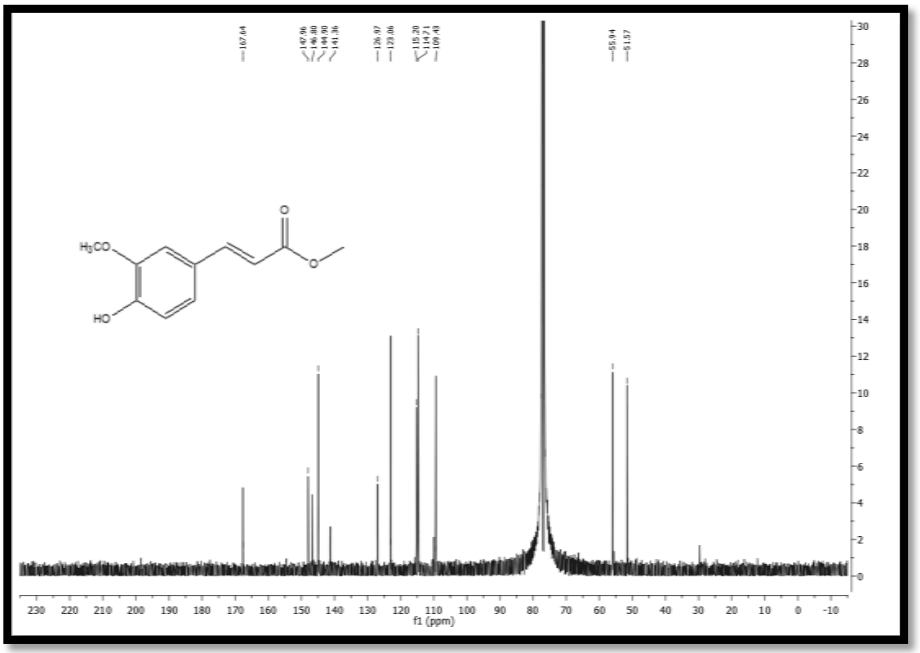

Figure 140. ^{13}C NMR spectrum (100 MHz) of compound **29** measured in $CDCl_3$

Withanolide A (30)

Withanolide A (**30**) was identified by comparison of the ^{1}H (Figure 141) and ^{13}C (Figure 142) NMR chemical shifts with literature values.[162]

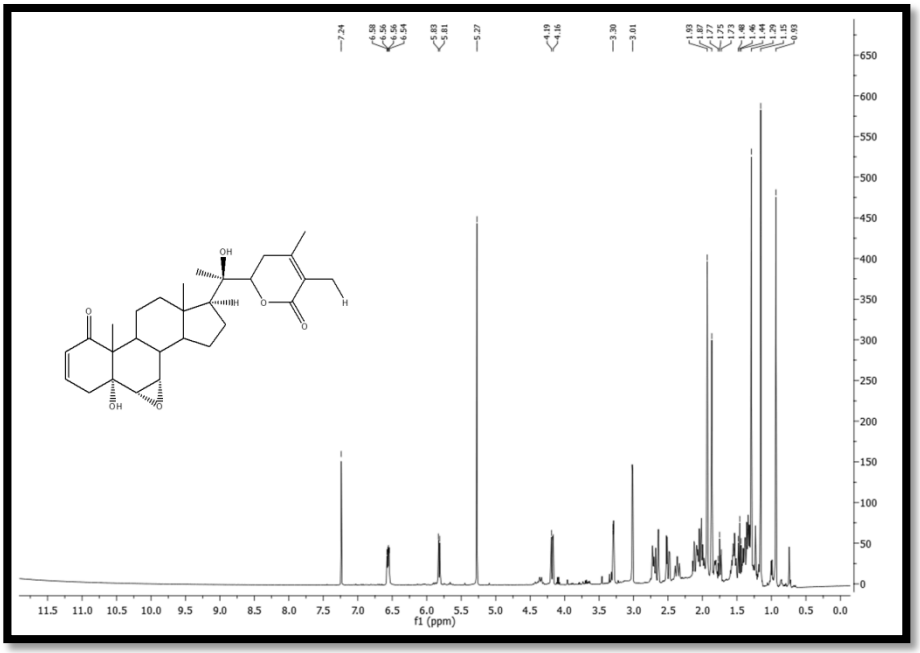

Figure 141. ^{1}H NMR spectrum (500 MHz) of compound **30** measured in $CDCl_3$

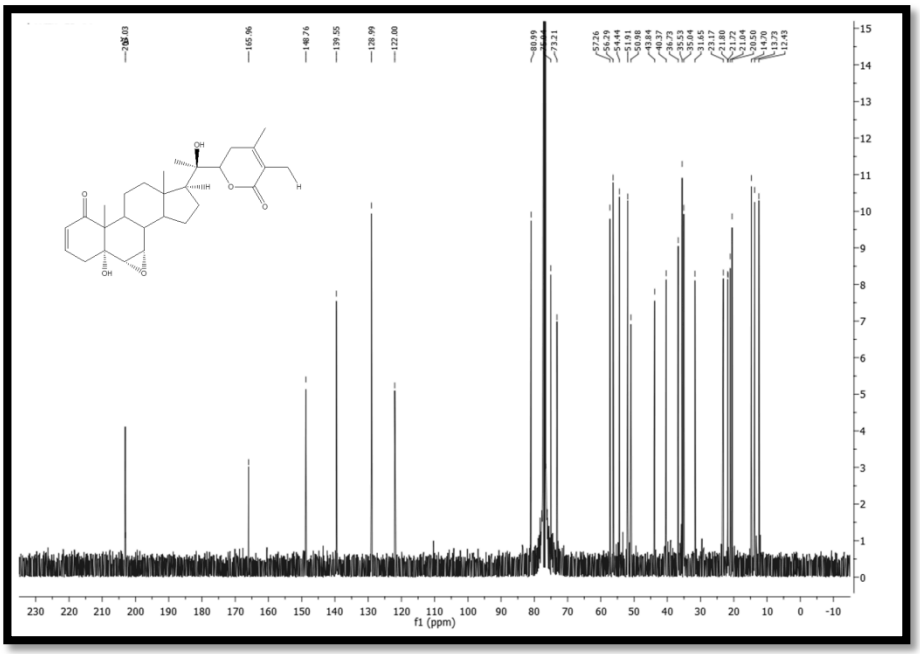

Figure 142. ^{13}C NMR spectrum (500 MHz) of compound **30** measured in $CDCl_3$

Withanone (31)

Withanone (**31**) was identified by comparison of the ^{1}H (Figure 143) NMR chemical shifts with literature values.[162]

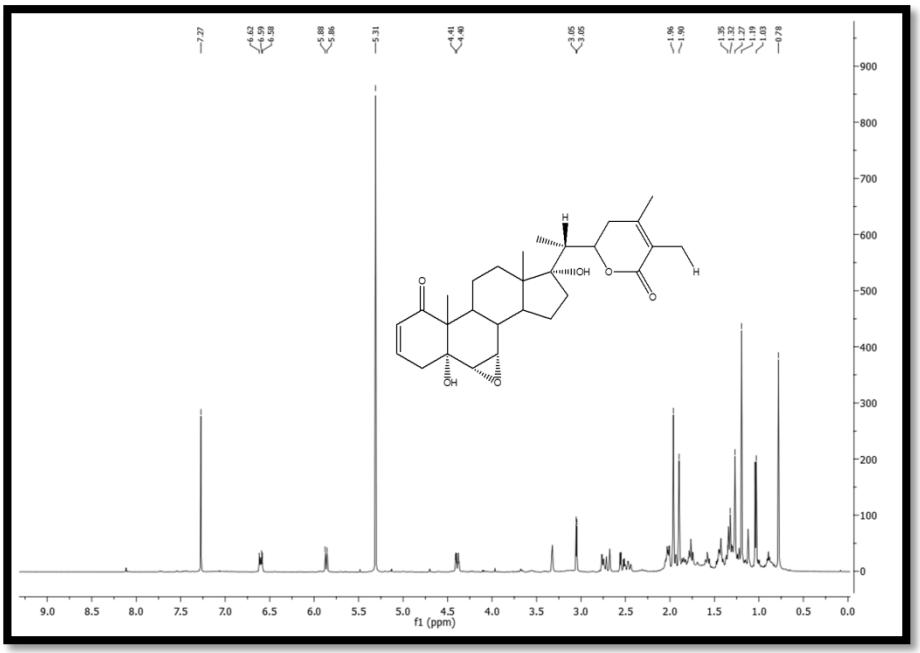

Figure 143. ^{1}H NMR spectrum (500 MHz) of compound **31** measured in $CDCl_3$

Withaferin A (32)

Withaferin A (**32**) was identified by comparison of the 1H (Figure 144) and APT (Figure 145) NMR chemical shifts data with literature values.[163]

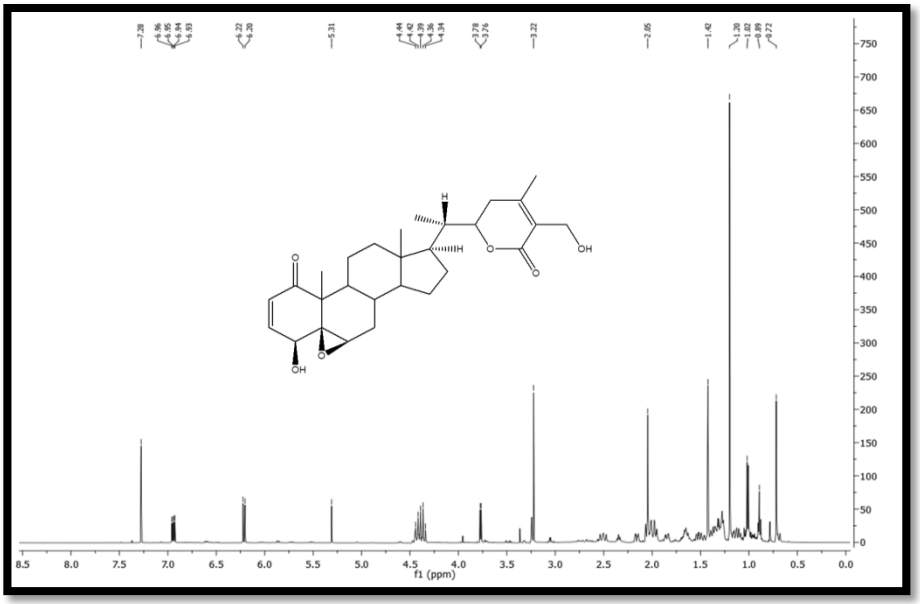

Figure 144. ^{1}H NMR spectrum (500 MHz) of compound **32** measured in $CDCl_3$

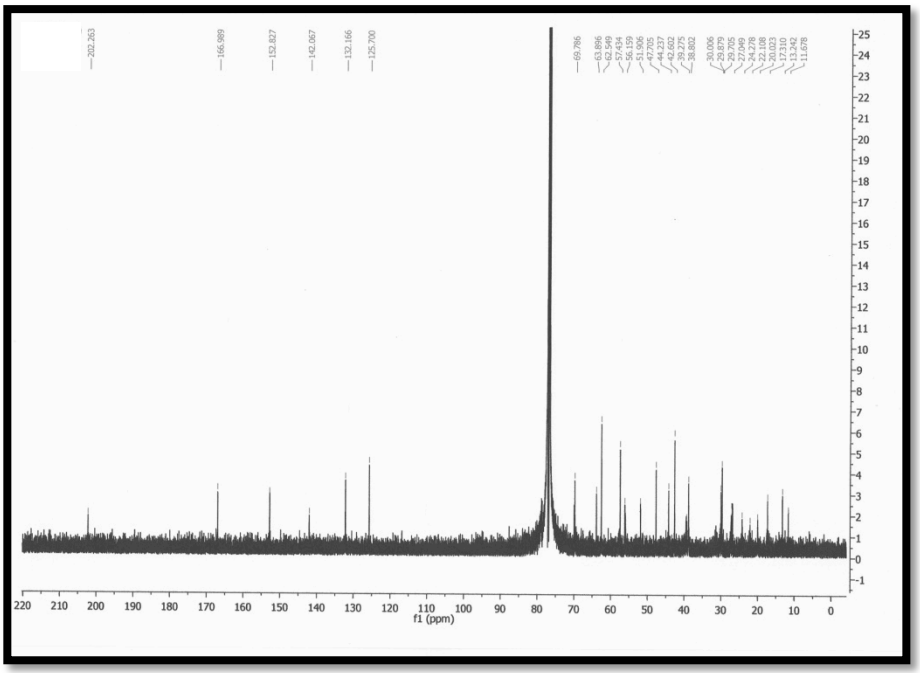

Figure 145. ^{13}C NMR spectrum (100 MHz) of compound **32** measured in $CDCl_3$

12. BIOLOGICAL RESULTS

12.1 Opioid and Cannabinoid Binding Affinity of Compounds Isolated from *O.maritimus*

As shown in table 8, DCM extract from *O. maritimus* exhibited the highest affinity for the CB1 and CB2 receptor with K_i values of 2.2 μg/ml and 1.3 μg/ml respectively. The same extract was able to bind to μ and δ with K_i values higher than those showed in the CB radioligand screening assay. All the isolated amides (**1**-**10**), the known pontica epoxide (**11**) and the new neo-lignan (**12**) were evaluated for the first time, except **6**, for their binding affinity to the μ and δ opioid as well as to the CB1 and CB2 receptors and the corresponding K_i values were expressed in μM (Table 8).

1-[(2*E*,4*E*,8*Z*)-tetradecatrienoyl]piperidine (**10**) was the most potent binder to both CB1 and CB2 receptors with a K_i value of 0.8 μM and 0.16 μM, respectively. It showed also the most CB2 selectivity with a K_iCB1/K_iCB2 = 5 (Table 1). Compound **9** compared with **10** displayed a strong reduced CB2 affinity (K_iCB2 about 150 times higher). Compound **10** with respect to **9** contain a further double bond with

Z configuration at C8 position of the acyl chain that seems to be essential for a high affinity of the piperidide to the CB2 receptor.

The influence of *Z* double bond at C8 of the tetradeca-2*E*,4*E*-dienoic acid isobutylamides to CB2 receptor affinity was decisively minor but still valuable as observed for amides **7** and **8** (Table 1). In the case of Δ^8-containing compound (**8**) 2 fold increased affinity, as compared to **7**, was observed. The influence of double bonds geometry in dodeca-tetraenoic acid isobutylamides with regards to CB2 receptor affinity has been reported previously by Matovic et al.[141] They found that tetraenes alkylamides with 8*Z,* 10*Z* geometry displayed high binding affinity for CB2 receptor.

Among the thienylheptatrienamides (**1**-**5**), piperidide **3** showed the highest affinity and selectivity to CB2 receptors (K_iCB2 = 1.24 μM; K_iCB1/K_iCB2 = 3.3). The substitution of piperidinyl group in **3** with a 2,3-dehydropiperidinyl ring, as in compound **4**, significantly reduced binding affinity to CB2 receptor (K_i = 13.5 μM) and annulled the CB1 binding affinity (K_i > 50 μM). The replacement of piperidinyl moiety of **3** with an amino-isopentyl, amino-isobuthyl or 5-amino-2-pentenyl 3-methylbutanoyl group reduced CB2 and increased CB1 affinity. The new neo-lignan **12** exhibited moderate affinity to CB1 (K_i = 2.7 μM) and CB2 (K_i = 4.2 μM) receptors.

Furthermore, compounds **1-12** were screened for inhibition of binding to μ and δ receptors (MOR and DOR) (Table 8).

The most active compounds resulted amides **8**-**10** and the new compound 9-isovaleroxy balanophonin (**12**) displaying moderate binding affinity to both MOR and DOR with K_i values ranging from 3.8 to 9 μM. The *Z* double bond at C8 of tetradeca acid isobutylamides increased once a time the receptor binding but did not influence the affinity for piperidides. In fact, despite what we observed in the CB receptors screenings, piperidinyl amide **10** showed MOR and DOR affinity comparable to that of **9**. Interestingly, alkylamide **6** had the highest MOR to DOR selectivity (K_iDOR/K_iMOR = 5.2) among all tested compounds. In the thienylheptatrienamides series a N-isopentyl chain improved the affinity for MOR while a N-2-pentenyl 3-methylbutanoyl moiety increased the affinity for DOR as compared to compound **2** containing a N-isobutyl chain. In our previous work[164] we found that falcarinol, a polyacetilene relatively widespread in Apiaceae and Araliaceae, bound CB1 receptor as covalent inverse agonist. On the basis of the structural similarity between falcarinol and pontica epoxide (**11**), we evaluated the binding affinity also for polyyne **11**,

but we did not find any affinity neither for CB nor for opioid receptors up to 50 μM (Table 8).

Up to now, it is believed that, for a high affinity to CB2 receptors, alkylamides should be N-substituted with an isobutyl or dimethylbutyl group and represented by a secondary alkylamide as the amide proton seems to be involved in the CB2 receptor interaction.[165]

Our findings are somewhat surprising because among all tested compounds the most potent and selective alkylamide resulted the tertiary amide 1-[(2*E*,4*E*,8*Z*)-tetradecatrienoyl]piperidine (**10**) which contain a piperidinyl moiety linked to a C14 acyl chain. Compound **10** showed CB2 affinity higher than that of dodeca-2*E*,4*E*-dienoic acid isobutylamide **6**, that is one of the active principles of *Echinacea* species. In our hands, compound **6** displayed a K_iCB2 value of 0.9 μM that is higher than that reported by Raduner et al.[5] (K_iCB2 = 0.06 μM) but lower in respect to that measured by Woelkart et al.[71] (K_iCB2 = 9.694 μM). As reported in a previous work,[5] the discreancy between the *K*i values could be due to the different source of CB2 receptors, as well as experimental condition.[135] Docking experiments into CB2 receptor of compounds **6** and **10** by means of GlideXP[136] (see in silico modeling study,

11.3.4, p.106) revealed that the presence of the secondary amide as donor group is not critical for activity, confirming the high binding affinity of alkilamide **10**.

Table 8. K_i values of DCM extract and isolated compounds for cannabinoid and opioid receptors

Extract/ Compd	Receptor Affinity (μM)		CB2 Selectivity	Receptor Affinity (μM)		MOR Selectivity
	***K*iCB2**	***K*iCB1**	***K*iCB1/*K*iCB2**	***K*iMOR**	***K*iDOR**	***K*iDOR/*K*iMOR**
DCM	1.3 ± 0.3[a]	2.2 ± 0.9[a]	1.69 : 1	10 ± 0.7 [a]	8.5 ± 1.3[a]	0.85 : 1
1	5 ± 0.1	2.2 ± 1	0.44 : 1	8.1 ± 0.1	26.5 ± 1.5	3.27 : 1
2	8.25 ± 1.4	8.8 ± 2.2	1.07 : 1	52 ± 0.5	25.5 ± 1.5	0.49 : 1
3	1.24 ± 0.3	4.1 ± 0.8	3.3 : 1	12.8 ± 3.3	8 ± 1	0.63 : 1
4	13.5 ± 0.5	> 50	-	29 ± 4	11.5 ± 2.1	0.40 : 1
5	10.2 ± 2.3	5.6 ± 0.3	0.55 : 1	41.5 ± 13	11 ± 2	0.27 : 1
6	0.9 ± 0.2	2.6 ± 0.4	2.89 : 1	8.2 ± 0.8	43 ± 9	5.24 : 1
7	1.17 ± 0.28	1.4 ± 0.1	1.20 : 1	51 ± 0.4	22.5 ± 2.5	0.44 : 1
8	0.55 ± 0.07	1.2 ± 0.3	2.18 : 1	7.5 ± 0.73	7.7 ± 1.4	1.03 : 1
9	24 ± 2.5	6.7 ± 1.4	0.28 : 1	5.75 ± 0.25	6.5 ± 1.6	1.13 : 1
10	0.16 ± 0.04	0.8 ± 0.1	5 : 1	7.4 ± 0.1	3.8 ± 0.7	0.51 : 1
11	> 50	> 50	-	> 50	> 50	-
12	4.2 ± 1.2	2.7 ± 0.3	0.64 : 1	9 ± 1.3	3.8 ± 1	0.42 : 1

[a]Values expressed in μg/mL.
K_i values were obtained from four independent experiments carry out in triplicate and are expressed as mean ± standard error.

12.2 Opioid Binding Affinity of Compounds Isolated from *S.glutinosa*

Affinities for δ and μ opioid receptors from mouse brain membranes were computed by displacement of [^{3}H-DPDPE] and [^{3}HDAMGO], respectively, in binding assays (Table 9). The DCM extract from S. glutinosa exhibited an interesting affinity for the μ and δ opioid receptors with Ki values of 10.3 μg/ml and 9.0 μg/ml, respectively. Among the isolated compounds, xanthomicrol (**17**) displayed the strongest opioid binding affinity to both μ and δ opioid receptors (K_i for MOR = 0.825 μM, K_i for DOR = 3.6 μM). It showed also the most MOR selectivity with a K_iDOR/K_iMOR = 4.4. The presence of a further hydroxy group at 3' position, as in sideritoflavone (**18**), significantly reduced binding affinity to MOR (K_i = 18.5 μM) while the replacement of this group with a methoxy moiety, as in 8-methoxycirsilineol (**19**), annulled the affinity to the MOR (Ki > 50 μM). In the semi-synthetic derivative of 1, 5-demethyltangeretin (**23**), the 4'-hydroxy group has been substituted with a methoxy moiety and the Ki value indicated that 5-demethyltangeretin had no significant affinity for μ (K_i > 50 μM) receptor, as compared to **17**. When both the free hydroxy groups of compound **17** were

methoxylated, as in tangeretin (**24**), the affinity for the MOR was 20-fold lower than that of **17**. Taken together, these results suggested that, for a high affinity to μ receptors, 5-hydroxy-6,7,8-trimethoxyflavones should be substituted with only one free hydroxyl group at 4' position of B ring. Roseostachenone (**21**) exhibited very low affinity to μ (K_i = 40.5 μM) and δ (K_i = 23.5 μM) receptors.

Table 9. K_i values of DCM extract and isolated compounds for opioid receptor

Extract/Compound	**Receptor Affinity (μM)**		**MOR Selectivity**
	***K*$_i$MOR**	***K*$_i$DOR**	***K*$_i$DOR/*K*$_i$MOR**
DCM	10.3 ± 0.2[a]	9.0 ± 1[a]	0.87 : 1
17	0.825 ± 0.025	3.6 ± 0.8	4.36 : 1
18	18.5 ± 0.8	12.5 ± 1	0.68 : 1
19	>50	37.5 ± 4	-
20	28 ± 0.4	12.0 ± 2	0.43 : 1
21	40.5 ± 7.5	23.5 ± 0.5	0.58 : 1
23	>50	>50	
24	16.3 ± 1.5	7.0 ± 0.5	0.43 : 1

[a]Values expressed in μg/ml.
K_i values were obtained from four independent experiments carry out in triplicate and are expressed as mean ± standard error.

12.2.1 Effects of Xanthomicrol on Morphine-induced Analgesia

Since the μ receptor is thought to be primarily responsible for the mediation of opioid anti-nociception, we evaluated the anti-nociceptive activity of xanthomicrol in the tail flick test. To evaluate the pharmacological effect of the most potent methoxyflavone **17**, antinociceptive effect of xanthomicrol was assayed in animal model of acute pain (tail-flick test).

Figure 146 showed the effects of xanthomicrol (40 and 80 mg/Kg, body wt. i.p.) pre-treatment on morphine-induced analgesia in the tail-flick, carried out in mice. Xanthomicrol alone was devoid of analgesic activity in the tail-flick test. Morphine alone, at the dose of 5 mg/kg, increased the tail-flick latency along 60 min after its administration [$F_{treatment}(1,37)= 33.63$, $P<0.0001$; $F_{treatment\ x\ time}(2,74)=6.83$, $P<0.005$; Tukey's test, $P<0.05$ *vs.* vehicle + saline-treated mice]. Xanthomicrol pre-treatment, at the dose of 80 mg/kg, completely suppressed the analgesic effect of morphine [$F_{pre\text{-}treatment}(2,37)= 7.51$, $P<0.005$; $F_{pre\text{-}treatment\ x\ treatment}(2,37)=3.61$, $P<0.05$; $F_{pre\text{-}treatment\ x\ time}(4,74)=1.09$, $P=0.37$; $F_{pre\text{-}treatment\ x\ treatment\ x\ time}(4,74)=0.52$, $P=0.72$]. On the contrary, 40 mg/kg of xanthomicrol

failed to reduce the analgesic activity of morphine (Tukey's test, $P<0.05$ *vs.* vehicle + saline-treated mice).

Our data demonstrated that pretreatment of xanthomicrol inhibited morphine-induced anti-nociception in the tail flick test, suggesting an antagonistic effect at μ opioid receptor.

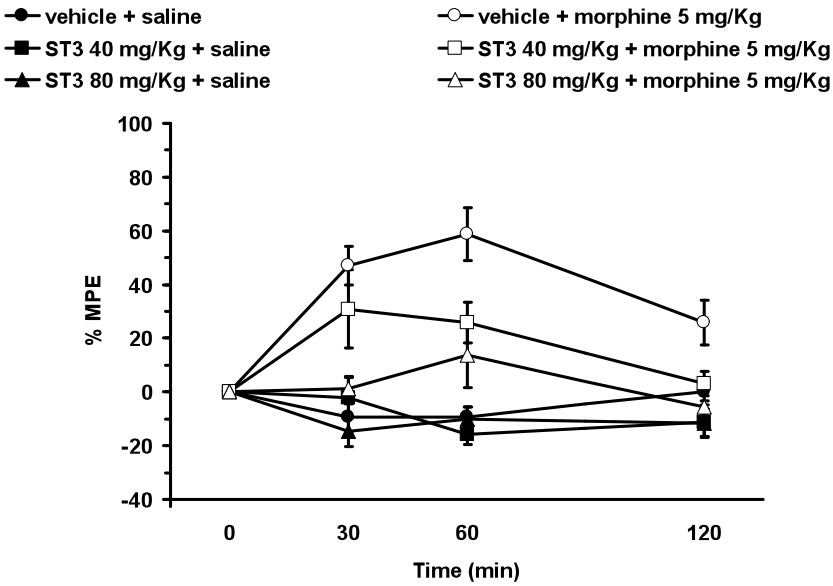

Figure 146. Effect of xanthomicrol pre-treatment on morphine-induced analgesia in the tail-flick test. Saline or xanthomicrol (40 and 80 mg/kg, i.p.) were administered 30 min before 5 mg/Kg, s.c. morphine injection. Basal algesia was assessed right before saline or xanthomicrol pre-treatment (baseline). The effects of the drugs were evaluated 30, 60 and 120 min after morphine treatment. Results are expressed as % MPE. Each point represent the mean ± S.E.M. of 3-11 mice per group. *P<0.05 *vs*. vehicle + saline-treated mice (three-way ANOVA followed by Tukey's post-hoc test).

12.2.2 Receptor Binding Affinity of Methanol and Alkaloid Extract from *W. somnifera* (WSE and WSAE)

We examined the affinity of *Withania somnifera* MeOH extract (WSE) towards opioid (μ, δ, k), cannabinoid (CB_1, CB_2), GABAergic ($GABA_A$), receptors using radioligand receptor binding assays. As shown in table 10, WSE exhibits the highest affinity for the $GABA_A$ receptors (K_i = 13 μg/ml). It is worth noting that WSE binds to $GABA_A$ with an affinity 15 times greater than that δ opioid receptors. In contrast, WSE showed a very weak binding affinity to μ, δ, and k opioid receptors and to CB_1 receptor and no binding affinity for the CB_2 receptors.

The alcaloid fraction of WSE (WSAE), respect to the *in toto* extract, showed an increased affinity towards all the tested receptors except for k (K_i = 700 μg/ml) and $GABA_A$ (K_i = 14 μg/ml).

Table 10. Binding affinity of *W. somnifera* MeOH extract (WSE) and alcaloid extract (WSAE)

Receptor affinity (μg/ml)						
Extract	**μ**	**δ**	**k**	**CB_1**	**CB_2**	**$GABA_A$**
WSE	385 ± 14	166 ± 11	775 ± 56	837 ± 74	>1000	13 ± 2
WSAE	60 ± 7	25.5 ± 6	700 ± 120	23.5 ± 1	20.3 ± 2	14 ± 0.5

Results are mean ± SEM of four independent experiments assayed in triplicate.

12.2.3 Analgesia Experiments

The interesting results of the binding assays for the μ, CB and GABA A receptors (Table 10) besides the observation that the administration of WSE blocked the development of tolerance to the analgesic effect of morphine,[166] prompted us to hypothesize that *W. somnifera* extracts could modulate additional aspects of morphine-induced analgesia. Therefore, we aimed to determine whether the combined administration of WSE with morphine could enhance or prolong the antinociceptive effect of morphine in the tail-flick and hot plate tests.

12.2.4 Effects of WSE on Morphine-induced Analgesia

The effects of WSE (100 mg/Kg) pre-treatment on morphine-induced analgesia were evaluated using the tail-flick (Figure 147) and the hot plate tests (Figure 148). WSE alone failed to alter the nociceptive reaction time. Morphine (2.5, 5 and 10 mg/Kg) elicited a dose-dependent antinociceptive effect in both tests, although its efficacy was higher when the tail-flick test was used. The peak in the analgesic effect was reached 60 min after morphine administration. Co-administration of WSE with morphine modulated its analgesic

activity depending on the dose of morphine and on the behavioural test used.

In the tail-flick test (Figure 147) morphine alone at the dose of 2.5 mg/Kg increased the tail-flick latency along 60 min after its administration [$F_{treatment}(1,30)= 46.16$, $P<0.0001$; $F_{treatment \times time}(4,120)=8.35$, $P<0.0001$; Tukey's test, $P<0.05$ *vs.* saline + saline-treated mice], and along 120 min following 5 mg/Kg [$F_{treatment}(1,26)=135.99$, $P<0.0001$; $F_{treatment \times time}(4,104)=10.97$, $P<0.0001$; Tukey's test, $P<0.05$ *vs.* saline + saline-treated mice] or 10 mg/Kg morphine administration [$F_{treatment}(1,31)=260.48$, $P<0.0001$; $F_{treatment \times time}(4,124)=5.61$, $P<0.005$; Tukey's test, $P<0.05$ *vs.* saline + saline-treated mice]. Interestingly, although WSE co-administration failed to modulate the antinociceptive effect elicited by 2.5 mg/Kg morphine [$F_{pre\text{-}treatment}(1,30)=0.78$, not significant (N.S.); $F_{pre\text{-}treatment \times treatment}(1,30)=2.28$, N.S.; $F_{pre\text{-}treatment \times time}(4,120)=0.66$, N.S.; $F_{pre\text{-}treatment \times treatment \times time}(4,120)=1.19$, N.S.], it protracted the analgesic effect induced by 5 mg/Kg morphine [$F_{pre\text{-}treatment}(1,26)=5.76$, $P<0.05$; $F_{pre\text{-}treatment \times treatment}(1,26)=7.66$, $P<0.05$; $F_{pre\text{-}treatment \times time}(4,104)=2.82$, $P<0.05$; $F_{pre\text{-}treatment \times treatment \times time}(4,104)=2.66$, $P<0.05$], and 10 mg/Kg morphine [$F_{pre\text{-}treatment}(1,31)=2.10$, N.S.; $F_{pre\text{-}treatment \times treatment}(1,31)=3.57$, N.S.; $F_{pre\text{-}treatment \times time}(4,124)=19.54$,

P<0.0001; $F_{\text{pre-treatment x treatment x time}}(4,124)=2.85$, *P*<0.05). In fact, the analgesic effect was still evident 240 min after 5 mg/Kg morphine treatment in mice pre-treated with WSE (78 ± 11% MPE) compared to mice pre-treated with saline (16 ± 7% MPE) (Tukey's test, *P*<0.05 vs. saline + saline-treated mice and vs. saline + morphine-treated mice). Likewise, analgesia was still evident at 240 min (55 ± 7% MPE) and 360 min (45 ± 11% MPE) after 10 mg/Kg morphine treatment, in mice pre-treated with WSE when compared to mice pre-treated with saline, in which the % MPE was respectively 20 ± 4% and 10 ± 3% (Tukey's test, *P*<0.05 *vs*. saline + saline-treated mice and *vs*. saline + morphine-treated mice).

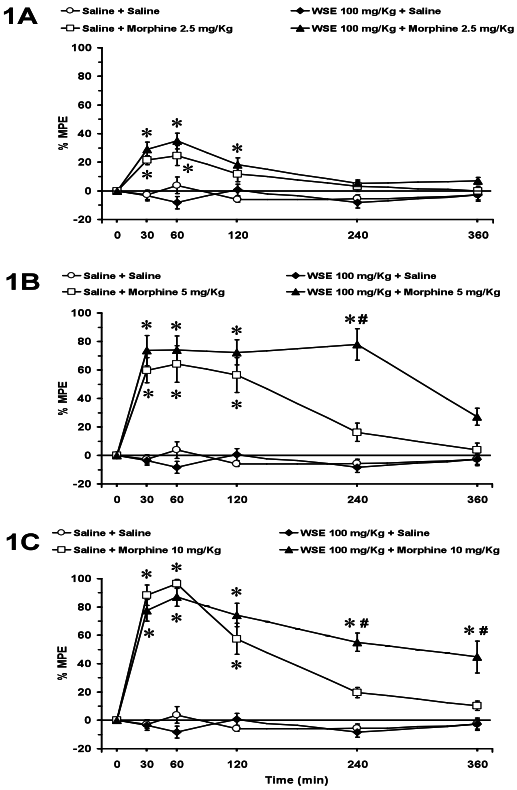

Figure 147**.** Effect of WSE pre-treatment on morphine-induced analgesia in the tail-flick test. Saline or WSE (100 mg/Kg, i.p.) were administered 30 min before 2.5 (a), 5 (b) and 10 (c) mg/Kg, s.c. morphine injection. Basal algesia was assessed right before saline or WSE pre-treatment (baseline). The effects of the drugs were evaluated 30, 60, 120, 240 and 360 min after morphine treatment. (See *Material and Method* for further details). Results are expressed as %MPE. Each point represent the mean±S.E.M. of 6-10 mice per group. **P*<0.05 *vs*. saline + saline-treated mice; # *P*<0.05 *vs.* saline + morphine-treated mice (three-way ANOVA followed by Tukey's post-hoc test).

A different picture was observed in the hot plate test (Figure 148) in which morphine, at the dose of 2.5 mg/Kg had no analgesic effect [$F_{treatment}(1,30)=0.35$, N.S.; $F_{treatment\ x\ time}(4,120)=5.4$, $P<0.0001$]; on the contrary, 5 and 10 mg/Kg increased the reaction time respectively along the first 60 min [$F_{treatment}(1,26)=46.53$, $P<0.0001$; $F_{treatment\ x\ time}(4,104)=5.61$, $P<0.0001$; Tukey's test, $P<0.05$ vs. saline + saline-treated mice], and along the first 120 min [$F_{treatment}(1,31)=58.72$, $P<0.0001$; $F_{treatment\ x\ time}(4,124)=10.27$, $P<0.0001$; Tukey's test, $P<0.05$ vs. saline + saline-treated mice]. WSE pre-treatment failed to modulate the analgesic effect induced by 2.5 mg/Kg [$F_{pre\text{-}treatment}(1,30)=0.41$, N.S.; $F_{pre\text{-}treatment\ x\ treatment}(1,30)=0.17$, N.S.; $F_{pre\text{-}treatment\ x\ time}(4,120)=0.17$, N.S.; $F_{pre\text{-}treatment\ x\ treatment\ x\ time}(4,120)=0.28$, N.S.], 5 mg/Kg [$F_{pre\text{-}treatment}(1,26)=0.0003$, N.S.; $F_{pre\text{-}treatment\ x\ treatment}(1,26)=0.27$, N.S.; $F_{pre\text{-}treatment\ x\ time}(4,104)=0.82$, N.S.; $F_{pre\text{-}treatment\ x\ treatment\ x\ time}(4,104)=0.48$, N.S.] and 10 mg/Kg morphine [$F_{pre\text{-}treatment}(1,31)=0.07$, N.S.; $F_{pre\text{-}treatment\ x\ treatment}(1,31)=0.30$, N.S.; $F_{pre\text{-}treatment\ x\ time}(4,124)=1.18$, N.S.; $F_{pre\text{-}treatment\ x\ treatment\ x\ time}(4,124)=0.55$, N.S.].

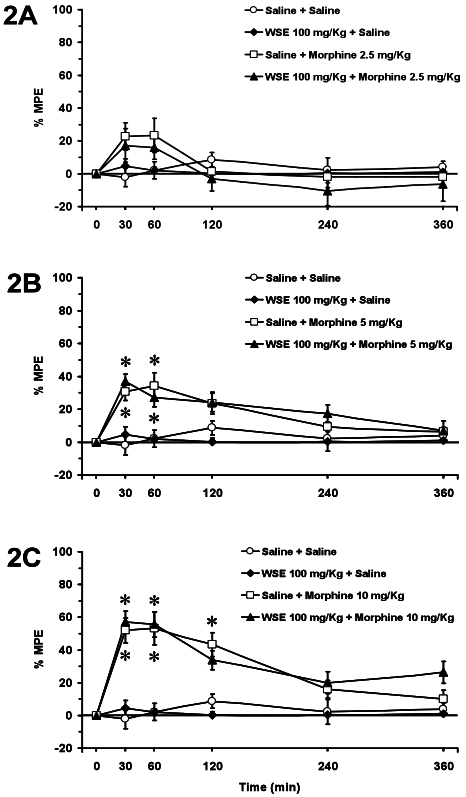

Figure 148. Effect of WSE pre-treatment on morphine-induced analgesia in the hot plate test. Saline or WSE (100 mg/Kg, i.p.) were administered 30-min before 2.5 (a), 5 (b) and 10 (c) mg/Kg, s.c. morphine. Basal algesia was assessed right before saline or WSE pre-treatment (baseline). The effects of the drugs were evaluated 30, 60, 120, 240 and 360 min after morphine treatment. Results are expressed as %MPE. Each point represent the mean±S.E.M. of 6-10 mice per group. *P<0.05 *vs*. saline + saline-treated mice (three-way ANOVA followed by Tukey's post-hoc test).

12.2.5 Effect of WSE on Morphine-induced Hyperalgesia

The effects induced by WSE (100 mg/Kg) pre-treatment on morphine-induced hyperalgesia were evaluated using the low-intensity tail-flick test (Figure 149). WSE alone failed to alter the nociceptive reaction time. In agreement with Gupta et al. (2001),[167] we found that a single injection of a low dose of morphine (2.5 mg/Kg) elicited a biphasic effect in the nociceptive response of CD1 mice. In fact, analgesia was reached at 30 and 60 after morphine administration [$F_{treatment}(1,32)=13.91$, $P<0.001$. $F_{treatment \times time}(6,192)=2.98$, $P<0.01$; Tukey's test, $P<0.05$ vs. saline + saline-treated mice]. This effect was followed by a gradual appearance of hyperalgesia; Tukey's test revealed that morphine administration reduced the nociceptive response (-65 ± 13% MPE) when compared to the nociceptive response of control mice (-4 ± 6% MPE) 360 min after morphine administration ($P<0.05$). Consistently with the results shown in Fig. 149, pre-treatment with WSE did not potentiate the analgesic effect of morphine during the first 120 min, however, it significantly prevented morphine-induced hyperalgesia [$F_{pre\text{-}treatment}(1,32)=7.25$, $P<0.05$; $F_{pre\text{-}treatment \times treatment}(1,32)=9.40$, $P<0.005$; $F_{pre\text{-}treatment \times time}(6,192)=2.98$, $P<0.001$; $F_{pre\text{-}treatment \times treatment \times}$

$_{time}$(6,192)=1.67, N.S.]. Tukey's test revealed that at 240, 300, 360 and 420 min after morphine administration the nociceptive threshold of mice pre-treated with WSE was higher when compared with the one observed in mice pre-treated with saline (*P*<0.05).

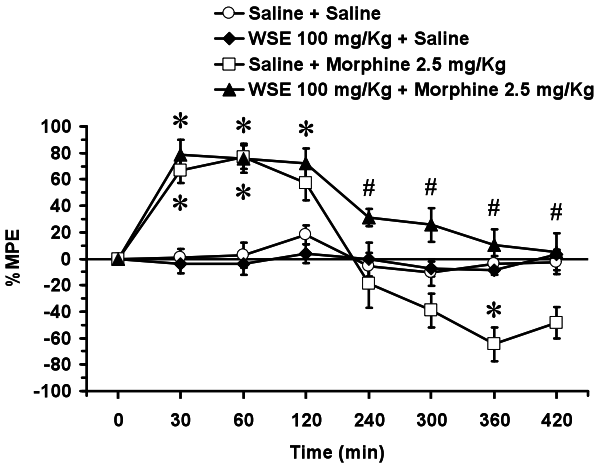

Figure 149. Effect of WSE pre-treatment on morphine-induced hyperalgesia in the low-intensity tail-flick test. Saline or WSE (100 mg/Kg, i.p.) were administered 30 min before morphine (2.5 mg/Kg, s.c.). Basal algesia was assessed right before saline or WSE pre-treatment (baseline). WSE pre-treatment (baseline). The effects of the drugs were evaluated 30, 60, 120, 240, 300, 360 and 420 min after morphine treatment. (See *Material and Method* for further details). Results are expressed as %MPE. Each point represent the mean±S.E.M. of 7-11 mice per group. *P<0.05 *vs*. saline + saline-

treated mice; # $P<0.05$ *vs.* saline + morphine-treated mice (three-way ANOVA followed by Tukey's post-hoc test).

12.2.6 Effect of WSE on Morphine-induced Hyper-locomotion

Figure 150 shows the effects of WSE on spontaneous motor activity and on morphine-induced (5 and 10 mg/Kg) hyper-locomotion. Repeated measures three-way ANOVA of the average distances travelled revealed that morphine increased motor activity in a dose dependent manner [$F_{treatment}(2,38)=18.43$, $P<0.0001$; $F_{treatment\ x\ time}(8,152)=19.61$, $P<0.0001$; Tukey's test, $P<0.05$ vs. saline + saline-treated mice]. WSE pre-treatment failed to alter both spontaneous motor activity and morphine-induced hyper-locomotion [$F_{pre\text{-}treatment}(1,38)=0.09$, N.S.; $F_{pre\text{-}treatment\ x\ treatment}(2,38)=0.18$, N.S.; $F_{pre\text{-}treatment\ x\ time}(4,152)=0.11$, N.S.; $F_{pre\text{-}treatment\ x\ treatment\ x\ time}(8,152)=0.60$, N.S.]. Specifically, Tukey's post-hoc analysis revealed that 10 mg/Kg morphine, alone and in combination with WSE increased motor activity 120, 240 and 360 min after administration (Tukey's test, $P<0.05$ vs. saline + saline-treated mice), but WSE pre-treatment did not affect morphine-induced hyper-locomotion.

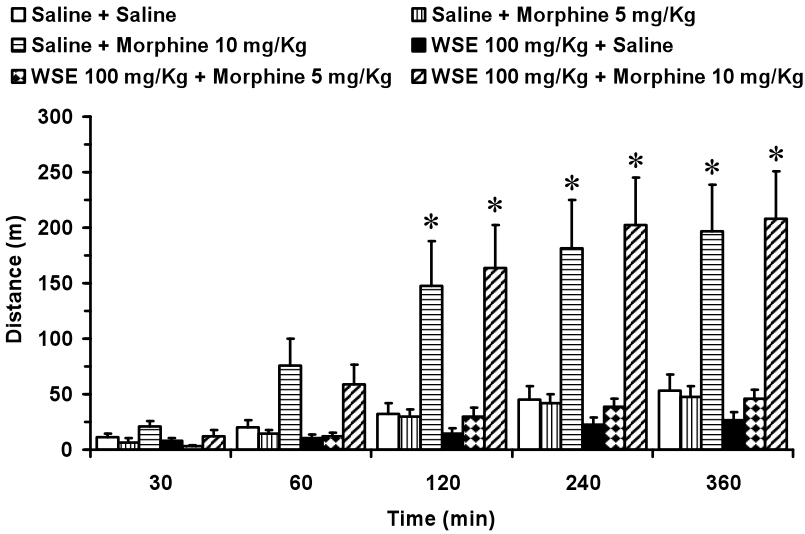

Figure 150. Effect of WSE pre-treatment on morphine-induced hyper-locomotion. After 30 min of habituation in the motor activity chambers, mice were pre-treated with saline or WSE (100 mg/Kg, i.p.) 30 min before saline or morphine (10 mg/Kg, s.c.) administration. Immediately after morphine administration, mice were returned to the motor activity chambers, and motor activity was recorded for 360 min. Results are expressed as average of distance travelled (m). Each bar represent the mean±S.E.M. of 5-11 mice per group. *P<0.05 *vs*. saline + saline-treated mice (three-way ANOVA followed by Tukey's post-hoc test).

13. CONCLUSIONS

Based on the receptor binding assays, it was possible to choose from a number of different plant extracts, four extracts from three different plants. Two of these have been obtained by percolation with dichloromethane of the roots of *Otanthus maritimus* (OME) and of the aerial parts and *Stachys glutinosa* (SGE), plants which grows wild in Sardinia. The third was a methanol extract (WSE) obtained by maceration of the roots of *Withania somnifera* and was provided by Natural Remedies Pvt. Ltd., Bangalore, India. The fourth was an alkaloids fraction (WSAE) obtained by liquid/liquid partition of the WSE.

A total of 30 secondary metabolites were isolated from the extracts. Two semisynthetic derivatives were also prepared.

The OME yielded two new alkylamides (**1**, **5**) and one new *neo*-lignan (**12**), along with thirteen known compounds. Among the constituents identified, 1-[(2E,4E,8Z)-tetradecatrienoyl]piperidine (**10**) was the most potent binder to both CB1 and CB2 receptors with a K_i value of 0.8 μM and 0.16 μM, respectively. Alkylamides **6**

and **8** compared with **10** showed minor affinity to CB2 receptors but still significant, with K_i values at low micromolar concentrations.

As far as we know, this is the first report of fatty acid piperidides and thienylheptatrienamides CB receptors screening. Since the presence of secondary amide group was described to be essential for the CB2 binding affinity of *Echinacea* alkylamides,[5] we decided to explore the nature of the ligand-receptor interactions carring out docking experiments into CB2 receptor by means of GlideXP. We focused on the compound **6** and **10**, which showed interesting activity but differed for the presence of secondary and tertiary amide moiety, respectively. The molecular modeling approaches applied in this study put in evidence, important requirements for the activity of this series of compounds. In particular, both compounds **6** and **10** are able to establish a strong hydrogen bond with Asn188: in the former compound the amide group behaves as a donor, while in the latter as an acceptor. Therefore, the presence of the secondary amide as donor group is not critical for activity. The derived information gives several hints for the design of optimized CB2 ligands.

From the SGE one new *neo*-clerodane, 3,4α-epoxyroseostachenol along four known flavones (eupatilin, sideritoflavone, xanthomicrol,

and 8-methoxycirsilineol) and one *neo*-clerodane diterpene (roseostachenone), were isolated. In order to find a structure-activity relationships, two metoxyflavones (5-demethyltangeretin, and tangeretin) were synthesized by methoxylation of xanthomicrol. Our results showed that xanthomicrol, the main constituent of *S. glutinosa* aerial parts (2% of the dried extract) is the principal responsible of the observed opioid binding affinities of the extract. We found that, among all the tested polymethoxyflavones (PMF_S), xanthomicrol presented the highest inhibition of the binding of the selective tritiated ligand [^{3}H]DAMGO to μ opioid receptor, with a K_i value of 0.825 μM. Moreover, structure-activity relationship studies indicated that the presence of only one free hydroxyl group at 4' position of B ring seems to be important for a high affinity of 5-hydroxy-6,7,8-trimethoxyflavones to the MOR receptor. Since the μ receptor is thought to be primarily responsible for the mediation of opioid anti-nociception, we evaluated the anti-nociceptive activity of xanthomicrol in the tail flick test. Our data demonstrated that pretreatment of xanthomicrol inhibited morphine-induced anti-nociception in the tail flick test, suggesting an antagonistic effect at μ opioid receptor. As far as we know, we reported for the first time that a flavone administered intraperitoneally in mice significantly

reduced morphine-induced antinociception in a dose-dependent manner in the tail flick test, and it seems that its action is mediated, at least in part, by opioid systems. Our findings show that xanthomicrol represents a structure for further development into potential MOR antagonist.

As regards WSE and WSAE, the results of the binding assays (Table 10) for the μ, CB and $GABA_A$ receptors suggested a possible anti-nociceptive effect of *W. somnifera*. Starting from these preliminar data and from previous studies demonstrating that *Withania somnifera* prevented the development of tolerance to the analgesic effect of morphine,[166] using behavioral appoaches we demonstrate for the first time the ability of WSE pre-treatment to prolong analgesia and to prevent the development of rebound hyperalgesia in mice treated with morphine.

Biochemical analyses suggest a potential involvement of $GABA_A$, CB, and opioid receptors in the observed behavioral effects. This study suggests the therapeutic potential of WSE as a valuable adjuvant agent in opioid-sparing therapies.

From WSE and WSAE three withanolides (withanolide A, withanone and withaferin A), four alkaloids (anaferine, (+)-sedridine, tropine, choline) along ferulic acid methyl ester have been isolated. Binding

experiments are currently undergoing in our laboratories in order to evaluate the affinity to CB, opiod and $GABA_A$ receptors of the secondary metabolites isolated from *W. somnifera*.

14. EXPERIMENTAL SECTION

14.1 General Experimental Procedures

Optical rotations were measured in $CHCl_3$ at 25 °C using a Perkin-Elmer 241 polarimeter. UV spectra were recorded on a GBC Cintra 5 spectrophotometer. IR spectra were performed with a Perkin-Elmer system 2000 FT-IR spectrophotometer using KBr mulls. NMR spectra were recorded at 25 °C on Unity Inova 500NB high-resolution spectrometer (Agilent Technologies, CA, USA) operating at 500 MHz for ^{1}H and 100 MHz for ^{13}C, respectively. All spectra were measured at 25 °C in $CDCl_3$ and referenced against residual $CHCl_3$ in $CDCl_3$ (^{1}H 7.27 ppm) and $CDCl_3$ (^{13}C 77.0 ppm). HR-ESIMS were measured on a Agilent 6520 Time of Flight (TOF) MS instrument while ESIMS experiments were performed on a Varian 1200 L triple quadrupole. Column chromatography was carried out under TLC monitoring using silica gel (40-63 μm, Merck), and Sephadex LH-20 (25-100 μm, Pharmacia). For vacuum-liquid chromatography (VLC), silica gel (40-63 μm) (Merck) was used. TLC was performed on silica gel 60 F_{254} or RP-18 F_{254} (Merck). Semi-preparative HPLC was conducted by means of a Varian 920 LH instrument fitted with an autosampler module

with a 1000 μL loop. The columns were a 250 x 10 mm Spherisorb silica, particle size 5 μm (Waters) and a 250 x 10 mm Polaris C-18-A, particle size 5 μm (Varian). The UV detection wavelength was 254 nm. For molecular modeling a PC Spartan Pro software program (Wavefunction Inc.) was used.

14.2 *O. maritimus* Plant Material

Otanthus maritimus roots were collected in November 2008 at Costa Rei beach, (Villasimius), Sardinia, Italy. The plant material was identified by Dr. Marco Leonti (University of Cagliari, Department of Life and Environmental Sciences) and a voucher specimen (No. 0455) was deposited in the Herbarium of the Department of Life and Environmental Sciences, Drug Sciences Section, University of Cagliari.

14.3 *O. maritimus* Extraction and Isolation

Air-dried and powdered roots of *O. maritimus* (780 g) were ground and extracted with CH_2Cl_2 (5 L) by percolation at room temperature to give 29.3 g dried extract. An aliquot (20 g) of the CH_2Cl_2 extract was subjected to vacuum-liquid chromatography (VLC) (silica gel, 90

g) using a step gradient of *n*-hexan/CH_2Cl_2/EtOAc (9 : 1 : 0 to 0 : 1 : 9, 500 mL each) to yield 11 main fractions (F1-F11). Fraction F3 (0.62 g) eluted with *n*-hexan/CH_2Cl_2 (5:5) was separated by column chromatography (CC) over silica gel using *n*-hexan/EtOAc (9.75:0.25) as eluent to obtain compound **11** (7.2 mg). Fraction F6 (*n*-hexan/CH_2Cl_2, 2.5:7.5) yielded compound **16** (1.29 g). Fraction F8 (1.26 g) was purified by CC over silica gel using *n*-hexan/EtOAc (7.5:2.5) as eluent giving seven subfractions (F8.1-F8.7). F8.6 (300 mg) was further chromatographed over silica gel (CH_2Cl_2/EtOAc, 9.5:0.5) to obtain four subfractions (F8.6.1-F8.6.4). F8.6.4 (44.5 mg) was purified by RP-HPLC using acetonitrile/H_2O (8.5:1.5, flow 2.5 mL/min) as eluent to give compound **6** (3.2 mg, t_R 10.0 min), compound **7** (20.8 mg, t_R 13.9 min) and compound **8** (8.8 mg, t_R 10.6 min). F8.7 (150 mg) was subjected to CC over silica gel using CH_2Cl/EtOAc (9.5:0.5) as eluent to obtain three subfractions (F8.7.1-F8.7.3). F8.71 (29.4 mg) was purified by solid-phase extraction (SPE) (RP-18) using acetonitrile/H_2O (8:2) as eluent and then with RP-HPLC using acetonitrile/H_2O (7:3, flow 3 mL/min) as eluent to give compound **15** (7.1 mg, t_R 7.0 min). Fraction F9 (4.99 g) was subjected to a further VLC (silica gel, 11 g) using a step gradient of *n*-hexan/EtOAc (3 : 1 to 0 : 9, 500 mL each) to yield 10 main fractions

(F9.1-F9.10). F9.2 (824 mg) was purified CC over silica gel using CH_2Cl/EtOAc (9.5:0.5) as eluent to give eleven subfractions (F9.2.1-F9.2.11). F9.2.4 yielded compound **14** (5.7 mg). F9.2.6 (140 mg) was subjected to CC over silica gel using *n*-hexan/EtOAc (7:3) to give compound **12** (4.7 mg). F9.2.6 yielded compound **3** (79.6 mg). F.9.2.8 (40.5 mg) was purified by NP-HPLC using *n*-hexan/*tert*-butyl methyl ether (2:8, flow 4 mL/min) to give compound **5** (12.3 mg, t_R 12.8 min). F9.5 was chromatographed by RP-HPLC using acetonitrile/H_2O (8.5:1.5, flow 2.5 mL/min) to yield compound **13** (8.7 mg, t_R 6.0 min). F9.7 (742 mg) was subjected to CC over silica gel using CH_2Cl/EtOAc (9.5:0.5) as eluent to obtain five subfractions (F9.7.1-F9.7.5). F9.7.3 (96 mg) was separated by CC on Sephadex LH-20 with MeOH as eluent to give compound **4** (7.0 mg). F9.7.4 (40 mg) was chromatographed by RP-HPLC using acetonitrile/H_2O (8:2, flow 2.5 mL/min) to yield compound **1** (9.6 mg, t_R 7.4 min). F9.7.5 (75 mg) was purified by RP-HPLC using acetonitrile/MeOH/trifluoroacetic acid (TFAA) (8.95:1:0.05, flow 2.5 mL/min) to yield compounds **10** (7.7 mg, t_R 9 min) and **9** (6.5 mg, t_R 12 min). F9.8 yielded compound **2** (60 mg).

14.4 Analitical and Spectroscopic Data of the New Compounds

(2*E*,4*E*,6*E*)-*N*-isopentyl-7-(2-thienyl)-2,4,6-heptatrienamide (**1**). Yellow amorphous powder. UV (CH_2Cl_2) λ_{max} (log ε) 259 (0.6), 353 (1.8), 369 (1.6).). ^1H ($CDCl_3$, 500 MHz) and ^{13}C ($CDCl_3$, 100 MHz) NMR, see Table 1. HR-TOF-ESIMS (*m/z*) 276.1408 $[M + H]^+$ (calcd. for $C_{16}H_{21}NOS$ 276.1417). EIMS (*m/z*) 276 $[M + H]^+$. FT-IR (KBr) ν_{max} 3295, 1690, 1615, 1585, 1000 cm^{-1}.

(2*Z*)-5-{[(2*E*,4*E*,6*E*)-7-(2-thienyl)-2,4,6-heptatrienoyl]amino}-2-pentenyl 3-methylbutanoate (**5**). Yellow amorphous powder. UV (CH_2Cl_2) λ_{max} (log ε) 259 (0.3), 353 (0.7). ^1H ($CDCl_3$, 500 MHz) and ^{13}C ($CDCl_3$, 100 MHz) NMR, see Table 1. HR-TOF-ESIMS (*m/z*) 374.1785 $[M + H]^+$ (calcd. for $C_{21}H_{27}NO_3S$ 374.1784). EIMS (*m/z*) 374 $[M + H]^+$, 396 [M + Na], 769 [2M + Na].

9-isovaleroxy balanophonin (**12**). Yellowish oil. $[\alpha]_D^{25}$ + 9.3° (*c* 0.08, CH_2Cl_2). UV (CH_2Cl_2) λ_{max} (log ε) 207 (1.0), 229 (0.2), 341 (0.4). ^1H ($CDCl_3$, 500 MHz) and ^{13}C ($CDCl_3$, 100 MHz) NMR, see Table 1. HR-TOF-ESIMS (*m/z*) 441.1908 $[M + H]^+$ (calcd. for $C_{25}H_{28}O_7$ 441.1908). EIMS (*m/z*) 441 $[M + H]^+$.

14.5 *Stachys glutinosa* Plant Material

Stachys glutinosa aerial parts were collected in April 2006 at Capoterra, Sardinia, Italy. The plant material was identified by Dr. Marco Leonti (University of Cagliari, Department of Life and Environmental Sciences). A voucher specimen (No. 0425) was deposited in the Herbarium of the Department of Life and Environmental Science, Drug Sciences Section, University of Cagliari.

14.6 *Stachys glutinosa* Extraction and Isolation

Air-dried and powdered leaves of *Stachys glutinosa* (547.83 g) were ground and extracted with CH_2Cl_2 (5 L) by percolation at room temperature to give 52.42 g dried extract. An aliquot (20 g) of the CH_2Cl_2 extract was subjected to vacuum-liquid chromatography (VLC) (silica gel, 90 g) using a step gradient of *n*-hexan/CH_2Cl_2/EtOAc/MeOH (7.5 : 2.5 : 0 : 0 to 0 : 0 : 7.5 : 2.5 , 500 mL each) to yield 8 main fractions (F1-F8). Fraction F3 (1.13 g) eluted with CH_2Cl_2 was separated by column chromatography (CC) over silica gel using CH_2Cl_2/MeOH (9.9:0.1) as eluent to obtain compound **19** (12.0 mg).). An aliquot (0.5 g) of fraction F4 (3.06 g)

eluted with CH_2Cl_2/AcOEt (7.5:2.5) was purified by CC over sephadex LH-20 using MeOH as eluent giving five subfractions (F4.1-F4.5). F4.3 (230 mg) was further chromatographed over sephadex LG-20 (MeOH) to obtain four subfractions (F4.3.1-F4.3.4). F4.3.3 (44.5 mg) was subjected to C18 SPE using acetonitrile/H_2O (7:3) as eluent to give compound **20** (15.2 mg). F5 (0.91 g) was washed with EtOAc under vacuum and the insoluble give compound **17** (404.4 mg). F8 (1.48 g) was cromatographated on silica gel using as eluent CH_2Cl_2/MeOH (9.9:0.1) to give five subfractions (F8.1-F8.5). F8.3 (145.3 mg) was purified by sephadex LH-20 (MeOH) to give **18** (15.0 mg) and **22** (40 mg). F6 (0.70 g) was subjected to CC (silica gel) using *n*-hexan/EtOAc (6.5 : 3.5) as eluent to obtain **21** (47.7 mg).

14.7 *Semi-synthesis* of 5-demethyltangeretin (23)

A mixture of xanthomicrol (**17**) (50.0 mg, 0.1453 mmol) and K_2CO_3 (1.2 equiv. 24.1 mg) in mixture of acetone/DCM (1:1, 8 ml) was added Me_2SO_4 (16.5 µl, 0.1744 mmol), and then refluxed for 4 h. The resulting solution was cooled and added Na_2CO_3 (25 ml, 10%). The solution was extracted with CH_2Cl_2 (3 x 10 ml). The organic layer was concentrated under vacuum and the methylated derivative was subsequently purified over silica gel using MeOH/DCM (9.9 : 0.1) to give **23** (23.2 mg, 44.6%) as a white solid: mp 172-173 °C (hexane); spectroscopic data (UV, MS, NMR) identical to those reported in the literature.[150]

14.8 *Semi-synthesis of* tangeretin (24)

A mixture of xanthomicrol (**17**) (65.9 mg, 0.1916 mmol) and K_2CO_3 (2.5 equiv. 66.2 mg, in mixture of acetone/DCM (1:1, 10 ml) was added Me_2SO_4 (45.3 µL, 0.479 mmol), and then refluxed for 4 h. The resulting solution was cooled and added Na_2CO_3 (35 ml, 10%). The solution was extracted with CH_2Cl_2 (3 x 10 ml). The organic layer was concentrated under vacuum and the residue was subsequently purified over Sephadex LH-20 (MeOH) to give **23** (21.8 mg, 31.8%)

and **24** (5.4 mg, 8%). Tangeretin (**24**) was obtained in 8% yield as white solid: mp 151-152 °C (hexane); spectroscopic data (UV, MS, NMR) identical to those reported in the literature.[151,152]

14.9 *W. somnifera* Plant Material

Standardized root methanolic extract of WS (*Withania somnifera* Dunal, Natural Remedies Pvt. Ltd., Bangalore, India) was given by Dr. Amit Agarwal (Natural Remedies Pvt Ltd. Bangalore, India).

14.10 *W. SOMNIFERA* EXTRACTION AND ISOLATION

14.10.1 Extraction and Separation Procedure of Alkaloids

Approximately 100 g of methanol extract have been dissolved in a mixture of MeOH/H_2O (3 : 1) (500 ml) and the obtained solution was subsequently treated with diluted HCl (2 N) up to pH 2. The acidic solution was exhaustively extracted with dichloromethane (DCM) to remove non-alkaloid compounds. The remaining aqueous solution was made alkaline with diluted NH_4OH up to pH 9 and extracted with DCM by liquid-liquid partition in a separation funnel.

The organic phase was evaporated under reduced pressure resulting in a light brown crude residue (WSa, 1.77 g) that gave a positive response to the alkaloids reagent (Dragendorff). The basic aqueous extract was evaporated at reduced pressure to obtain a dark brown solid that was treated with MeOH and the resulting mixture filtered under vacuum to remove the insoluble residue. The obtained solution was concentrated under vacuum to give a rubbery dark brown solid (36.31 g) mainly represented by inorganic salts (WSb).

The crude residue (DCM2) was purified by gel-chromatography (Sephadex LH-20) with MeOH as eluent to give 30 fractions. After comparison of the 30 fractions by Silica gel thin layer chromatography (TLC) they were combined, according to visual similarities, and to positive response to Dragendorff reagent, in three main fractions (F1-F3). The alkaloid-containing fraction (F2, 0.5123 g), was purified by column chromatography (CC) using basic alumina (activity grade II) as stationary phase eluting with toluol/MeOH (7: 3) to obtain four subfractions (F2.1-F1-4) and then with MetOH/H_2O (8: 2) to give the subfraction F2.5.

F2.5 (69.7 mg) was separated by CC on silica gel eluting with MeOH, then with MeOH/H_2O (7: 3) (8A4, 100 ml) and finally with H_2O/MeOH/trifluoroacetic acid (7 : 3 : 0.025). The fractions eluted

with MeOH/H_2O (7: 3) gave (+)-sedredine (**25**) (16.0 mg) and those eluted with H_2O/MeOH/trifluoroacetic acid (7 : 3 : 0.025), anaferine (**26)** (68.5 mg). Anaferine was isolated as meso isomer, according to Schwarting et al.[120]

Fraction F1 (63.2 mg), which resulted negative to the Dragendorff reagent, was purified by CC on silica gel using *n*-hexane-ethyl acetate (3: 7) as eluent yielding ferulic acid methyl ester (**29**) (8.5 mg).

An aliquot (10 g) of WSb was purified by Vacuum-Liquid Chromatography (VLC) (neutral alumina) using a step gradient of DCM/MeOH (9 : 1 to 0 : 10) to yield 5 main fractions (A1-A5).

Fraction A5 (347 mg) was cromatographated using neutral alumina as stationary phase and DCM/MeOH (8 : 2) as eluent, to give tropine (**27**) (12.3 mg) and choline (**28**) (8.5 mg).

14.10.2 Separation Procedure of Withanolides

20 g of dry MeOH extract were purified by VLC using a step gradient of *n*-hexane/DCM (9 : 1 to 0 : 10) to yield 4 main fractions (B1-B5). Fraction B2 (579 mg) was chromatographed by Sephadex LH-20 using MeOH as eluent to yield three subfractions (B2.1-B2.3). B2.2 (96.5 mg) was further purified by CC on silica gel using *n*-

hexane/ethyl acetate (7 : 3) to give withanone (**31)** (9 mg). Subfraction B2.3 (400 mg) was separated by CC over silica gel using hexane/EtOAc (7 : 3) as eluent to obtain withanolide A (**30**) **(**68.1 mg).

Fraction B3 (480 mg) was purified by CC over silica gel using hexane/EtOAc (6 : 4) as eluent to obtain 400 fractions. The collection 346-377 was dissolved in thert-but-met-ether and then washed with hexan to obtain withaferin A (**32**)(15.5 mg).

15. MOLECULAR MODELING

15.1 Ligands Preparation

Ligands were docked in the global minimum energy conformation as determined by molecular mechanics conformational analysis performed with Macromodel software.[168] Theoretical 3D models of the most active compounds were built by means of Maestro GUI. The inhibitors structures were then submitted to a conformational search of 1000 steps with an energy window for saving structure of 10 kJ/mol. The algorithm used was the Monte Carlo method with MMFFs (Merck molecular force fields)[170] followed by an energy minimization carried out using the MMFFs, the GB/SA[171] water implicit solvation model and the Polak-Ribier Coniugate Gradient (PRCG) method, converging on gradient with a threshold of 0.01 kJ(mol•Å)$^{-1}$.

15.2 Protein

The CB2 receptor was obtained has reported by Ruhl[138].

15.3 Docking and Post-Docking Experiments

Glide XP was applied for docking experiments[136]. Then, to take into account induced fit mechanism, the resulting top ranked theoretical complexes were subject to 10000 steps of the Polak-Ribier conjugate gradient (PRCG) energy minimization method using OPLS_2005 force field. The residues, located in a radius of 5 Å around the ligand, were left free to move. The optimization process was performed up to the derivative convergence criterion equal to 0.01 kJ/(mol•Å)$^{-1}$. The binding interaction energies were computed applying molecular mechanics and continuum solvation models with the molecular mechanics generalized Born/Surface area (MM-GBSA) method.[171] Depictions were taken by means of Pymol (PyMOL Molecular Graphics System, Version 1.5.0.4 Schrödinger, LLC)

16. BIOLOGY ASSAY

16.1 Animals

Male CD1 mice (Charles River, Calco, Italy) 20-25 g were used. Animals were housed in an animal facility on a 12h light/dark cycle (lights on from 08:00 AM), at a constant room temperature of 21 ± 1°C (relative humidity approximately 60%). Standard rodent chow and water were available ad libitum. Animals were allowed to adapt to the animal facility conditions for at least two weeks after arrival. Procedures involving animals and their care were conducted in accordance with the institutional guidelines that are in compliance with national (D.L. number 116, Gazzetta Ufficiale, supplement 40, February 18, 1992; Circolare number 8, Gazzetta Ufficiale, July 14, 1994) and international laws and policies (EEC Council Directive 86/609, OJL 358, 1, Dec. 12, 1987; Guide for the Care and Use of Laboratory Animals, U.S. National Research Council, 1996). Every effort was made to minimize animal pain and discomfort and to reduce the number of experimental subjects.

16.2 Drugs and Chemicals

Morphine hydrochloride (Salars, Como, Italy) was dissolved in saline (NaCl 0.9%) and administered subcutaneously (s.c.) in a volume of 5 ml/Kg. The standardized root methanolic extract of WS (*Withania somnifera* Dunal, Natural Remedies Pvt. Ltd., Bangalore, India) was dissolved in saline for analgesia experiments [administered intraperitoneally (i.p.) in a volume of 5 ml/Kg] and in dimethyl sulfoxide (DMSO, Sigma-Aldrich, Milan, Italy) for binding assay. The dose of WSE for analgesia experiments was selected on the basis of previous studies[173,174] [^{3}H]-DAMGO ([d-Ala2, N-Me-Phe4,Gly-ol5]-enkephalin), [^{3}H]-DPDPE ([D-Pen^2, D-Pen^5]-enkephalin), [^{3}H]-U-69,593, [^{3}H]-CP55,950, [^{3}H]-MK801, [^{3}H]-Muscimol, [^{3}H]-Baclofen, [^{3}H]-Clonidine and [^{3}H]-Ketanserine were purchased from Perkin Elmer, Monza (MB), Italy. CP-55,940, Naloxone, U-69,593, muscimol, MK801, yohimbine and methysergide were obtained from Tocris Cookson Ltd (Bristol UK).

16.3 [^{3}H]-DAMGO-[^{3}H]-DPDPE (opioid receptors) Binding Assay

Ligand binding assays were carried out according to the procedure described by Ruiu et al.[173] Briefly, the whole brain minus cerebellum was homogenized with Polytron in 50 volumes (w/v) of 50 mM Tris-HCl (pH 7.4), centrifuged at 48,000xg for 20 minutes at 4°C, re-suspended in 50 volumes of the same buffer solution, and incubated at 37 °C for 45 minutes. After a further centrifugation step at 48,000xg for 20 minutes at 4 °C, the final pellet was re-suspended in the same buffer solution. Brain membranes (150-200 µg of protein) were incubated with the appropriate concentration of [^{3}H]-DAMGO [(D-Ala^2, N-Me-Phe^4, Gly^5-ol-) enkephalin] (1 nM) or [^{3}H]-DPDPE [(D-Pen 2,5)-enkephalin] (1 nM) in Tris-HCl buffer at 25 °C for 60 minutes in the absence or presence of naloxone (1 µM). The binding reaction was stopped by rapid filtration under vacuum through glass-fibre filters (Whatman GF/B) using a Brandell 36-sample harvester (Gaithesburg, MD, USA) and thereafter the filters were washed with 4×5 ml ice-cold 50 mM Tris–HCl buffer (pH 7.4). The affinity of compounds **1**-**21** was compared with that of the reference

compound Morphine hydrochloride (MOR *K*ì = 1.2 ± 0.03 nM; DOR *K*ì = 100 ± 12 nM).

16.4 [^{3}H]-CP-55,940 (cannabinoid receptors) Binding Assay

The whole brain minus cerebellum and spleen were homogenized in 20 volumes (w/v) of ice-cold TME buffer (50 mM Tris-HCl, 1 mM EDTA and 3.0 mM MgCl2, pH 7.4), centrifuged at 1,086xg for 10 minutes at 4 °C, and the resulting supernatants were centrifuged at 45,000 x g for 30 min, at 4 °C. [^{3}H]-CP-55,940 binding was performed by the method previously described by Ruiu et al.[174]. Briefly, the membranes (30-80 µg of protein) were incubated with 0.5 nM of [^{3}H]-CP-55,940 for 1 h at 30 °C in a final volume of 0.5 ml of TME buffer containing 5 mg/ml of fatty acid-free bovine serum albumin (BSA). Non-specific binding was estimated in the presence of 10 µM of CP-55,940. All binding studies were performed in disposable glass tubes pre-treated with Sigma-Cote (Sigma Chemical Co. Ltd., Poole, UK), in order to reduce non-specific binding. The reaction was terminated by rapid filtration through Whatman GF/C filters presoaked in 0.5% polyethyleneimine (PEI) using a Brandell 96-sample harvester (Gaithersburg, MD, USA). Filters were washed five

times with 4 ml aliquots of ice cold Tris HCl buffer (pH 7.4) containing 1 mg/ml BSA. The affinity of compounds **1**-**12** was compared with that of the reference compound SR144528 (CB1 *K*ì = 70 ± 10 nM; CB2 *K*ì = 0.28 ± 0.04 nM).

16.5 [^{3}H]-Muscimol ($GABA_A$ receptor) Binding Assay

Ligand binding assays were carried out according to the procedure described by Beaumont et al. (1978)[175] with slight modifications. Briefly, the cerebral cortex were homogenized in 0.32M sucrose, centrifuged at 1,000xg and the resulting supernatants were centrifuged at 20,000xg. The resulting pellet was suspended in ice-cold water, homogenised and centrifuged at 8,000xg. The supernatant together with the buffy layer on the pellet was then centrifuged at 48,000xg. The resulting pellet was re-suspended in water, and once more centrifuged at 48,000xg. The final pellet was frozen and stored at -80°C. On the day of analysis, membrane pellet was allowed to thaw at 4°C before re-suspension in 50 mM Tris–citrate buffer, pH 7.1, containing 0.05% Triton X-100 and incubated for 30 min at 37°C. Following incubation, the suspension was

centrifuged at 48,000xg. The washing step was repeated three more times and the final pellet was then re-suspended in the binding buffer. Non-specific binding was estimated in the presence of 200 µM of GABA.

16.6 Analysis of samples

Displacement curves were carried out using serial dilutions ranging from 1 mg/ml to 0.001 mg/ml of DCM extract and from 100 µM to 0.01 µM of all other compounds. To avoid possible undesired effects on radioligand binding, DMSO concentration in the different assays never exceeded 1% (v/v).

Filter-bound radioactivity were counted in a liquid scintillation counter (Tricarb 2900; PerkinElmer Life Sciences, Boston, MA, USA) using Ultima Gold as scintillation fluid (Packard, USA). Protein content was determined using the Bio-Rad Dc Kit (Bio-Rad Laboratories GmbH, Munich, Germany) and following manufacture instructions. Data from radioligand inhibition experiments were analyzed by nonlinear regression analysis of a Sigmoid Curve using GraphPad Prism program (Graph Pad Software, Inc., San Diego, CA,

USA). K_i values were calculated from the obtained IC_{50} values by means of the equation of Cheng and Prusoff[176].

All receptor binding experiments were performed in triplicate and results were confirmed in at least four independent experiment.

17. ANALGESIA EXPERIMENTS

17.1 WSE Tail-flick and Hot-plate Test

The antinociceptive effects were quantified using the tail-flick test and the hot plate test.[174] An automated device (model 7360, Ugo Basile, Italy) was used to determine the tail-flick latency, defined by the time (s) at which the animals withdraw the tail from a radiant heat source. Mice were held and gently restrained above the apparatus; the light beam was focused 1.5 cm from the tip of the ventral surface of the tail. The stimulus intensity was adjusted to result in a mean pre-drug control latency of 2-3 s, and a cut-off time of 12 s was applied to avoid tissue damage.

A semi-automated device (model 7280, Ugo Basile, Italy) was used to determine the reaction of mice placed on the hot plate, defined by the time (s) at which mice exhibited a nociceptive response or discomfort (licking or fanning the paws, jumping). A 50 cm high Plexiglas cylinder was suspended over the hot plate and the temperature was maintained at 55 ± 0.2 °C; to avoid skin damage, after 15 s mice were removed from the hot plate. Mice were pre-treated with saline or WSE 100 mg/Kg 30 min before saline or

morphine treatment; increasing doses of morphine were used (2.5, 5 and 10 mg/Kg). Basal algesia was assessed right before saline or WSE pre-treatment (baseline). The effects of the drugs were evaluated 30, 60, 120, 240 and 360 min after morphine treatment.

17.2 Tail-flick Test of xanthomicrol

The anti-nociceptive effects were quantified using the tail-flick test.[177] An automated device (model 7360, Ugo Basile, Italy) was used to determine the tail-flick latency, defined by the time (s) at which the animals withdraw the tail from a radiant heat source. Mice were held and gently restrained above the apparatus; the light beam was focused 1.5 cm from the tip of the ventral surface of the tail. The stimulus intensity was adjusted to result in a mean pre-drug control latency of 2-3 s, and a cut-off time of 12 s was applied to avoid tissue damage.

Mice were pre-treated with saline or xanthomicrol (40 and 80 mg/kg) 30 min before saline or morphine (5 mg/kg) treatment. Basal algesia was assessed right before saline or xanthomicrol pre-treatment (baseline). The effects of the drugs were evaluated 30, 60 and 120 min after morphine treatment.

17.3 Morphine-induced Hyperalgesia Experiment

The ability of WSE to inhibit the development of morphine-induced hyperalgesia was evaluated using the low-intensity tail-flick test according to Gupta and colleagues (2011)[167] with few modifications. Briefly, the stimulus intensity was adjusted to result in a mean pre-drug control latency of 5-7 s, and a cut-off time of 10 s was applied. Mice were pre-treated with saline or WSE 100 mg/Kg 30 min before saline or morphine treatment (2.5 mg/Kg). Basal algesia was assessed right before saline or WSE pre-treatment (baseline). The effects of the drugs were evaluated 30, 60, 120, 240, 300, 360 and 420 min after morphine treatment.

17.4 Spontaneous and Morphine-induced Motor Activity Experiments

In order to evaluate the ability of WSE to modulate further pharmacological effects induced by morphine, spontaneous and morphine-induced motor activity experiments have been carried out [173]. Mice were tested in chambers made of transparent Plexiglas (40Lx30Wx40H cm) interfaced to a computer equipped with a TSE software (TSE Systems, Bad Homburg, Germany). The distance

travelled (m) by mice inside the chambers was detected by 8 horizontal photocells. Mice were habituated to the chambers for 30 min. Immediately after habituation, mice were treated with saline or WSE 100 mg/Kg and 30 min later were injected with saline or morphine (5 or 10 mg/Kg). Motor activity was evaluated for 360 min after morphine administration.

17.5 Data Analysis

Treatment-induced variations in tail-flick and hot plate response were calculated as the percentage of maximal possible effect (MPE) according to the following formula: MPE [%]: [(T1-T0)/(T2-T0)] x 100, where T0 and T1 are the latency before (baseline) and after treatment, and T2 is the cut-off time (12 s in the tail-flick, 15 s in the hot plate and 10 s in the low-intensity tail-flick tests). Data from behavioural experiments are expressed as mean ± standard error (S.E.M.) of %MPE. The %MPE in tail-flick and hot plate experiments were analyzed separately by repeated measure three-way analysis of variance (ANOVA) with pre-treatment (saline and WSE) and treatment (saline and morphine) as between-subjects factors, and time as within-subjects factor (repeated measures).

In the spontaneous and morphine-stimulated motor activity experiments, the average distance travelled (m) after WSE pre-treatment and morphine treatment was analyzed by repeated measures three-way ANOVA, with pre-treatment (saline and WSE) and treatment (saline and morphine) as between-subjects factors and time (min) as within-subjects factor (repeated measures).

For each of the statistical analysis described above, when appropriate, post-hoc comparisons were done using Tukey's test.

18. REFERENCES

1. Balick, M.J. , Cox , P.A. , *Plants,People and Culture: the Science of Ethnobotany*. Ed.Scientific American Library, New York, NY (1997)
2. Giroud, C. Felber F., Augsburger M. *Forensic Sci. Intern.* 112, 143–150 (2000).
3. Gertsch J., Pertwee R.G., Di Marzo V. *Br. J. of Pharmacol.* 160, 523-529, (2010)
4. Low Dog, T. *"Botanicals in the management of pain in Contemporary pain medicine: the science and practice of contemporary and alternative medicine in pain management"*. (Audette JF, and Bailey A, Eds.), Umana Press, Totowa, NJ, 447-470. (2008)
5. Raduner, S. Majewska, A.; Chen, J.-Z.; Xie, X.-Q.; Hamon, J.; Faller, B.; Altmann, K.-H.; Gertsch, J. *J. of Biol. Chem.* 281, 14192-14206, (2006)
6. Newman D.J., Gragg G.M., *J. Nat. Prod.* 75, 311-335, (2012)
7. Goodman & Gilman's: *"The pharmacological basis of therapeutics"*, 9th ed. , 265-557, McGraw Hill (2010)

8. Kreek, MJ, Koob, GF,. *Drug Alcohol Depend*, ,51,23-47(1998)
9. Davis, M.P., Pasternack, G.W.,.*Oxford University Press*, 1-27. (2005)
10. Giordano, J. *Pain Physician* 8, 277-290. (2005)
11. Aley, K.O., Kulkarni, S.K. *Methods and Findings in Experimental and Clinical Pharmacology* (10), 597-601 (1989)
12. Bergman, S.A., Wynn, R.L., Williams, G.,. *Anesth. Prog*. 35, 190-194. (1988)
13. Kissin, I., Lee, S.S., Arthur, G.R., Bradley, E.L. Jr.,. *Anesthesia & Analgesia* 85, 182-187(1997)
14. Yaksh TL. *Acta Anaesthesiol. Scand.*, ,41:94-111. 1997
15. Fischer, B.D., Carrigan, K.A., Dykstra, L.A.,. *J. Pain* 6, 425-433. 2005
16. Newman D.J., Gragg G.M., *J, Nat. Prod.* 75, 311-335, (2012).
17. Prevatt-Smith K.M., Prisinzano T.E., *Nat. Prod. Rep.* 27, 23-31, (2010)
18. Thomas E. Prisinzano *AAPS J.* 7, 61(2005)
19. Howlett, AC. *Prostaglandins Other Lipid Mediat*. 68, 619–31 (2002)
20. Mackie K , J. *Neuroendocrinol*. 20, 10–14 (2008)

21. Sylvaine G, Sophie M, Marchand J, Dussossoy D, Carriere D, Carayon P, Monsif B, Shire D, LE Fur G, Casellas P. *Eur. J. Biochem*. 232, 54–61(1995)
22. Matsuda LA, Lolait SJ, Brownstein MJ, Young AC, Bonner TI. *Nature* 346,561–564 (1990)
23. Gérard CM, Mollereau C, Vassart G, Parmentier M. *Biochem. J.* 279, 129–34 (1991)
24. Pacher P, Mechoulam R ,. *Prog Lipid Res.* 50, 193–211 (2011)
25. Begg M, Pacher P, Bátkai S, Osei-Hyiaman D, Offertáler L, Mo FM, Liu J, Kunos G,. *Pharmacol. Ther*. 106, 133–145 (2005)
26. Mathison R, Ho W, Pittman QJ, Davison JS, Sharkey KA,. Br. *J. Pharmacol*. 142, 1247–1254 (2004)
27. Desroches J.,Beaulieu P.,*Current Drug Targets* 11,462-473(2010)
28. Elphick, M. R.; Egertova, M. *Philosophical Transactions of the Royal Society B: Biological Sciences* 356, 381-390(2001)
29. Godlewski G, Malinowska B, Schlicker E., *J. Pharmacol.* 142,701–708 (2004)
30. Fride E.,*Eur. J. Pharmacol.* 500,289–297 (2004)
31. Mathison, R.; Ho, W.; Pittman, Q.; Davison, J.; Sharkey, K.. *Br. J. Pharmacol.* 142, 1247–1254(2004)

32. Varga, K.; Wagner, J. A.; Bridgen, D. T.; Kunos, G. *FASEB J.* 12, 1035–1044 (1998)
33. Han K.H., Lim S., Ryu J., Lee C.W., Kim Y., Kang J.H., Kang SS., Ahn Y.K., Park S., Kim J.. *Cardiovasc. Res*. 84, 378–86 (2009)
34. Pertwee R.G.,.*Br. J. Pharmacol*., 156, 397–411(2009)
35. De Luca, M. A. Solinas, M.; Bimpisidis, Z. Goldberg, S. R. Di Chiara, G. ,. *Neuropharmacol.* 63, 161–168(2011)
36. Pacher P, Mechoulam R. *Prog Lipid Res*. 50, 193–211. (2011).
37. De Fonseca FR, Schneider M. *Addict. Biol*. 13, 143–6. (2008).
38. Wright KL, Duncan M, Sharkey KA. *Br. J. Pharmacol*. 153 , 263–270 (2008)
39. Capasso R, Borrelli F, Aviello G, Romano B, Scalisi C, Capasso F, Izzo AA. *Br. J. Pharmacol*. 154, 1001–1008 (2008)
40. Pacher P, Bátkai S, Kunos G. *Pharmacol. Rev*. 58 (3): 389–462. (2006)
41. A. C. Howlett, F. Barth, T. I. Bonner et al., *Pharmacol. Rev*. 54, 161–202 (2002)
42. L. S. Melvin, M. R. Johnson *J. Med. Chem*. 27, 67–71. (1984)
43. M. A. Huestis, D. A. Gorelick *Arch. Gen. Psychiatry*, 58, 322–328. (2001)

44. *"Marinol-the legal medical use for the Marijuana plant*".Drug Enforcment Administration.
45. *"Sativex Oromucosal Spray"* medicines.org.uk. 2011-06-09.
46. Pickens, JT . *Br.J. of Pharmacol.* 72, 649–56 (1981)
47. Burns, T. L. Ineck, J.R. *Ann. Pharmacother.* 40, 251–260 (2006)
48. Marinol (dronabinol) capsule drug label/data at Daily Med from U.S. National Libreray of Medicine,National Institutes of Health.
49. McKim, William A. Drugs and Behavior: *An Introduction to Behavioral Pharmacology* (5th ed.). Prentice Hall. (2002) p. 400.
50. K. Mackie, Annu. Rev. *Pharmacol. Toxicol*. 46, 101–122 (2006)
51. M. Rinaldi-Carmona, F. Barth *FEBS Lett*. 350, 240–244 (1994)
52. L. F. Van Gaal, A. M. Rissanen *Lancet*, 365, 1389–1397 (2005)
53. F. Chaperon, P. Soubri *Psychopharmacology* 135, 324–332.(1998)
54. T. De Vries, J. Homberg, et al., *Psychopharmacology*, 168, 164–169 (2003)
55. M. Solinas, L. V. Panlilio, et al., *J. Pharmacol. Exp. Ther*. 306, 93–102 (2003)
56. G. Cossu, C. Ledent *Behav. Brain Res*. 118, 61–65. (2001)
57. C. Cohen, G. Perrault *Behav. Pharmacol*. 13, 451–463 (2002)

58. S. R. Wachtel, H. de Wit, *Drug Alcohol Depend*. 59, 251–260 (2000)
59. J.E.Gallate, P. E. Mallet and I. S. McGregor *Psychopharmacology*, 173, 210–216 (2004)
60. Gertsch J., Leonti M., Raduner S., Racz I., Chen J.Z., Xie X.Q. Altmann K.H. *Proc. Natl. Acad*. Sci. USA 105, 9099–9104 (2008)
61. Klauke A.L., Racz I., Pradier B., Markert A., Zimmer A.M., Gertsch J., Zimmer A.Eur. *NeuroPsychopharmacol*. doi: 10.1016/j.euroneuro.2013.10.008
62. Pignatti S.,"Flora d'Italia". Vol.III, p. 85, Edagricole, Bologna (1982)
63. Camarda, I. Valsecchi, F. *Piccoli arbusti liane e suffrutici spontanei della Sardegna*; C. Delfino Ed. p. 273 (1992)
64. Reutter, L., *Traite de matiere medicale et de chimie vegetale*; Paris Librairie J.B. Baillière et Fils; p. 829, (1923)
65. Bohlmann, F.; Zdero, C.; Suwita, A. *Chem. Ber*., 107, 1038. (1974)
66. Pascual Teresa, J.de.; San Feliciano, A.; Barrero, A.F.; Medarde, M.; Tomé, *F. Phytochemistry*, 20, 166 (1981)
67. Christodoulopoulou, L., Tsoukatou, M. Tziveleka, L.A., Vagias, C., Petrakis, P.V., Roussis, V. J. *Agr. Food Chem*., 53, 1435-1439 (2005)

68. Jakupovic, J. Boeker, R., Grenz, M., Paredes, L., Bohlmann, F., Seif El-Din, A. *Phytochemistry*, 27, 1135 (1988)
69. De Pascual Teresa, J., Barrero, A.F., Caballero, E., Medarde, M. *An. Quim*., 75, 323 (1979)
70. Khafagy, S.M.; Sabri, N.N.; Salam, N.A.A.; Seif El-Din, A. *Pharmazie*, 36, 507 (1981)
71. Woelkart, K., Xu, W., Pei, Y., Makriyannis, A., Picone, R.P., Bauer, *R. Planta Med*. 71, 701-705 (2005)
72. Goel, V., Lovlin, R., Barton, R., Lyon, M.R. Bauer, R., Lee, T.D., Basu, T.K. *J. Clin. Pharmacol*. Ther., 29, 75 (2004)
73. Dietz, B. Heilmann, J. Bauer, R. *Planta Med.* 67, 863-864 (2001)
74. Matthias, A., Addison, R.S., Penman, K.G., Dickinson, R.G., Bone, K.M., Lehmann, R.P. *Life Sci*., 77, 2018 (2005)
75. Ardjomand-Woelkart, K., Kollroser, M., Magnes, C., Sinner, F., Frye, R.F., Derendorf, H., Bauer, R., Butterweck V. *Planta Med.*, 77, 1794-1799 (2011)
76. Cappelletti C.,"*Trattato di Botanica*",UTET,Torino,1975.
77. Pignatti S., "*Flora d'Italia*". Vol. II, p. 468, Edagricole, Bologna (1982)
78. Atzei A.,"*Le Piante della tradizione popolare in Sardegna*",Carlo Delfino Editore,(2003)

79. Loy M.C. Poli F., Sacchetti G., Selenu M.B., Ballero M. *Fitoterapia* 75,277-295 (2004)
80. Ballero M. *Fitoterapia* 64,141 (1993)
81. Paulis G.*,"I Nomi Popolari delle Piante in Sardegna*",Carlo Delfino Editore (1992)
82. Mariotti G.P. *Rivista Italiana EPPOS* 7, 536-540(1996)
83. Pintore G. Marchetti M, Chessa M, Sechi B, Scanu N, Mangano G, Tirillini B. *Nat. Prod. Comm*. 1133-36 (2006)
84. Mariotti G.P. *Flav. Frag. J.*,12, 205-209,(1999)
85. Serrilli A.M. Ramunno A., Piccioni F., Serafini M., Ballero M., Bianco A. *Nat. Prod. Res.* 20,648-652 (2006)
86. Merrit A.T.,Ley S.V., *Nat.Prod.Rep*. 9, 243-287 (1992)
87. Chinou I., *Curr.Med.Chem*. 12,1295-1317 (2005)
88. Bruno M. Piozzi F,, Rosselli S. *Nat. Prod. Rep.*19,357-378 (2002)
89. T. M. Orgiyan and D. P. Popa. *Chem. Nat. Comp.* 5, 5-6 (1969)
90. Popa D. P., Orgiyan T. Samek, M. Z. Dolejs L. *Chem. Nat. Comp.* 8, 292-295 (1972)
91. M. Adinolfi, G. Barone, R. Lanzetta, G. Laonigro, L. Mangoni and M. Parrilli. *J. Nat. Prod*. 47, 541-543(1984)
92. F. R. Melek, A. S. Radwan, M. A. El-Ansari, O. D. El-Gindi, S. H. Hilal and A. A. Genenah .*Fitoterapia* 63, 276 (1992).

93. T. M. Orgiyan , *Aktual. Probl. Izuch. Ef. Rast. Efim. Masel* 160-161 (1970)
94. D. P. Popa, T. M. Orgiyan, and Kh. Sh. Kharitov. *Chem*. *Nat. Comp*. 10, 324-330 (1974)
95. D. P. Popa and T. M. Orgiyan. *Chem. Nat. Comp*. 10, 410 (1974)
96. A. I. Derkach. *Rastitel'nye Resursy* 34, 57-61 (1998)
97. C. Fazio, S. Passannanti, M. P. Paternostro and F. Piozzi (1992). *Phytochemistry* 31, 3147-3149.
98. C. Fazio, M. P. Paternostro, S. Passannanti and F. Piozzi, *Phytochemistry* 37, 501-503 (1994)
99. C. Fazio, S. Passannanti, M. P. Paternostro, N. A. Arnold ,. *Planta Med*. 60, 499. (1994)
100. T. Konishi, M. Takasaki, H. Tokuda, S. Kiyosawa, T. Konoshima *Biol. Pharm. Bull*. 21, 993-996 (1998)
101. K. Dimas, C. Demetzos, V. Vaos, p. Ioannidis and T. Trangas, T *Leuk. Res.* 25, 449-454 (2001)
102. C. Demetzos, S. Mitaku, M. Couladis, C. Harvala, D. Kokkinopoulos *Planta Med*. 60, 590-591 (1994)
103. E. Kalpoutzakis, I. Chinou, S. Mitaku, A. L. Skaltsounis C. Harvala *Nat. Prod. Lett*. 11, 173-179 (1998)

104. M. P. Paternostro, A. M. Maggio, F. Piozzi, O. Servettaz *J. Nat. Prod*. 63, 1166-1167 (2000)

105. A. Garcia-Granados, M. B. Jimenez, A. Martinez, A. Parra, F. Rivas, J. M. Arias, 1994. *Phytochemistry* 37, 741-747.

106. A. Garcia-Granados, E. Linan, A. M. Martinez, F. Rivas, C. M. Mesa-Valle, J. J. Castilla-Calvente, A. Osuna *J. Nat. Prod*. 60, 13-16 (1997)

107. N. Fokialakis, E. Kalpoutzakis, B. L. Tekwani, A. L. Skaltsounis, S. O. Duke *Biol. Pharm. Bull.* 29*,* 1775-1778 (2006).

108. Rajeswara Rao B.R., Rajput D.K., Nagaraju G, Adinarayana G. *J. Pharmacogn.* 3, 88-91 (2012)

109. Singh S. and Kumar S. *Withania Somnifera: The Indian Ginseng Ashwagandha*, 293 (1998)

110. Mukhopadhya B., Chakraborti A., Ghosal S. *Immunomodulatory properties of some Indian medicinal plants*. eds. Emerging Drugs. Vol. 1, PJD Publications, Westbury, USA, p. 445-460 (2001)

111. Weiner M.A., Weiner J. *Ashwagandha (Indian ginseng). In: Herbs that heal.* Quantum Books, Mill Valley, CA, 70-72 (1994)

112. *The Aurvedic Pharmacopoeia of India*. New Delhi: the controllor of Publications Civil Lines, Vol 1(2001)

113. Sharma, P.C., Yelne, M.B., Dennis, T.J. *Database of Medicinal Plants Used in Ayurveda*. New Dehli: Central Council for Reseaarch in Ayurveda & Siddha, Vol. 3 (2001)

114. Kulkarni S.K., Dhir A. *Prog. in Neuropsycopharmacol. Biol. Psychiatry* 32, 1093-1105 (2008).

115. Choudhary S, Kumar P, Malik *J. Pharmacogn Rev*. 7, 81-91 (2013)

116. Wollen K.A. Altern. *Med. Rev*. 15, 223-244 (2010)

117. Prakash J., Yadav S.K., Chouhan S., Singh S.P. *Neurochem. Res.* 38, 972-80 (2013)

118. Andrade C., Aswath A., Chaturvedi S.K., Srinivasa M., Raguram R*., Indian J. Psychiatry*, 42, 295-301 (2000)

119. Chaurasiya N.M., Uniyal G.C., Lal P., Misra L., Sangwas N.S., Tuli R. *Phytochem. Anal*. 19, 148-1554 (2008)

120. Schwarting A.E., Bobbitt J.M., Rother A., Atal C.K., Khanna K.I., Leary J.D., Walter W.G. *Lloydia* 26, 258-273 (1963)

121. Schröter H.B., Neumann D. *Tetrahedron* 22, 2895-2897 (1966)

122. Wim Vanden Berghe, W.V., Sabbe A., Kaileh M., Haegeman G., Heyninck K. *Biochem Pharmacol*. 84, 1282-1291 (2012)

123. Chen L.-X., He H., Qiu F. *Nat. Prod. Rep*. 28, 705−740 (2011)

124. Moncrief J.W., Heller K.S*., Cancer Res*. 27, 1500-1502 (1967)

125. Santagata S., Xu Y.M., Wijeratne E.M., Kontnik R., Rooney C., Perley CC. *ACS Chem. Biol.* 7, 340–349 (2011)

126. Kaileh M., Vanden Berghe W., Heyerick A., Horion J., Piette J., Libert C. *J. Biol. Chem*. 282, 4253-4264 (2007)

127. Min K.J., Choi K., Kwon T.K. *Int. Immunopharmacol*. 11, 1137-42 (2011)

128. Mehrotra A., Kaul D., Joshi K. *Mol. Cell Biochem.* 349, 41-55 (2011)

129. Choudhary M.I., Yousuf S., Nawaz S.A., Ahmed S., Atta-ur-Rahman. *Chem. Pharm. Bull*. 52, 1358-1361 (2004)

130. Schliebs R., Liebmann A., Bhattacharya S.K., Kumar A., Ghosal S., Bigl V. *Neurochem. Int*. 30,181-190 (1997)

131. Greger, H., Hofer, O. *Phytochemistry* 23, 1173 (1984)

132. Crombie, L., Fischer, D. *Tetrahedron Lett*. 26, 2481 (1985)

133. Sy, L.K., Brown, G.D. *Phytochemistry*, 50, 781 (1999)

134. Gertsch, J. *Planta Med*. 74, 638-650 (2008)

135. Raduner, S., Bisson, W., Abagyan, R., Altmann, K.-H., Gertsch, J. *J. Nat. Prod*., 70, 1010-1015 (2007)

136. Friesner, R.A.; Murphy, R.B.; Repasky, M.P.; Frye, L.L.; Greenwood, J.R.; Halgren, T.A.; Sanschagrin, P.C.; Mainz, D.T. J. *Med. Chem*., 49, 6177(2006)

137. Xu, F.; Wu, H.; Katritch, V.; Han, G.W.; Jacobson, K.A.; Gao, Z.-G.; Cherezov, V.; Stevens, R.C. *Science*, 332, 322. (2011)

138. Ruhl, T.; Deuther-Conrad, W.; Fischer, S.; Gunther, R.; Hennig, L.; Krautscheid, H.; Brust, P. *Org. Med. Chem Lett*. 2, 32. (2012)

139. Kollman, P.A.; Massova, I.; Reyes, C.; Kuhn, B.; Huo, S.; Chong, L.; Lee, M.; Lee, T.; Duan, Y.; Wang, W.; Donini, O.; Cieplak, P.; Srinivasan, J.; Case, D.A.; Cheatham, T. E. *Acc. Chem. Res.*, 33, 889 (2000)

140. Song, Z.H.; Slowey, C.-A.; Hurst, D.P.; Reggio, P.H. *Mol. Pharmacol*., 56, 834 (1999)

141. Matovic, N.; Matthias, A.; Gertsch, J.; Raduner, S.; Bone, K.M.; Lehmann, R.P.; DeVoss, J. J. Org. *Biomol. Chem*., 5, 169 (2007)

142. 142 Li, Y.; Zhang, Y.; Huang, Z.; Cao, X.; Gao, K. Can. *J. Chem*. 82, 622 (2004)

143. Tang, G.-H.; Chen, D.-M.; Qiu, B.-Y.; Sheng, L.; Wang, Y.-H.; Hu, G.-W.; Zhao, F.-W.; Ma, L-J.; Wang, H.; Huang, Q.-Q.; Xu, J.-J.; Long, C.-L.; Li, J. *J. Nat. Prod*., 74, 45 (2011)

144. Abarbri, M.; Parrain, J.L.; Duchêne, A. *Synth. Commun*., 28, 239 (1998)

145. Bohlmann, F.; Abraham, W.R.; *Phytochemistry*, 20, 855. (1981)

146. Greger, H.; Grenz, M.; Bohlmann, F. *Phytochemistry*, 20, 2579 (1981)

147. Takeya, T., Ara, Y., Tobinaga, S. *Chem. Pharm. Bull*., 31, 1970. (1995)

148. Kanlayavattanakul, M., Ruangrungsi, N., Watanabe, T., Ishikawa, T. *Heterocycles*, 61, 183 (2003)

149. Bohlmann, F., Rao, N. *Chem. Ber*. 106, 303. (1973)

150. Morimoto, M., Kumeda, S., Komai, K. J. *Agric. Food Chem*. 48, 1888-1891 (2000)

151. Li, S., Lo, C.-Y., Ho, C.-T., *J. Agric. Food Chem*. 54, 4176–4185 (2006)

152. Iinuma, M., Matsuura, S., Kusuda, K.,.. *Chem. Pharm. Bull.* 28, 708-716(1980)

153. Manabe S. et al., *Tetrahedron* 42,3461–3470 (1986)

154. Jahaniani, F., Ebrahimi, S.A., Rahbar-Roshandel, N., Mahmoudian, M. *Phytochemistry* 66, 1581-1592 (2005)

155. Kuhnt, M., Rimpler, H., Heinrich, M., *Phytochemistry* 36, 485-489 (1994)

156. Oshitari, T., Okuyama, Y., Miyata, Y., Kosano, H., Takahashi, H., Natsugari, H. *Bioorg. Med. Chem*. 19, 7085-7092 (2011)

157. Agrawal, P.K., *Carbon–13 NMR of flavonoids*, Elsevier, Amsterdam, p. 154 (1989)

158. Takahata H, Kubota M, Ikota NJ. *Org. Chem* 64, 8594-8601 (1999)

159. Blechert S, Stapper C. *J. Org. Chem.* 2855-2858 (2002).

160. Lazny R., Ratkiewicz A., Nodzewska A., Wynimko A., Siergiejczyk L. *Tetrahedron* 68, 6158-6163 (2012)

161. Pieters L., Van Dyck S., Gao M., Bai R, Hamel E., Vlietinck A., Lemière G. *J Med Chem* 42, 5475-5481 (1999)

162. Chatterjee S., Srivastava S., Khalid A., Singh N., Sangwan R.S., Sidhu O.P, Roy R., Khetrapal C.L., Tuli R. *Phytochemistry* 71, 1085–1094 (2010)

163. Huaping Z., Abbas K., Samadi *J. Nat. Prod*. 74, 2532-2544 (2011)

164. Leonti M., Casu L., Raduner S., Cottiglia F., Floris, C., Altmann K.-H., Gertsch J. *Biochem. Pharmacol*. 79, 1815-1826 (2010)

165. Gertsch, J. *Planta Med.* 74, 638-650 (2008)

166. Kulkarni, S.K., Ninan, I.,. *Journal of Ethnopharmacology* 57(3), 213-217. (1997)

167. Gupta, L.K., Gupta, R., Tripathi, C.D. *Clin. Exp. Pharmacol. Physiol.* 38, 592-597 (2011)

168. Mohamadi F., Richards N.G.J., Guida W.C., Liskamp R., Lipton M., Caufield, C., Chang, G., Hendrickson, T., Still W.C. J., *Comput. Chem*. 11, 440 (1990)

169. Halgren, T.J. *Comput. Chem*., 17, 520 (1996)

170. Hasel W., Hendrickson T.F., Still, W.C., *Tetrahedron Comput. Methodol*. 1, 172 (1988)

171. Kollman P.A., Massova I., Reyes C., Kuhn B., Huo S., Chong L., Lee M., Lee T., Duan Y., Wang W., Donini O., Cieplak, P., Srinivasan J., Case D.A., Cheatham T. E. *Acc. Chem. Res.*, 33, 889 (2000)

172. Kasture S., Vinci S., Ibba F., Puddu A., Marongiu M., Murali B., Pisanu A., Lecca D., Zernig G., Acquas E. *Neurotox. Res.* 16, 343-355 (2009)

173. Ruiu S., Longoni R., Spina L., Orrù A., Cottiglia F., Collu M., Kasture S., Acquas E. *Behav. Pharmacol.* 24, 133-143 (2013)

174. Ruiu S., Pinna G.A., Marchese G., Mussinu J.M., Saba P., Tambaro S., Casti P., Vargiu R., Pani L. *J. Pharmacol. Exp. Ther.*306, 363-370 (2003)

175. Beaumont, K., Chilton, W., Yamamura, H.I., Enna, S.J.. *Brain Research* 148, 153-162 (1978)

176. Cheng Y., Prusoff W.H., *Biochem. Pharmacol.* 22, 3099-3108 (1973)

177. Orrù A., Marchese G., Casu G., Casu M.A., Kasture S., Cottiglia F., Acquas E., Mascia M.P., Anzani N., Ruiu S. *Phytomedicine*http://dx.doi.org/10.1016/j.phymed.2013.10.021. In press

19. PUBLICATIONS AND PRESENTATIONS

Publications

S., Ruiu, **N., Anzani**, A., Orrù, C., Floris, P., Caboni, E., Maccioni, S., Distinto, S., Alcaro, F., Cottiglia. N-Alkyl dien- and trienamides from the roots of *Otanthus maritimus* with binding affinity for opioid and cannabinoid receptors. *Bioorganic & Medicinal Chemistry*, **21**, 7074-7082 (2013).

A., Orrù,G. Marchese, G., Casu, M.A., Casu, S. Kasture, F. Cottiglia, E., Acquas,M. P. Mascia, **N. Anzani**, S., Ruiu. *Withania somnifera* root extract prolongs analgesia and suppresses hyperalgesia in mice treated with morphine. *Phytomedicine*, http://dx.doi.org/10.1016/j.phymed.2013.10.021. In press.

S., Ruiu, **N., Anzani**, A., Orrù, E., Maccioni, C., Floris, F., Cottiglia. Xanthomicrol, a Flavone from *Stachys glutinosa,* Inhibited the Anti-nociceptive Effect of Morphine in Mice. Submitted to *Planta Medica.*

Oral Presentation

N. Anzani. Attività antitopoisomerasica di derivati fenantridinici isolati dal *Pancratium illyricum*. Annual meeting of: "La Parola ai Giovani", Società Chimica Italiana, Sezione Sardegna. University of Cagliari, June 24th, 2011, Cagliari Italy.

N. Anzani. N-alkylamides from *Otanthus maritimus*: structure elucidation, binding affinity for cannabinoid receptors and computational study. 3rd Meeting of the Paul Ehrlich MedChem Euro-PhD Network, 27th-29th September 2013 Santa Margherita di Pula, Cagliari, Italy.

Poster Presentation

S., Ruiu, A.,Orrù, C., Floris, P.,Caboni,F., Cottiglia. N-alkyl dien- and trienamides with binding affinity for opioid and cannabinoid receptors. 7th meeting of "Nuove Prospettive in Chimica Farmaceutica", Società Italiana di Chimica, Divisione di Chimica Farmaceutica, 29th-31th May 2013, Savigliano, Cuneo,Italy.